A Review of Aeronautical Fatigue and Integrity Investigations in China June 2015-May 2017

Presented at the 35th conference of the International Committee of Aeronautical Fatigue and Structural Integrity (ICAF)

Compiled by

Dong Dengke, Cui Degang and Su Shaopu

Table of contents

1 Introduction

This review summarizes the studies on the research of aeronautical fatigue and integrity investigations in China during the period June 2015 to May 2017 and is presented at the 35th conference of the International Committee Aeronautical Fatigue and Structural Integrity (ICAF) in Japan.

This report includes the research on the structure integrity analysis of advanced material, advanced methods, widespread fatigue damage, maintenance and repair, corrosion fatigue and resistances, structure health monitoring, load acquisition and spectrum compilation, and full-scale fatigue testing etc.

After China was fully accepted by ICAF organization in the 34th conference of ICAF，China Delegation ICAF Office under the leadership of Chinese Aeronautical Establishment (CAE) has been established to make better communication with ICAF organization and all the partners. The office organizes relevant professional institutions and academics to carry out the research inside China and cooperate with ICAF partners. The China National Review is integrated and compiled by China Delegation ICAF Office based on the recent researches progress contributed by the following organizations.

1 AVIC Aircraft Strength Research Institute

2 AVIC Shenyang Aircraft Design & Research Institute

3 AVIC Helicopter Design & Research Institute

4 AVIC Chengdu Aircraft Design & Research Institute

5 AVIC Beijing Aeronautical Manufacturing Technology Research Institute

6 AVIC Harbin Aircraft Industry Group Co.,LTD, Aircraft Design and Research Institute

7 COMAC Shanghai Aircraft Design and Research Institute

8 COMAC Beijing Aeronautical Science & Technology Research Institute

9 Naval Aeronautical Engineering Institute

10 Civil Aviation University of China

11 Shanghai Jiao Tong University

12 Northwestern Polytechnical University

13 Institute of Nuclear Physics and Chemistry, China Academy of Engineering Physics

Each item of the report lists the corresponding contributors. The generous contributions provided by these aerospace industry and universities are sincerely acknowledged.

2 Advanced Materials and Process

2.1 Particulate Reinforced Aluminum Matrix Composite[1]

Particulate Reinforced Aluminum Matrix Composite is regarded as a kind of engineering materials with high performance, regular microstructure, fine particulate, interfacial compatibility (Figure 2. 1), low density, high rigidity, high stiffness, high specific strength and being suitable to mass production. Therefore, it has broad application prospects in high-tech area such as aviation, aerospace and national defense industry.

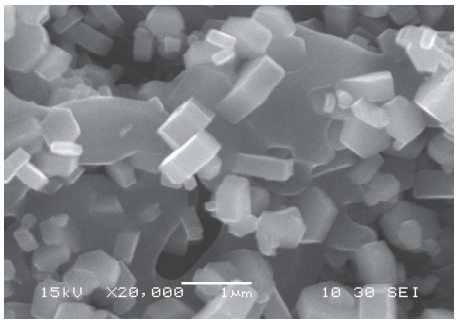

Figure 2. 1 Material Microstructure

1 Mechanical Property

The developed situTiB_2 Particulate Reinforced casting Aluminum Matrix Composite has obvious advantages in strength, modulus properties over the other matrix composites. In addition, it is suitable to product the huge, complex and thin-wall casting parts. Table 2. 1 shows the comparisons of mechanical properties between 10%TiB_2 /A356 and A356.

Table 2. 1 Mechanical Properties of 10%TiB_2 /A356 and A356

Mechanical parameters	A356 Matrix alloy	10%TiB_2 /A356 Composites
σ_b(MPa)	280～310	410 ～ 420
$\sigma_{0.2}$ (MPa)	180～230	340 ～ 350
E (GPa)	68～72	85 ～ 90
δ_5 (%)	3～5	2.0 ～ 2.5
ρ （gcm^{-3}）	2.70	2.77

2 Fatigue Properties

8% TiB_2 /A356 composite has a 40% higher Fatigue limit than A356 matrix alloy (Figure 2. 2).

[1] AVIC Aircraft Strength Research Institute

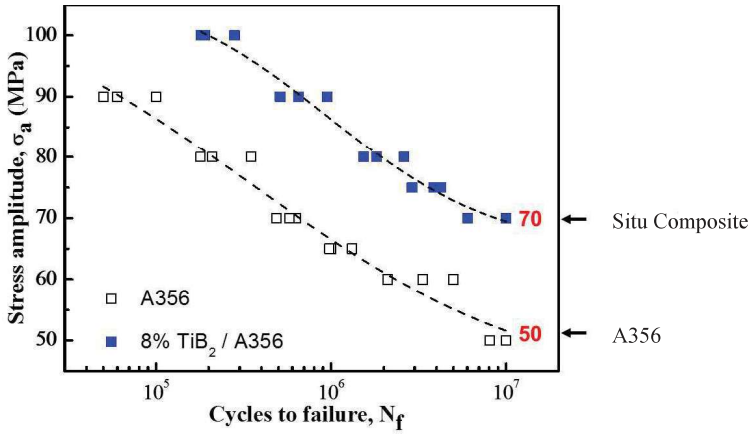

Figure 2. 2 Fatigue Limit Comparisons Between 8%TiB_2 /A356 Composite and A356 Matrix Alloy

3 Applications

In situTiB_2 Particulates Reinforced Aluminum Metal Matrix Composites has been used in various parts of the Tiangong-2 space lab for their high specific strength and specific modulus, low coefficient of thermal expansion, good damping capacity, casting formability and machinability (Figure 2. 3).

Figure 2. 3 The Application of Particulate Reinforced Aluminum Matrix Composite on Tiangong-2 space lab

2.2 Crack Growth Property of Glare in Fuselage Structure[1]

Fiber metal laminate can be classified as ARALL (Aramid Reinforced Aluminum Laminates), GLARE (Glass Reinforced aluminum laminates), CARE(Carbon Reinforced aluminum laminates), TiGr (Titanium/Graphite hybrid laminates) and so on.

Recently, the most globally focused and widely used laminate is GLARE. Since the 20th foreign institutions have conducted some wide research and tests regarding the fabrication and performance of the GLARE laminate structure. Lots of useful data have been obtained, and some analytical methods have been formed. Strengthen Reinforced (SR) structure has an excellent fatigue crack growth performance, which can obviously improve the fatigue life of aircraft structure and reduce the structure weight and inspection costs.

Based on C919 and follow-up models' market competitive requests, the circumferential crack growth properties (Figure 2. 6) of the panel are investigated in virtue of the test results of baseline structure (Figure 2. 4) and SR structure (Figure 2. 5). This work verifies the superiority of the SR structure crack growth performance.

[1] COMAC Shanghai Aircraft Design and Research Institute

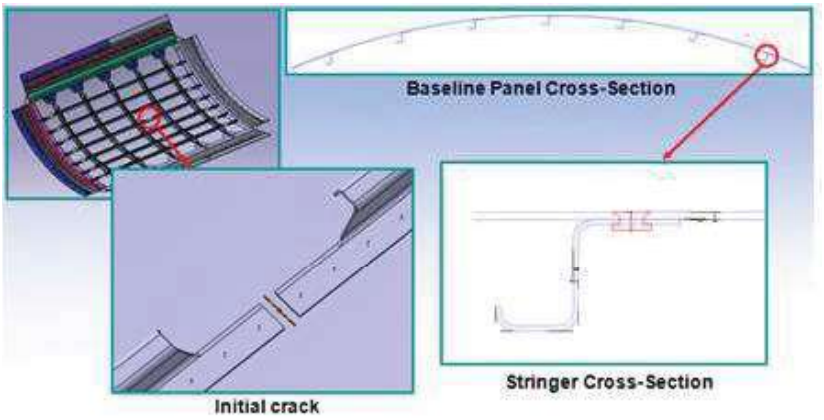

Figure 2.4 Baseline Panel

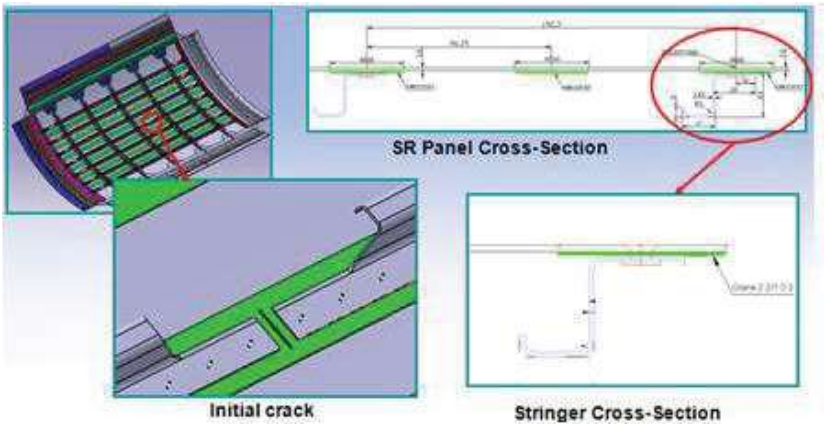

Figure 2.5 SR Panel

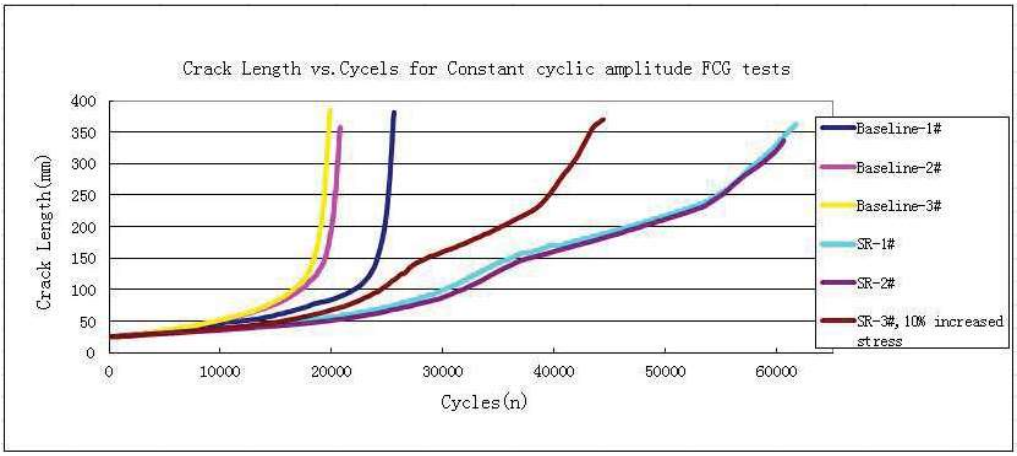

Figure 2.6 Crack Length VS. Cycles for Baseline and SR Specimen

2.3 Application and Research of Al-Li Alloy[1]

The third generation Al-Li alloy is favored by aircraft manufacturing companies recently in virtue of its

[1] COMAC Shanghai Aircraft Design and Research Institute

good performance, such as high strength, low density and high corrosion resistance. COMAC widely applies third-gen Al-Li alloy on fuselage panels of C919 and conducts lots of the corresponding research and tests. This paper introduces the static strength and fatigue performance of the 2060-T8E30、2099-T83 、 2198-T8 、 2196-T8511 Al-Li alloy under welding, shot peening and riveting process conducted by COMAC.

2.3.1 Strength Test of Al-Li Alloy in Welded Joint

As an advanced jointing technique, welding brings a simpler connection structure, better mechanical properties and lower weight compared with riveting. So it's widely applied in the area of aviation. COMAC focuses on the feasibility of the application of Friction Stir Welding (FSW) and Laser Beam Welding (LBW) on the fuselage panels, and conducts a series of basic research on process parameters and mechanical performance tests. The results show that FSW applied on the Al-Li skin lap joint and skin-stringer joint structure has better static and fatigue performance than the other described process.

1) Static Strength Test

The shear and tensile strength tests were carried out for skin lap joint and skin-stringer joint with riveting/FSW manufacture processes.

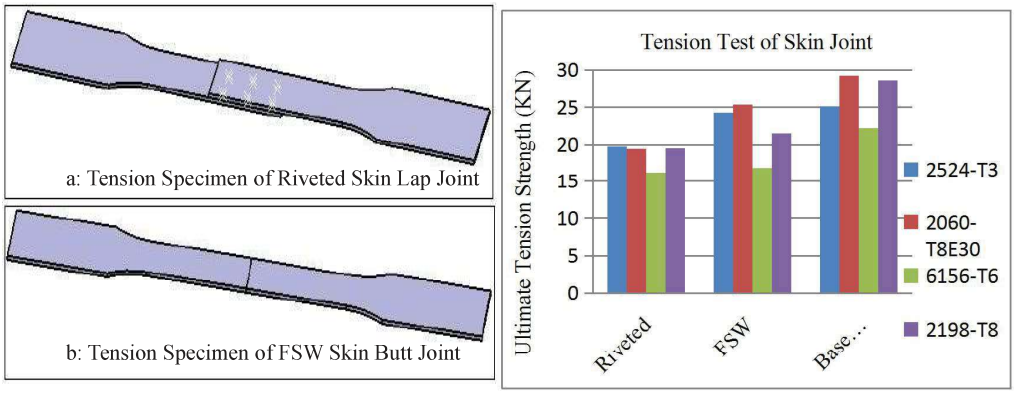

Figure 2. 7 Tension Test results of Riveted/Welded Skin Joint

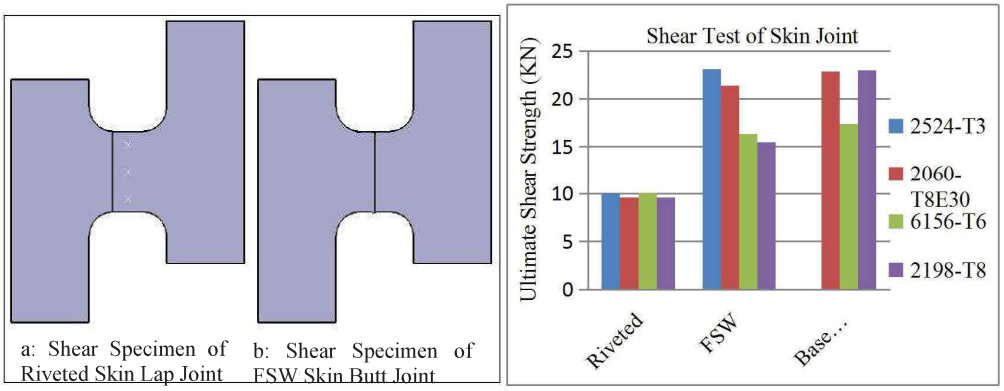

Figure 2. 8 Shear Test Results of Riveted/Welded Skin Joint

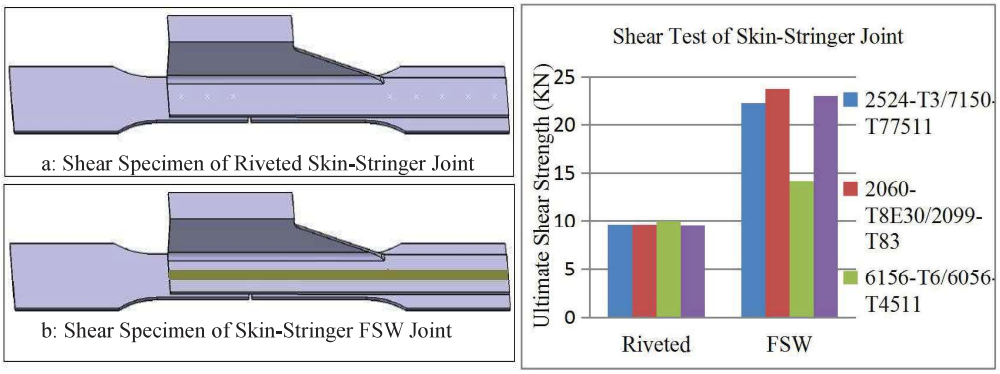

Figure 2. 9 Shear Test of Riveted/Welded Skin-Stringers Joint

2）Fatigue Strength Test

The fatigue strength tests were carried out on skin lap joint and skin-stringer joint with riveting/FSW/LBW processes.

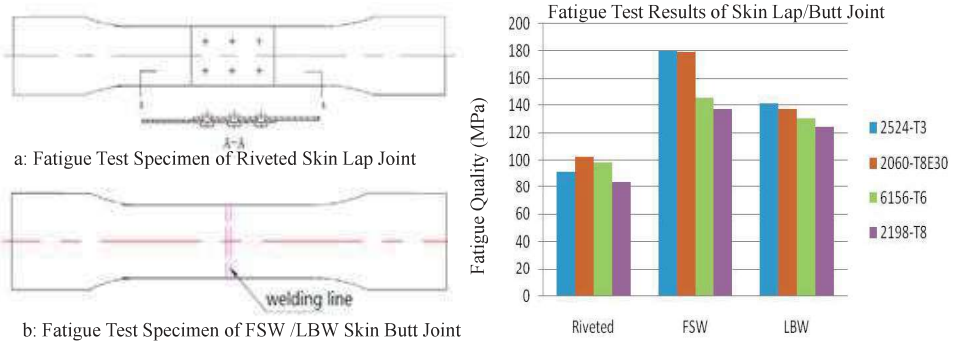

Figure 2. 10 Test Results of Riveted Skin Lap Joint / Welded Butt Joint

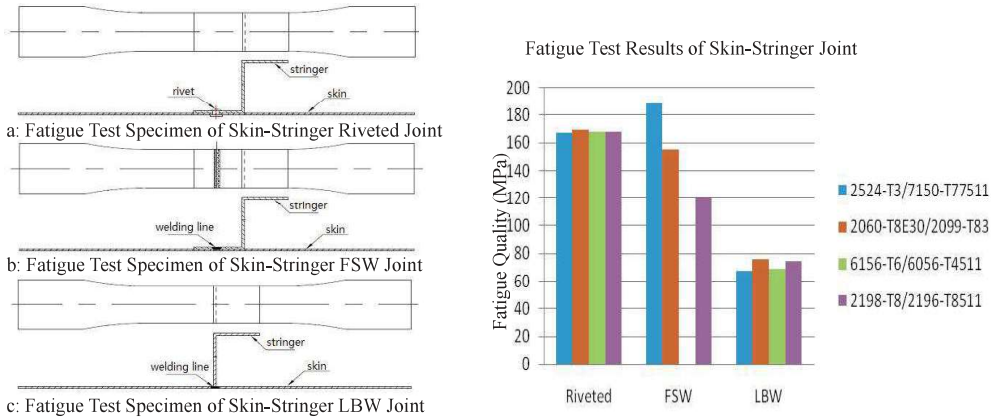

Figure 2. 11 Test Results of Skin-Stringer Rivet Joint / Welded Joint

Conclusions

a) The static and fatigue properties of FSW specimen on ordinary aluminum alloy or Al-Li alloy are better than riveted skin lap/butt joint.

b) For skin-stringer joint structure, 2524-T3/7150-T77511 and 2060-T8E30/2099-T83 are the best choice for FSW. The static performance of FSW structure is better than riveted ones, and the fatigue performance is comparatively equal.

c) The fatigue performance of LBW skin lap/butt joint is better than riveted ones; Yet LBW skin-stringer joint structure has much worse property than riveted structure.

2.3.2 Fatigue Property Test of Al-Li Alloy with Shot Peening Process

Shot peening is a surface treatment process that often used to improve the fatigue performance of parts. COMAC studies fatigue property of 2060-T8E30 with shot peening technique. The cast steel shots and ceramic shots are used to conduct a shot peening process on 2060-T8E30 Al-Li alloy sheets with different thickness. In addition, different shot peening intensity is applied on specimen and the fatigue performance is tested in this research. The results show that shot peening can improve significantly the fatigue performance of Al-Li alloy at an appropriate shot peening parameter.

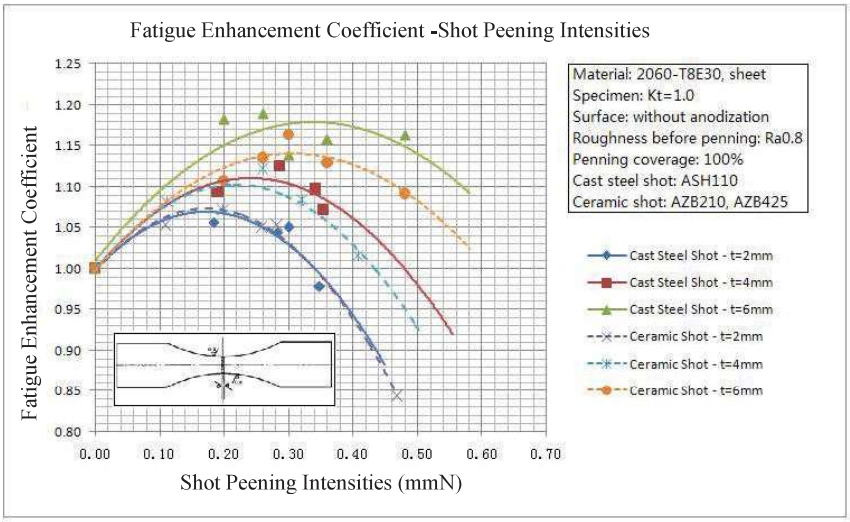

Figure 2. 12 Fatigue Enhancement Coefficient - Shot Peening Intensities

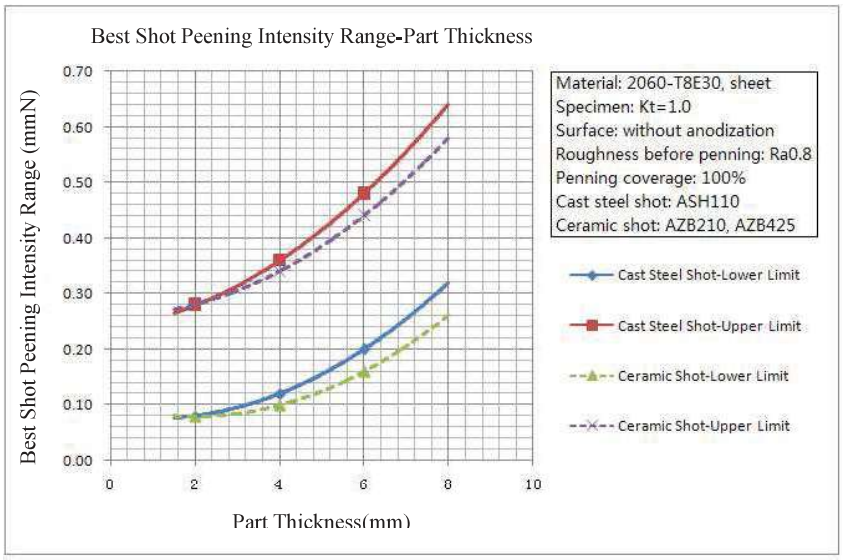

Figure 2. 13 Best Range of Shot Peening Intensity - Part Thickness

Conclusions:

1) The shot peening effects on the fatigue property of 2060-T8E30 Al-Li alloy specimen shows a trend of parabolic type curve against shot peening intensity. Fatigue enhancement coefficient increases at first and then decreases as shot peening intensity increases. Two much higher shot peening intensity will cause lower fatigue property than that of the base material. The shot peening intensity of the thin sheet should especially be strictly controlled.

2) The best range of shot peening intensity regarding fatigue performance of 2060-T8E30 Al-Li alloy increases with the sheet thickness increased. Moreover, the thick sheet has a larger improvement on

fatigue performance than that in thin sheet after shot peening.

3) The peening intensity in cast steel shot peening is much higher than ceramic shot peening for the thick plate.

2.3.3 Fatigue Property Test of Al-Li Alloy with Rivet Joint

For 2524-T3 alloy and 2060-T8E30 structures with different riveting forces, COMAC studied the expansion, fatigue performance of rivet hole and the rivet driven head sizes design. Compared with 2524-T3 alloy, the larger riveting force should be applied on 2060-T8E30 Al-Li alloy.

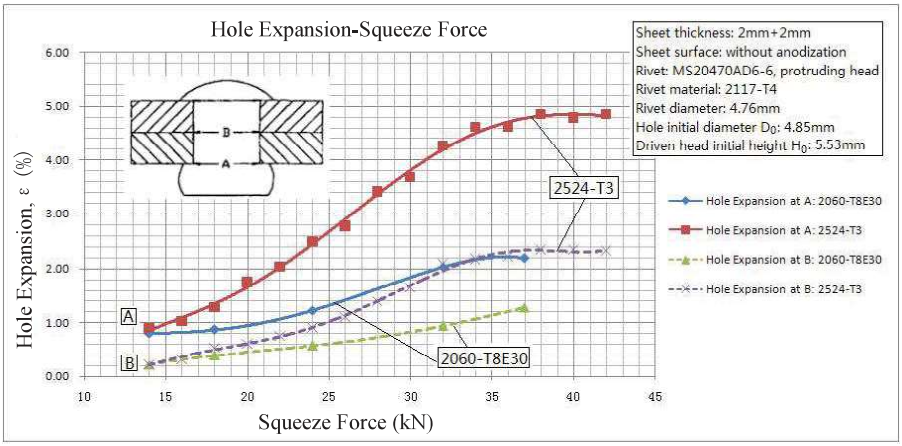

Figure 2. 14 Hole Expansion Measured at Different Locations

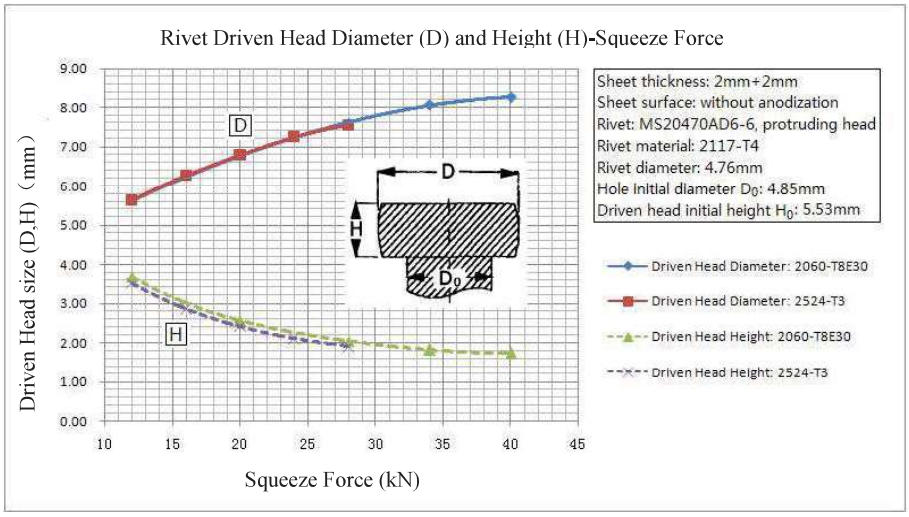

Figure 2. 15 Driven Head Diameter (D) And Height (H) on Different Materials

Conclusions

1) The interference of rivet hole increases with riveting force increasing. Under the same riveting force, the rivet-hole expansion of 2060-T8E30 Al-Li alloy sheet is lower than that of 2524-T3 aluminum alloy sheet.

2) The height of rivet driven head and the diameter of rivet hole vary linearly with the riveting force increasing, and the 2060-T8E30 Al-Li alloy sheet and 2524-T3 aluminum alloy sheet almost have the same height of rivet driven head while supposed on the same riveting force.

3) The fatigue quality of rivet hole shows a trend of a parabolic curve against the riveting force. To obtain the best fatigue performance, the 2060-T8E30 Al-Li alloy sheet needs higher riveting force than 2524-T3 aluminum alloy sheet.

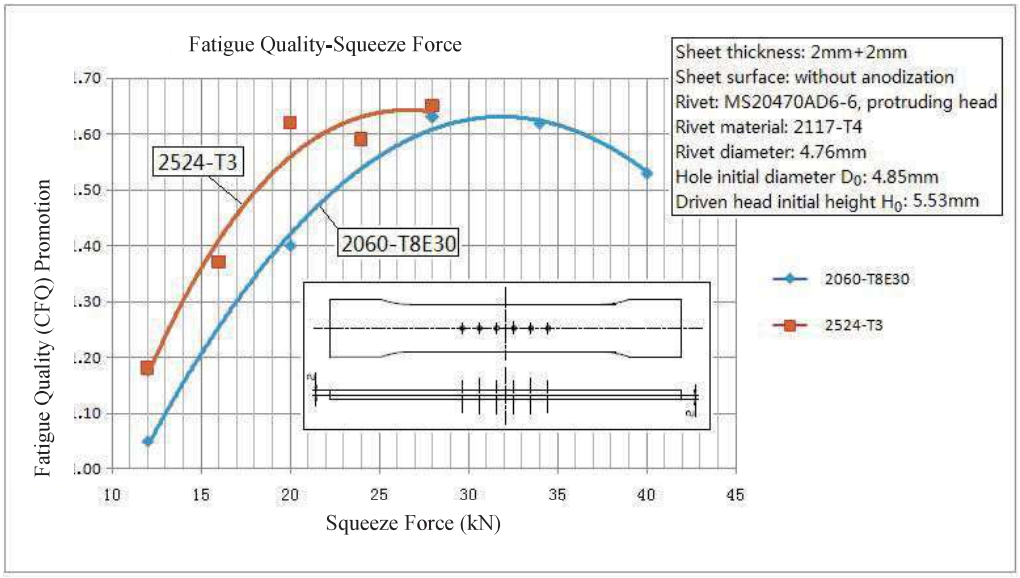

Figure 2. 16 Fatigue Quality at the Riveted Holes in 2060-T8E30 Sheet and 2524-T3 Sheet

2.4 Friction Stir Welding of 2060Al-Li Alloy[1]

The study shows the strength differences of FSW technique at different parameters. The FSW strength with a factor of 800/200 is relatively the highest (Figure 2. 17).

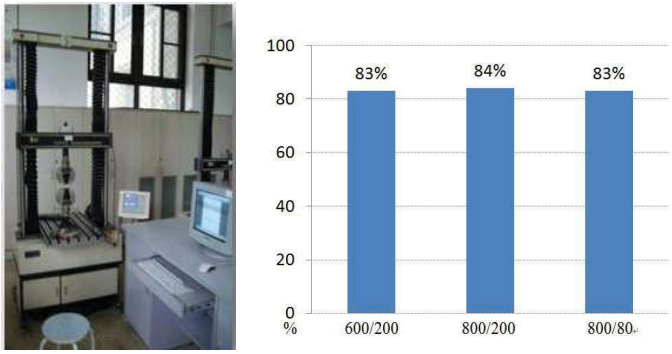

Figure 2. 17 Strength Difference of FSW Technique with Serial Factors

Based on the FSW factor of 800/200, the mechanical properties of tension, shear, compression and fatigue were tested and compared with the riveted structure:

1) The tension failure load of FSW structure is lower and more dispersive than design load;
2) The shear failure load of FSW structure is higher and more dispersive than the riveted one;
3) Initial buckling usually takes place on the skin supposed on compression load. The buckling deformation increases with the load increasing, the stringer separates from the skin and loses the load-carrying capacity. The initial buckling load is much lower than that of the riveted one while the failure load is close to it;

The Detailed Fatigue Ratio (DFR) value of the riveted structure is 97% of that of FSW structure.

[1] AVIC Beijing Aeronautical Manufacturing Technology Research Institute

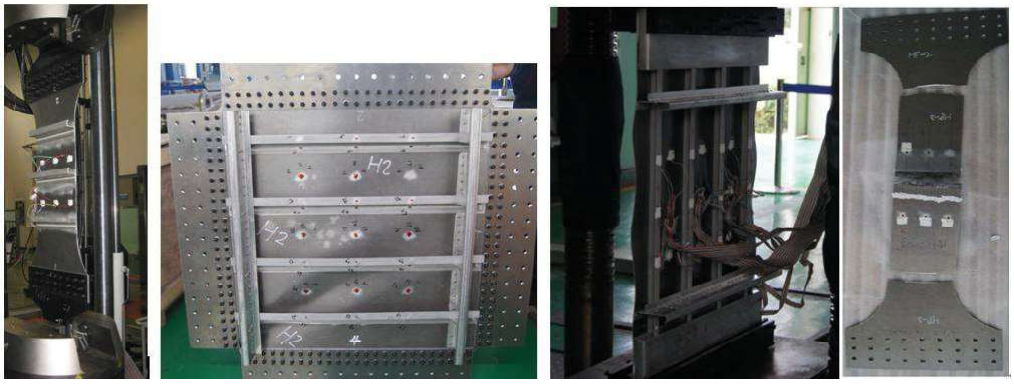

a) Tension Test b) Shear Test c) Compress Test d) Fatigue Test

Figure 2. 18 Strength Test of Friction Stir Welding of 2060Al-Li Alloy

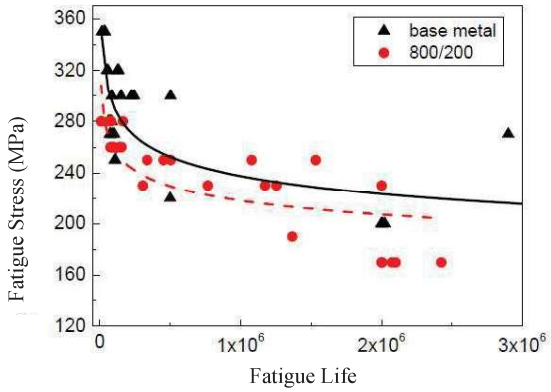

Figure 2. 19 Fatigue Property of Friction Stir Welding Technique of 2060Al-Li Alloy

2.5 Strength Researches into Additive-Manufactured Structures[1]

The relationship between EBWD (Electron Beam Wire Deposition) process parameters and the mechanical properties of EBWD titanium alloys were developed by tensile test and fractography analysis. The effect of solution temperature on mechanical properties of TC17 alloy specimen fabricated by EBWD is demonstrated in Figure 2. 20[1]. With solution temperature increasing, the tensile strength of EBWD TC17 increases while the plasticity decreases.

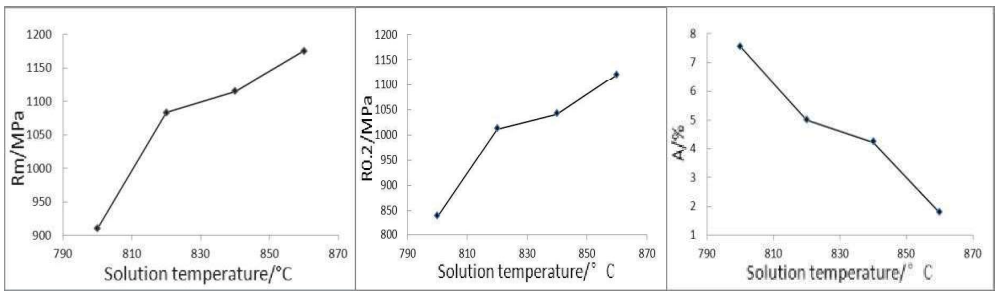

Figure 2. 20 Tensile Test Results of TC17 Alloy Specimen Fabricated by EBWD

With the improvement of deposition process and heat treatment, the static strength of TC4 alloy specimen fabricated by EBWD can be close to that of forged one, and the plasticity is increased dramatically as well. The S-N curve and fatigue limits at 10^7 cycles were determined by staircase

[1] AVIC Aircraft Strength Research Institute

method using smooth coupons, and the results are shown in Table 2. 2[2]. It can be seen that the fatigue limit of EBWD TC4 material is much higher than that of forged parts.

Table 2. 2 High Cycle Fatigue Limits of EBWD TC4 Material at Different Stress Ratios

Stress ratio	R=0.5	R=0.06	R=-1
Fatigue limit (MPa)	889.82	747.08	528.33

The organization and tensile properties of as-deposited, 400℃/3 h annealing, 900 ℃/3 h annealing state and hot isostatic-pressing (HIP) of 316 stainless steel by selective laser melting are studied. The test results are shown in Figure 2. 21. The fracture surfaces in different states are shown in Figure 2. 22[3]. The results show that the deposited organization is mainly composed of columnar crystals grown epitaxially. The organization of the as-deposited sample after 400 ℃/3 h annealing doesn't change significantly, the transverse and longitudinal strength increase slightly and the longitudinal elongation improves significantly, yet the transverse elongation decreases slightly; the coarse columnar crystals after 900 ℃/3 h annealing split into more slender columnar crystals. In the case of strength reducing, the transverse and longitudinal elongation improves significantly and the tensile strength and elongation attain the forging level; after HIP, the coarse columnar crystals split into small columnar crystals and tend to be equiaxial. The lateral and longitudinal strength decrease significantly, while the lateral and longitudinal elongation increase, the tensile strength and elongation attain the forging level. In view of the comparison results at four states, the tensile strength match the best with elongation at the post-process of 900°C/3h anneal.

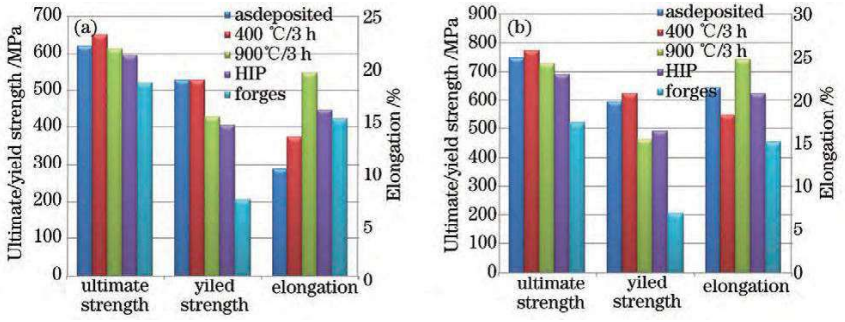

a) Vertical b) Horizontal

Figure 2. 21 Tensile Properties of 316 Stainless Steel by SLM Processing at Room Temperature

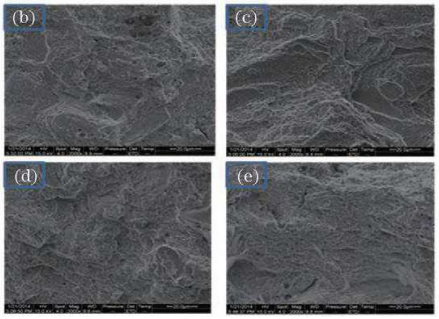

Figure 2. 22 Fracture Surface Characterizations of 316 Stainless Steel by SLM Processing at Different States.

(b) As-Deposited; (c) 400 ℃/3 h Heat-Treated; (d) 900 ℃/3 h Heat-Treated; (e) HIP

To research into the effects of heat treatment and surface condition on the residual stress distribution, fatigue and crack growth properties of SLM TC4 alloy, AVIC Aircraft Strength Research Institute designed a range of test coupons including optimized SLM process, heat treatment and isostatic pressing parameters. As-deposited, heat treated and isostatic pressed coupons are fabricated. Figure 2. 23 shows some fatigue coupons.

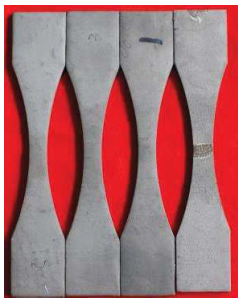

Figure 2. 23 TC4 Fatigue Coupons and Rough C(T) Coupons Fabricated by SLM

SLM processing, as an advanced process generates complex residual stress in manufacturing process, causes "curling" and "distortion" phenomena of metallic parts. The existence of residual stress restricts the application in particular aerospace and automotive. It will be potentially valuable to well understand the mechanism of residual stress and the effects of different manufactured parameters on it. We studied the distribution of residual stress in standard coupons by two measurement approaches, X radio and neutron diffraction. Considering the rough surface of coupons at as-deposited or machined state, we applied electrolytic polishing process to decrease the measured error. The residual stresses at the centre of coupons 3# (machined) and 4# (as-deposited) were respectively 278Mpa and 205Mpa in Y direction (Figure 2. 24) by X radio. The residual stress distribution of couple 4# was measured by neutron diffraction (Figure 2. 25), which showed that the coupon had a higher stress gradient in X direction than that in Y direction.

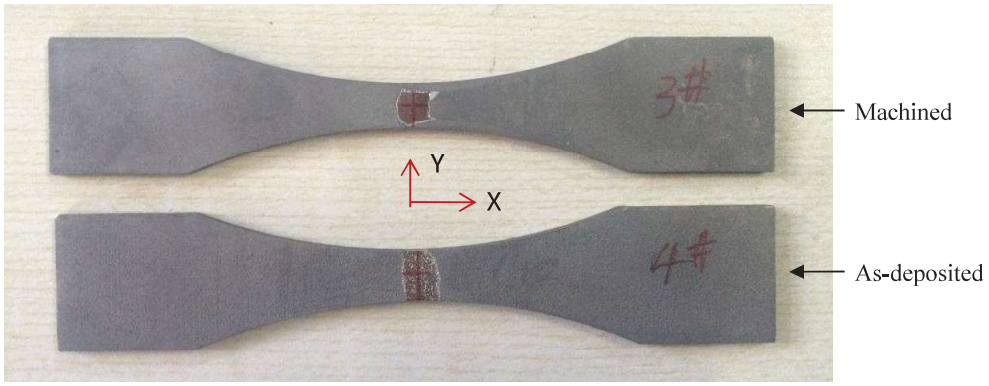

Figure 2. 24 Coupons for Residual Stress Measurement by X Radio Method

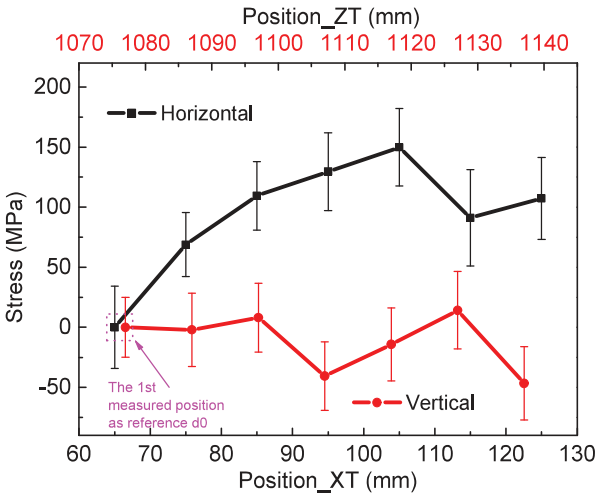

Figure 2. 25 Residual Stress Gradient Distributions of Coupon 3# in X and Y direction

Reference:

[1] Yang Yang, Suo Hongbo, Chen Zheyuan, Wang Lei. (2016). *Heat Treatment of Metals*, Vol. 41, 9., p.141-144.
[2] Huang Zhitao, Suo Hongbo, Gong Shuili, Yang Guang, Yang Yang, Dong Wei, Yang Fan.(2015). Manufacture Technology Research,4., p.14-17.
[3] Ding Li, Li Huaixue, Wang Yudai, Huang Zhitao. (2015).Chinese Journal of Lasers, Vol.42, 4., p.1-7.

2.6 Crack Location Effects on Fatigue Crack Growth Behavior of 2024-T3 Aluminum by Friction Stir Welding[1]

Friction Stir Welding (FSW) is a solid-state joining process emerging as an alternative technology to join high strength alloys which are difficult to weld with conventional techniques. Recently, great development of this advanced technology is being driven by aeronautics, aerospace and railway industries in China, and some important national projects of FSW have been accomplished/proceeding. As a major participant and principal of a national project, AVIC Aircraft Strength Research Institute (ASRI) has done a lot of work on FSW, including welding parameters, fatigue life correlation, test verifications and so on. A project regarding how to necessarily introduce the FSW technique into aircraft structure maintenance has been conducting in ASRI.

As an aspect of the ASRI project, a study of crack location effects on fatigue crack growth behavior of friction stir welded 2024-T3 aluminum is presented in this paper. First, two plates with same thickness (3.2mm) were welded using FSW technique. Then, the Middle Tensile (MT) specimen (400mm×100mm) was cut from welding plate. According to different distances from middle of nugget zone, two hole-edged cracks were precut in corresponding location. The mechanical behavior of MT specimen was studied in virtue of static and fatigue crack growth tests, and there are totally 18 specimens which for static test is 7 and for fatigue test is 11. The fatigue crack growth rates in different locations and in base material were analyzed. The fracture analysis of three classic different locations was made.

Figure 2. 26 Crack Growth Specimen Test

Figure 2. 27 and Figure 2. 28 present the N-a curves and △K-da/dN curves of the specimens with the crack in different locations. QH denotes the specimen with a crack appearing in middle nugget zone,Q2 denotes the specimen in which a crack distance to middle nugget zone is 2mm in advancing side, H17 denotes the specimen in which crack distance to middle nugget zone is 2mm in retreating side. The results show that the crack growth rate of QH specimen is the slowest, and the corresponding crack growth life is highest.

It was concluded that the crack growth rate of welded plate in nugget zone is lower than that of base material, yet it increases gradually as the displacement of crack location to the middle of nugget zone increases, and the peak is in junction of the welded zone and base material, which varies with the crack locations. The details of crack growth rate in different locations are also described in this work.

[1] AVIC Aircraft Strength Research Institute

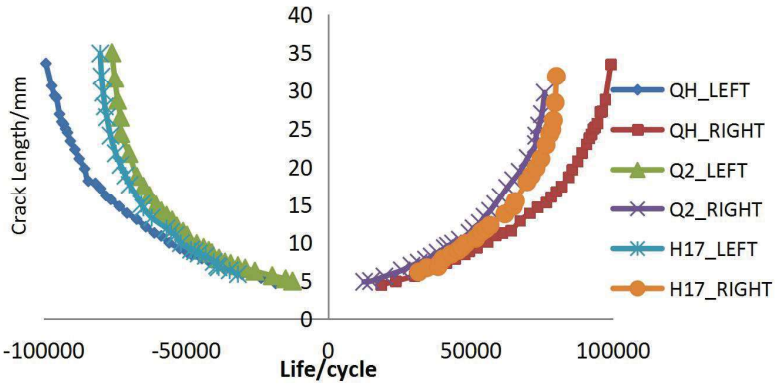

Figure 2. 27 Crack Growth Life Vs Crack Length Curves of the Specimens with Crack in Different Locations

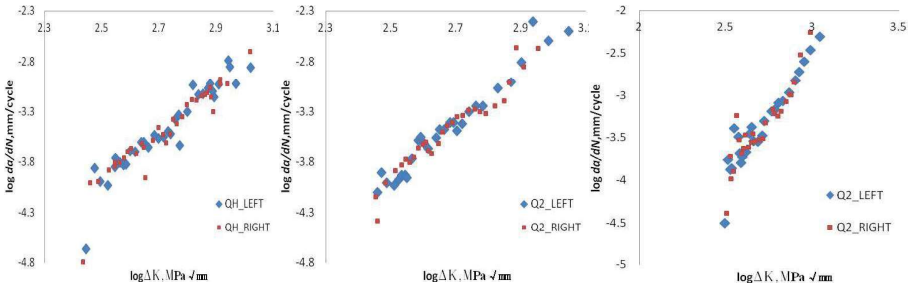

Figure 2. 28 da/dN VS ΔK Curves of the Specimens with a Crack in Different Locations in Three Specimens

The study provides some useful data for aircraft structure maintenance when using FSW technique. The data can be used to determine whether the fatigue life of structure by FSW maintenance can meet the requirements of airworthiness, economy and safety and where the rivet/bolt holes should be drilled in welded region of structure.

3 Advanced Analytical, Numerical Simulation Methods and Experiments

3.1 Research and Application on the Control Criterion of Composite Stability[1]

During the process of aircraft structure design, stability design criterion is a critical factor since losing stability is a serious problem for aircraft safety. Moreover, it plays a very important role on the weight reduction of the aircraft structure. Therefore, it is necessary to conduct a research and test validation on the control criterion of composite structure stability, which will give insight into the potential ability of bearing load.

If we broaden the design criterion of composite structure stability, the local buckling can happen to part of the structure even if it can still endure load. When the load is less than the limit load, the structure gets thinner and thinner, and it means that the state "losing stability- recovery-losing stability again" during the operation may happen to this part of structure. Once the composite structure has a big distortion, delamination collapses of part of the structures may occur. The delamination areas between the losing stability and the around area are highly absonant so that the appearance of debonding and the damage of bolt hole may lead to destroy. Even though the damage does not happen at single stability lost, we need to have a research and test validation on the effect of the repeat losing stability during flight on the fatigue life.

Based on the background above, we designed typical stiffened plate test pieces (in Figure 3. 1) in order

[1] AVIC Shenyang Aircraft Design & Research Institute

to conduct a validation on the ability of bearing load after post-buckling and losing stability fatigue of composite stiffened plate. Meanwhile, comparisons between the test results to the results of engineering theoretical computation and to the finite element analysis were performed. The specific structure form of test pieces is a combination of composite skin and cap shape stringers, and the material used in skin and stringers is T300/BA9913 prepreg. The space between stringers is 170 mm, the thickness of skin is 1.75 mm.

Under the axial compression situation, we adopted local buckling load formula to study the orthogonal anisotropy rectangular plate in engineering theoretical computation analysis:

$$N_{xcr} = \frac{2\pi^2 D_{22}}{b^2}\left(\frac{D_{11}}{D_{22}}\left(\frac{b}{a}\right)^2 m^2 + 2\left(\frac{D_{22}+2D_{66}}{D_{22}}\right) + \left(\frac{a}{b}\right)^2 \frac{1}{m^2}\right) \quad (a/b<4)$$

$$N_{xcr} = \frac{2\pi^2 D_{22}}{b^2}\left(\sqrt{\frac{D_{11}}{D_{22}}} + \frac{D_{12}+2D_{66}}{D_{22}}\right) \quad (a/b\geq 4) \qquad (3.1\text{-}1)$$

The formula of overall buckling load:

$$P_{cr} = \frac{P_\varepsilon}{1+\lambda P_\varepsilon/(G\bar{A})} \qquad (3.1\text{-}2)$$

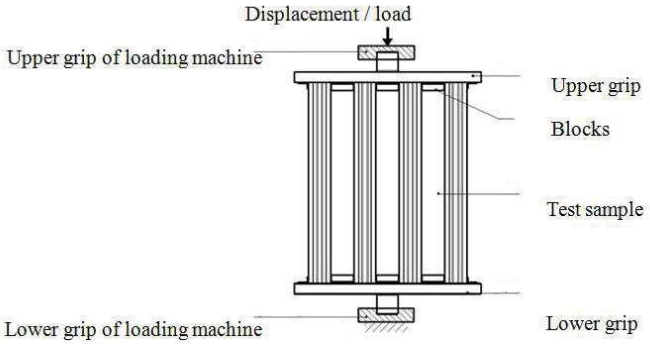

Figure 3. 1 Test on Ability of Bearing Load and Losing Stability Fatigue of Composite Stiffened Plate

The finite element computation adopted the modal method and the improved RIKS arc length method. The calculated results are shown in Figure 3. 2 and Figure 3. 3.

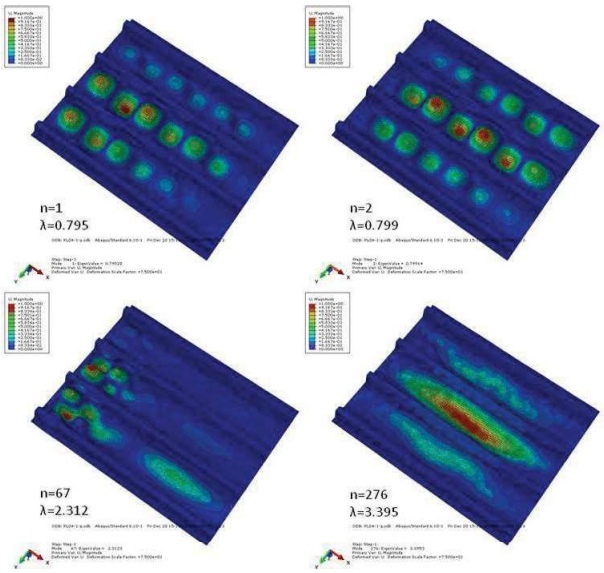

Figure 3. 2 Result of Finite Element Modal Method

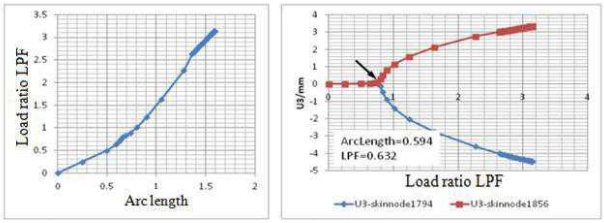

Figure 3. 3 Result of Improved RIKS Arc Length Method

By sorting the results of engineering computation, finite element analysis computation, and test, we got the critical load and failure load, as shown in Table 3. 1.

Table 3. 1 Contrast of Buckling Critical Load and Failure Load of Stiffened Plate

	Engineering computation	Modal method	Improved RIKS arc length method	Static test
Local buckling type	Skin local buckling	Skin local buckling	Skin local buckling	Skin local buckling
Critical load kN	40	139	111	90
Failure type	General buckling	General buckling	Skin bulge and strain transfinite	General buckling
Failure load kN	225	595	396	270
Bearing capacity after post-buckling	82%	77%	72%	66.7%

In Table 3. 1, it is obviously confirmed that the result from engineering computation is relatively conservative, and both the critical load and failure load are less than the ones in static test; Comparing with the result of the finite element analysis, the test result is smaller. The reason is that when the test pieces tend to lose stability, the clamped ends of test pieces are between pinned ends and fixed ends, especially the limitation of the angle. Moreover, the boundary constraints in the finite element analysis are idealized fixed ends.

In the process of fatigue test: first, test load was set as 1.33 times of the local buckling load 120kN, and the fatigue test was carried out until the objective life achieved. At this time, there is no damage occurred in the test pieces. Second, the test load was increased to 135kN, as 1.46 times of the local buckling load. During the fatigue process, also no damage occurred in the test pieces. Therefore, we can manifest the buckling of composite stiffened plate without prefabricated damage has no effect on the fatigue performance. Based on the above analysis, in the future we will carry out a Test on ability of bearing load and losing stability fatigue of composite stiffened plate with different energy and parts damage.

Based on the analysis and test validation, we get the following conclusions:

1) Calibrating the stability of composite stiffened plate in engineering computation is relatively conservative, but it is a safe result;

2) Calibrating in finite element analysis may be dangerous, so an appropriate safety factor is needed to revise it; Buckling of composite stiffened plate without prefabricated damage has no effect on the fatigue performance.

3.2 Fatigue Buckling Evaluation and Post-buckling Analysis of Stiffened Panel on Pure Shear[1]

Thin-walled panels are almost restricted to be used in the state of shear buckling in current aircraft structure design, whereas critical buckling load of aircraft fuselage and wing structure is merely

[1] AVIC Aircraft Strength Research Institute

20%~30% of failure load. If the critical amplitude of structure stability is chosen as a threshold of aircraft structure safety design, it will dramatically lower the material use efficiency. In addition, the inaccuracy calculation of critical buckling load probably puts the structure in the case of fatigue buckling. Consequently, it is necessary to give an efficient method for aircraft panels on fatigue buckling. A fundamental research of aircraft wing thin-walled structure was preceded by US NASA in the 1980s [1], achieving failure mechanism and analytical method for structure subjected to fatigue bending and shear load. Recently, some researchers applied continuum damage mechanics in shear buckling analysis of pure shearing structure, and predicted the fatigue life of crack initiation. Yet complicated FEM calculation limited its engineering application. This paper will provide an efficient approach to the durability evaluation of aero-structures on fatigue buckling. Besides, some references are presented to avoid fatigue buckling in aircraft structure design.

Detail Fatigue Rating (DFR) is a popular method to evaluate the structure fatigue life in engineering application. DFR value dependent on the structure loading form is always an important measurement of structure anti-fatigue capability. Due to the different buckling levels of stiffened panels at different maximum loads, the force forms of the rivets are different. The DFR value is different for the structure panels with different shear loading. In reference [2], we proposed a fatigue buckling evaluation method for pure shearing structure. The DFR basic value was proposed as

$$\mathrm{DFR}_{\mathrm{base}} = \frac{100}{\mathrm{a}+\mathrm{b}\times\tau/\tau_{\mathrm{cr}}} \tag{3.2-1}$$

where τ is the shear stress subjected on panel; τ_{cr} is structure critical buckling load; a and b are the coefficients dependent on material properties which can be determined by experiments in this paper. Based on DFR theory, the fatigue life can be calculated as described in [2].

A new design approach of test specimen was firstly applied to avoid the fatigue damage of noncritical failure of diagonal edged location. We applied the integrated under boarding with boned-riveting connection on skin to strength the weak zone. The feasibility of design could be verified by the coherence of theoretical value and experimental results (in part 3). In addition, we analyzed the critical buckling load and bucking modes adopting Digital Image Correlation (DIC) technology which presented a good agreement with the measurement of traditional strain gauge (Figure 3. 4). In virtue of experimental results of "diagonal tension" test, we illustrated the failure mechanism of fatigue buckling for pure shear panel in 2024 alloy, and found that the critical buckling load was gradually decreasing as the loading cycles increasing, and the variation would be larger after the structure has initial crack. This is the reason why the structure failure earlier than anticipation. Supposing that the DFR value of the structure might be changed with ultimate loads under fatigue buckling, we combined the proposed method (Formula 3.2-1) and the experimental results (when $\tau/\tau_{cr} = 1.56\ and\ 1.83$), then got a=0.686 and b=0.414. The feasibility of this efficient approach has been verified by experiments for structure subjected to pure shear stress (when $\tau/\tau_{cr} = 2.062$). The estimated life (7.8957e4 cycles) is consistent with the experiment result (8.0541e4 cycles), Figure 3. 5is the fatigue buckling failure of structure on pure shear.

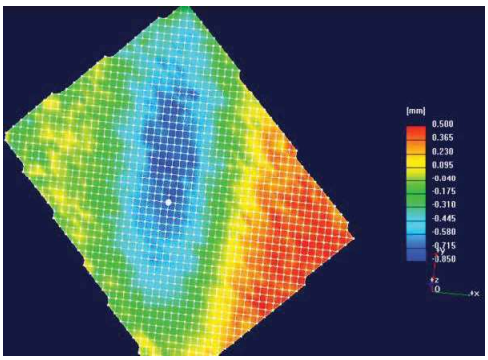

Figure 3. 4 Structure Buckling Mode Measured by DIC

Figure 3. 5 Fatigue Buckling Failure of Structure

The Finite Element Method was applied to analyze the structure buckling and post-buckling load-carrying capability. Comparisons among engineering methods, FEM analysis and the experimental results are presented (Figure 3. 6). The FEM result is in a good agreement with the experimental results, and the analysis predicted failure load is within 7.2% of the test result, which is 19% percent higher than engineering method.

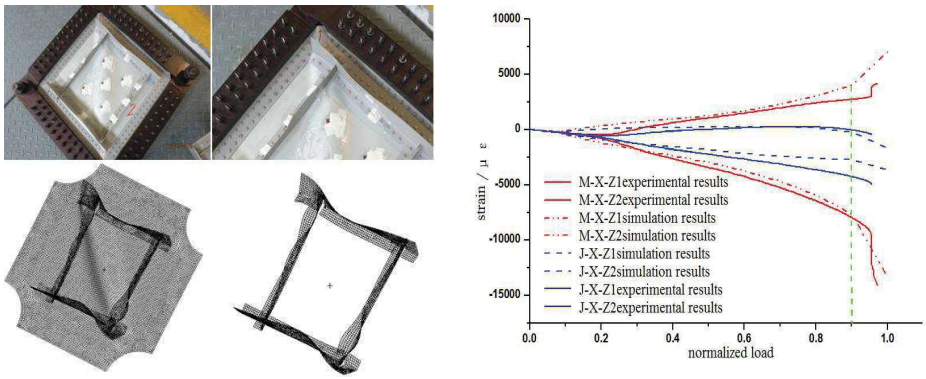

a) Structure Failure Mode on Static Loading b) Strain-Load Results

Figure 3. 6 Comparisons of FEM Analysis and Experimental Results on Failure Mode and Strain

References:
[1] J. Arl-Gur, J.Singer, A. Libai, Repeated buckling tests of stiffened thin shear panels.NASA Report.1982.
[2] J. Bierbaum, P. Horst. Crack propagation in aluminium panels due to shear forced bucking.
[3] Handbook of structure durability and damage tolerance design on civil structure, Aviation industry Press.2003.

3.3 Application of Multi-Axial Fatigue Life Estimation Methods to Aircraft Structural Components[1]

The majority of main load-carrying structures of an aircraft in service are impacted by complex loadings. Thus, the loading conditions of these bearing structures are usually in typical multi-axis stress status. Among them, ratio multi-axis stresses condition is a common one. The estimation of the fatigue life for these structures using traditional single-shaft stress method may cause serious errors. Thus, fatigue life analysis based on the multi-axis fatigue failure principles must be applied in the forecast of the life of these structures.

Three multi-axis fatigue analysis models based on critical plane have been chosen to analyze a typical airframe structure. The result of the analysis has been compared with the result from the method of singe-axis life estimation. The applicability of the critical plane method in such structures has also been discussed.

- Wang-Shang Model

[1] AVIC Shenyang Aircraft Design & Research Institute

$$\left[\Delta\varepsilon_{max}{}^2+\frac{1}{3}\left(\frac{\Delta\gamma_{max}}{2}\right)^2\right]^{\frac{1}{2}}=\frac{\sigma_f^{'}}{E}(2N_f)^b+\varepsilon_f^{'}(2N_f)^C \tag{3.3-1}$$

where, $\Delta\varepsilon_{max}$ is the maximum absolute shear strain between the two closest corners of a zigzag line; $\Delta\gamma_{max}/2$ is the amplitude of the maximum shear strain on the plane of the maximum shear strain; N_f is the fatigue life; $\sigma_f^{'}$、$\varepsilon_f^{'}$ and b are the material constants of strain fatigue, respectively; E is the Young's modulus of the material.

- SWT model

$$\frac{\sigma_{max}^1\Delta\varepsilon_{max}^1}{2}=\varepsilon_f^{'}\sigma_f^{'}(2N_f)^{b+c}+\frac{\sigma_f^{'2}}{E}(2N_f)^{2b} \tag{3.3-2}$$

where, $\Delta\varepsilon_{max}^1$ is the amplitude of the maximum tensile strain; σ_{max}^1 is the maximum tensile stress perpendicular to the plane of the maximum principal stress.

- Morrow-Brown-Miller Model

$$\frac{\Delta\gamma_{max}}{2}+S\Delta\varepsilon_n=A\frac{\sigma_f^{'}-2\sigma_{n,mean}}{E}(2N_f)^b+B\varepsilon_f^{'}(2N_f)^c \tag{3.2-3}$$

where, $\sigma_{n,mean}$ is the mean stress on the plane of the maximum shear strain, A=1.3+0.7S，B=1.5+0.5S，S is the coefficient of the effect of the principal strain; c is a material constant.

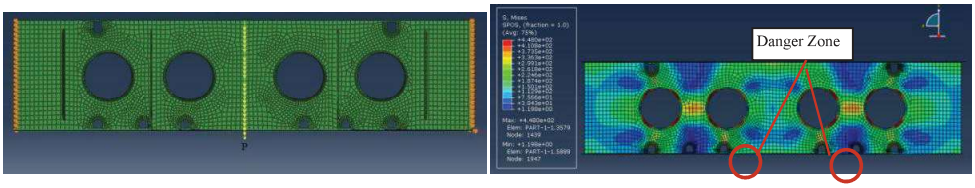

Figure 3. 7 Critical Fatigue Region of The Structure

Figure 3. 7 shows the critical fatigue region of the chosen structure.

Substituting the stress and strain values from these critical points into the Wang-Shang model to perform calculation, we can get the life (N_f) of the most critical point which is 10216 spectrum units.

Through analysis, when the maximum value of the equivalent strain is used, the fatigue life of the structure increases exponentially with respect to the increase of b (see Figure 3. 8 (a)); c has almost the same effect as b on the forecast of the fatigue life (see Figure 3. 8(a)); $\varepsilon_f^{'}$ has a linear relationship with the result of life, and it has a relatively small influence (see Figure 3. 8(b)); $\sigma_f^{'}$ has a exponential relationship with the result of life, but it has a big influence (see Figure 3. 8 (b)). Thus, when measuring the single-axis fatigue coefficient, b, c and $\sigma_f^{'}$should be measured with higher precision. The triangular region in the figure shows the position where the coefficients were obtained in this study case.

Also, substituting the stress and strain values of these critical points into the SWT model and Morrow-Brown- Miller model, we can get similar results. The life values are 23453 and 41157~44671(corresponding with the values of S, 1.8~2.8) spectrum units, respectively.

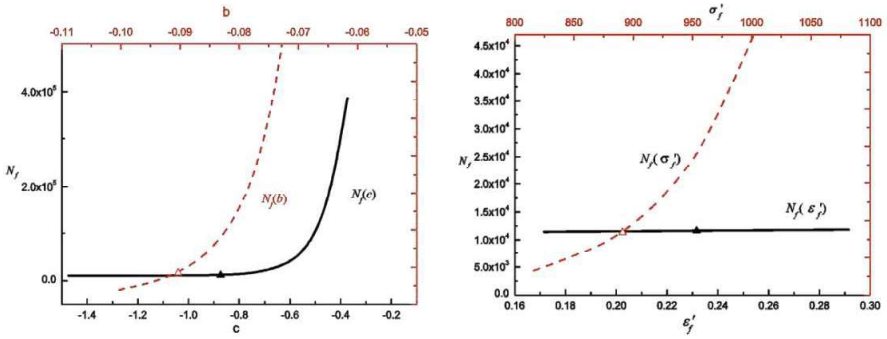

(a) Effects of b and c

(b) Effects of $\sigma_f^{'}$ and $\varepsilon_f^{'}$

Figure 3. 8 Effects of Material Constants on Fatigue Estimation Results (equivalent strain = 5.872×10^{-3})

Figure 3. 9 Test Setup and Specimen

Setting the result of 9631 spectrum units from test (Figure 3. 9) as a base value, we compared and analyzed the forecasting lives got from the three types of multi-axis models. We can find that all of the computational results of the three models are bigger than the base. The best forecast result is from the Wang-Shang model, while the biggest error comes from the Morrow-Brown-Miller model which is bigger than 320% (s=1.8~2.8). If the fatigue life is predicted with the single-axis low-circle fatigue function, called Mason-Coffin function, the predicted life can be given as 342945 units, and then the error will be higher.

According to the comparison between the predicted results and the test results, we can see that, considering the structures under multi-axis loadings, if the life is predicted with the method of single-axis life analysis, there will be a significant error in its result.

Wang-Shang model is applicable in the study of such structures in this paper. The precision of the computational result is engineering acceptable, and the result is better than those from SWT model and Morrow-Brown-Miller model.

A suitable S should be identified when using Morrow-Brown-Miller model in order to get a better computational result. In the case in this paper, the effect of S is not big. But in case of the absence of material coefficients, it will be not convenient for engineering application.

3.4 A Method of Fatigue Quality Determination for Splice Fastener Joints under Multiaxial Fatigue Loading[1]

Splice joints (Figure 3. 10) are most common type of fitting in airframes. These joints are also the primary source of fatigue failure in aircraft [1] and other structures.

In COMAC, a COMAC Fatigue Quality (CFQ) analysis system has been developed based on the experiences gathered from aviation manufacture and the large amount of coupon-level tests. This method is based on the well-established general fatigue theory and supported by large amount of pyramids tests on coupons, components, sub-assembly parts, section-scale and full-scale aircraft with the statistical analysis of the test results [3].

For the splice joint, CFQ is defined as: 1) large samples of test coupons or from a fleet with the typical structure feature under an applied uniaxial cyclic stress (or local reference stress) in a given direction with a given stress ratio 0.06 and maximum stress; 2) the given fatigue life $10^5$with a given reliability 95% and a given confidence 95%. Thus, the maximum applied stress or maximum reference stress is the fatigue quality CFQ of a splice joint in the airframe. The CFQ is often used as a design value to evaluate the fatigue life of aircraft in tests and service. The CFQ_s are commonly provided in two directions: 0 degree, which is orthogonal to the splice joint line, and the fatigue quality is denoted as CFQ_0; 90 degree, which is parallel to the splice joint line, and the fatigue quality is denoted as CFQ_{90} shown in Figure 3. 11 and Figure 3. 12.

[1] COMAC Shanghai Aircraft Design and Research Institute

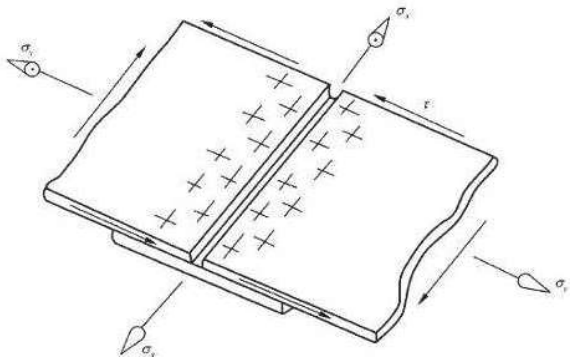

Figure 3. 10 A Typical Splice Joint

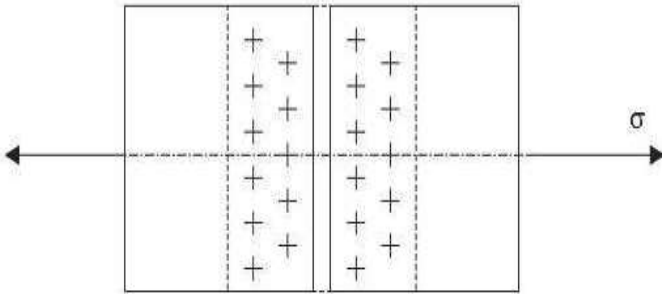

Figure 3. 11 CFQ_0 of A Lap Joint under Fatigue Loading

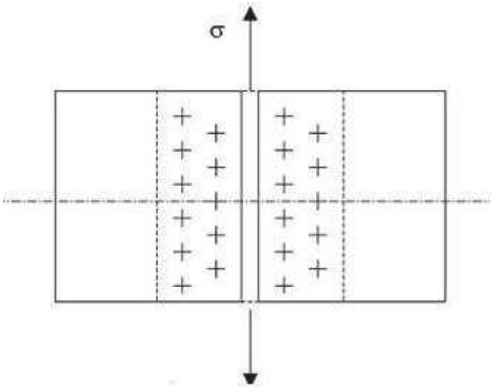

Figure 3. 12 CFQ_{90} of A Lap Joint under Fatigue Loading

For splice joint under general loading shown in Figure 3. 13, the CFQ calculation steps are as follows:

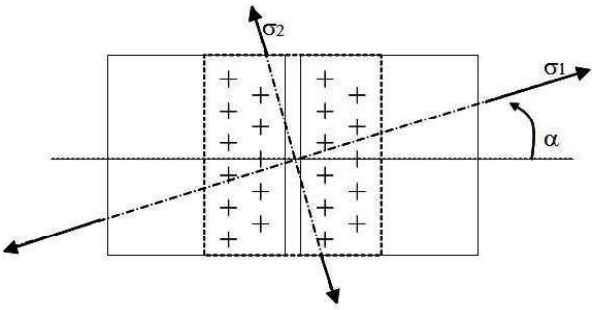

Figure 3. 13 Splice Joint General Case: Biaxial Stress Loading

Step 1: Obtain the fatigue spectrum in the form of local field stress (σ_x, σ_y, τ_{xy}) at the fatigue

calculation point and take the reference stress as, $\sigma_{ref} = max(\sigma_x, \sigma_y, |\tau_{xy}|)$

Step 2: Determine the fatigue qualities CFQ_0 and CFQ_{90} for the given material and manufacturer for the splice joint under the specified loading as shown in Figure 3. 13. Note that neither the fastener load nor secondary bending is considered when CFQ_{90} is determined. Then, we obtain $\gamma = \frac{CFQ_{90}}{CFQ_0}$

Step 3: Calculate two principal stresses and the principal stress angle as follows:

$$\sigma_1 = \frac{\sigma_x+\sigma_y}{2} + \sqrt{\left(\frac{\sigma_x-\sigma_y}{2}\right)^2 + \tau_{xy}^2}\ ,\ \sigma_2 = \frac{\sigma_x+\sigma_y}{2} - \sqrt{\left(\frac{\sigma_x-\sigma_y}{2}\right)^2 + \tau_{xy}^2}\ ,\ \alpha = \tan^{-1}\left[\frac{\tau_{xy}}{\sigma_1-\sigma_y}\right]$$

Step 4： The fatigue qualities CFQ_0^* and CFQ_{90}^* are calculated as

$$CFQ_0^* = \frac{CFQ_0}{1-\frac{\sigma_2}{3\sigma_1}}\ ,\ CFQ_{90}^* = \frac{CFQ_{90}}{1-\frac{\sigma_2}{3\sigma_1}+\frac{|\sigma_2|}{\sigma_1}(\gamma-1)}$$

Step 5: The fatigue quality CFQ_α^* is calculated as $CFQ_\alpha^* = \frac{CFQ_0^*+CFQ_{90}^*}{2} + \frac{CFQ_0^*-CFQ_{90}^*}{2}\cos(2\alpha)$

Step 6: Modify CFQ_α^* based on the chosen reference stress: $CFQ_\alpha^{**} = CFQ_\alpha^* \times \sigma_{ref}/\sigma_1$

Step 7: Calculate the fatigue life using the pre-defined fatigue method, the given spectrum, the obtained fatigue qualityCFQ_α^{**}, and the given SN function form, which includes the R-ratio effect.

Reference:

[1] Niu, M.C.Y., Airframe Structural Design, Chapter 7, 1988.
[2] Dong D., Cui D. and Chen X. A Review of Aeronautical Fatigue and Integrity Investigations in China (June 2008 – May 2015), ICAF 2015.

3.5 Research on Fatigue Behavior and Fatigue Mechanisms of Martensite Stainless Steel FV520B[1]

Martensite stainless steel is one of the most widely used materials for kinds of blade manufacturing (such as aero-engine and centrifugal compressor) due to its high strength, good corrosion resistance and perfect welding performance. As a consequence, martensite stainless steel is an attractive option in aircraft structural design.

Table 3. 2 Heat Treatment Process

Heat Treatment	Conditions	Holding time
Solution Treatment	1050±10℃, air cooling	1.5-2.5h
Refining Treatment	850±10℃, oil cooling	1.5-2.5h
Aging Treatment	480±10℃, air cooling	2.0-3.0h

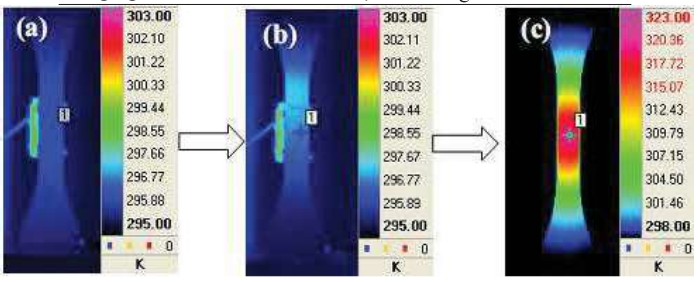

(a) 565MPa; (b) 833MPa; (c) 972Mpa

Figure 3. 14 Temperature Maps During Tensile Process

Experimental tests have been carried out for the purpose of studying the effects of heat treatments on the microstructures and mechanical properties of martensite stainless steels. The heat treatment procedures for different martensite steels is presented in Table 3. 2. During the static tensile test, an infrared camera was used to monitor the variation of the surface temperature field so as to assess the damage evolution process in real time. The thermal maps during the static loading process are shown in

[1] AVIC Aircraft Strength Research Institute

Figure 3. 14. Figure 3. 15 provides the relationships between the loading time to the temperature signal and the tensile stress.

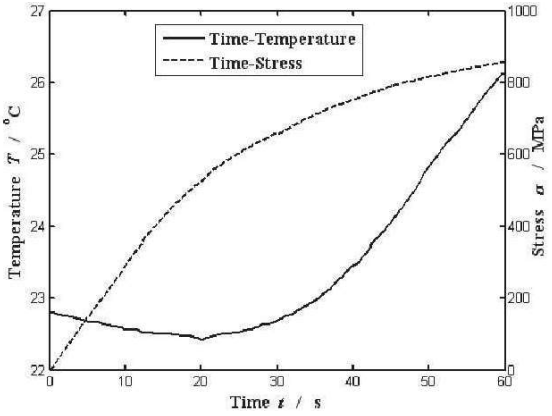

Figure 3. 15 Relationships between Loading Time to Temperature Signal and Tensile Stress

And based on the self-heating phenomenon, the fatigue limits of the original and heat-treated martensite steels were experimentally evaluated by using infrared thermographic technology. Accordingly, Figure 3. 16 gives the evaluated fatigue limits of the two kinds of martensite steels. Good agreements were achieved between the evaluated values and those obtained by the traditional fatigue testing method. In order to qualitatively analyze the relationship between the temperature field variation and the internal microstructrual evolution the surface temperature variation was also recorded by the infrared camera during the fatigue tests. Figure 3. 17 shows the temperature field evolution in several different stress levels until the specimen was fractured

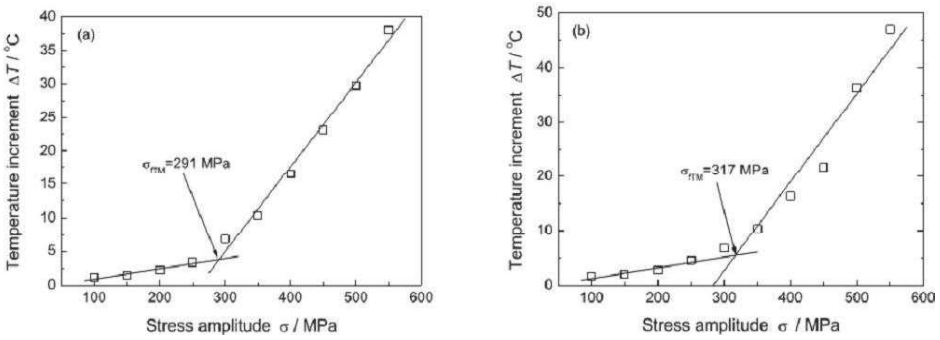

Figure 3. 16 Predicted Fatigue Limits by Thermographic Method

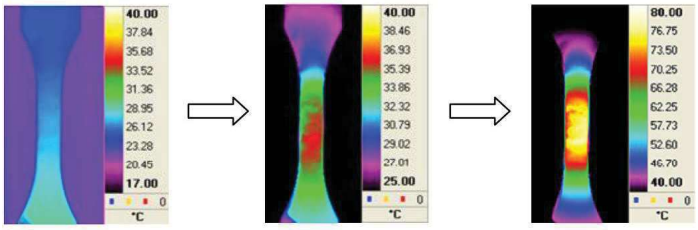

(a) 150MPa; (b) 350MPa; (c) 550Mpa

Figure 3. 17 Temperature Evolution for Different Stress Levels

The scanning electron microscope (SEM) was applied to observe the fatigue fracture surface for getting more detailed information about the fatigue crack initiation and propagation mechanisms. It is found that the fatigue microcrack initiating from the corner of the specimen surface is because of the stress concentration there. Figure 3. 18 presents the morphology of the fracture surface.

The metallographic analysis shows that the mechanical property improvement of the martensite steel is attributed to the formation of the fine tempered martensite along with the secondary phase particles

uniformly distributed at the grain boundary. Figure 3. 19 shows the microstructures of the original and heat treated steels, respectively. The present research work provides valuable and prospective material properties of martensite steels. This is quite important for the material selection during the aircraft structure design process.

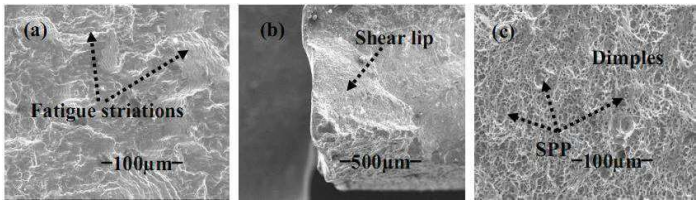

(a) Fatigue Striations; (b) Shear Lip; (c) Dimples

Figure 3. 18 Morphologies of Fracture Surface

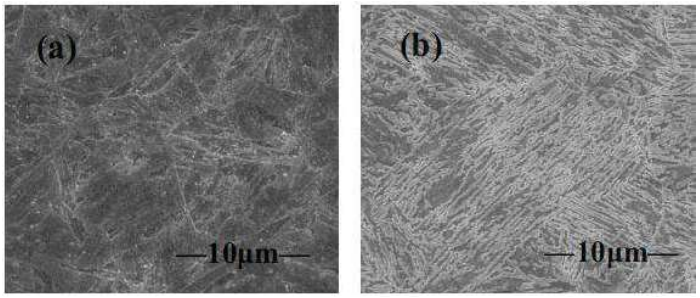

(a) Original Steel; (b) Heat-Treated Steel

Figure 3. 19 Microstructures

Acknowledgements

The work was sponsored by National Natural Science Foundation of China (contract No. 51601175 and 11602237).

3.6 Fatigue Assessment Based on Fatigue Thermography[1]

It has always been a challenge and hard problem to study the fatigue behaviour and failure mechanisms of engineering structural materials. Generally, because of the scatter characteristics of the materials it needs a large quantity of fatigue testing work to determine the fatigue parameters of materials. For the high-cycle and very high-cycle fatigue, the traditional fatigue test has fatal limitations, such as costly and time-consume. This is the bottleneck problem for the research and development of new structures and new aircraft models. As known, the energy dissipation process is actually responsible for the fatigue process. As a consequence, the researchers start to carry out scientific work based on fatigue energy theory.

Fatigue Behaviour Evaluation of Materials

The fatigue evolution process is actually the process of energy dissipation. It is an experimental fact that the surface and internal temperature signal of the material will simultaneously vary during the process. As a result, it is possible to predict the fatigue limit and fatigue life of materials based on the limiting energy theory. The model for fatigue limit prediction is:

$$\begin{cases} \Delta T_s = 0; & \sigma_a < \sigma_0 \\ \Delta T_s = A\sigma_a^2 + B; & \sigma_a > \sigma_0 \end{cases} \tag{3.6-1}$$

The theoretical model for fatigue life prediction is:

$$N_f = \frac{\Phi}{\Delta T_s} \tag{3.6-2}$$

[1] AVIC Aircraft Strength Research Institute

Figure 3. 20 a) presents the predicted result of the fatigue limit based on the temperature increase. Figure 3. 20 b) shows the fatigue S-N curve predicted by the energy theory. It is concluded that the predicted result is in good agreement with the traditional fatigue S-N curve.

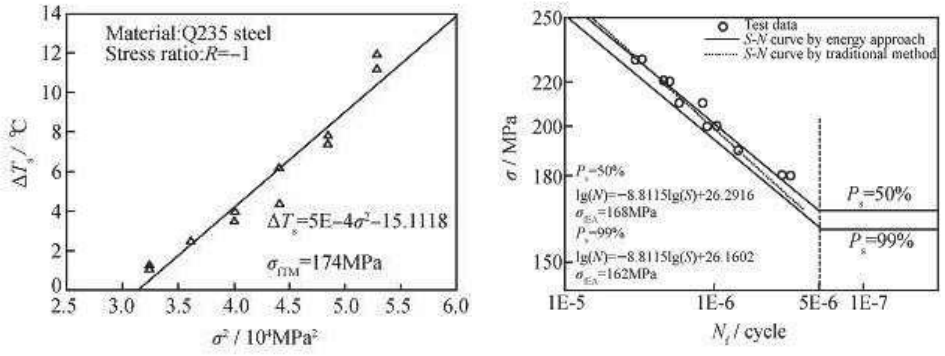

a) Predicted Fatigue Limit b) Predicted S-N Curve

Figure 3. 20 Predicted Results

Fatigue Behaviour Evaluation of Welded Joints

Similarly, the thermograph approach can be used to predict the fatigue parameters of welded joints, as shown in Figure 3. 21. Figure 3. 22 give the fatigue S-N curves by means of the traditional fatigue testing method and the energy theory. It is also concluded that fatigue thermograph gives insight into the rapid prediction of fatigue behaviour.

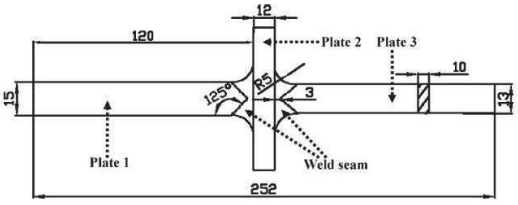

Figure 3. 21 A Welded Joint

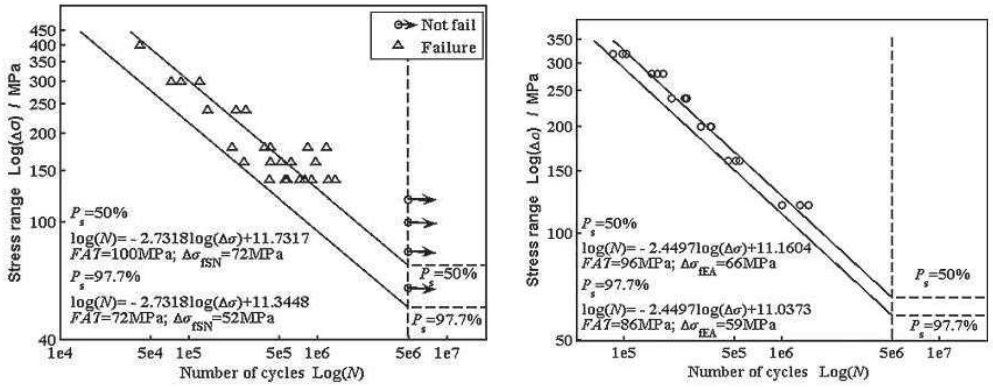

a) Traditional Result b) Predicted Result

Figure 3. 22 Results Respectively by Traditional method and Energy Theory

Thermo-Elastic Stress Evaluation

The lock-in thermograph is employed to analyze the stress concentration effect around a blind hole. According to the thermo-elastic stress theory, the fatigue notch coefficient is calculated as:

$$K_f = \frac{\sigma_{sf}}{\sigma_{df}} \tag{3.6-3}$$

Figure 3. 23 shows the stress distribution around the blind hole captured by the infrared camera. It is obviously found that the stress value perpendicular to the loading direction is the maximum principal stress. In Table 3. 3, the results calculated by the finite element method, thermo-elastic method and lock-in thermograph are compared. It is concluded that the developed method based on the thermo-elastic stress evaluation enables us to predict the fatigue notch coefficient accurately.

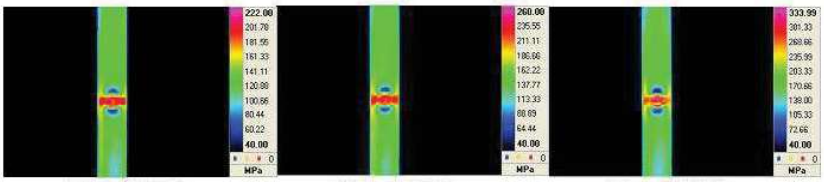

Figure 3. 23 Stress Distribution around Blind Hole

Table 3. 3 Comparison of fatigue notch coefficient

Depth / mm	FEM	TSA	LT
0.9	1.43	1.31	1.13
1.8	1.61	1.49	1.33
2.7	1.69	1.59	1.49

3.7 Study of the Influence of Different Damage Forms on Canopy PMMA Fatigue Life[1]

PMMA (Polymeric Methyl Methacrylate) is widely used in the airplane canopy. In outfield, the PMMA undertakes different damage forms, including scratching, collision and crazing etc. All of these damage forms will influence the carrying capacity and fatigue life of airplane canopy, and even lead to security risks. Based on this situation, it is necessary to carry out fault analysis for the PMMA structure with different damage forms. According to the previous research result, scratching is a representative damage form for airplane canopy, so in our work we take scratching damage as an example. The works are listed as follows:

1) The fatigue experiment of the PMMA with scratching

The fatigue experiments were carried out for the PMMA with the different scratching depths, including 0.1mm, 0.2mm, 0.3mm and 0.4mm. As a result, the S-N curves of the PMMA have been determined. The results with different scratching depths are shown in Table 3. 4 and Figure 3. 24.

Table 3. 4 Fatigue Experiment Results for Scratching Depths of 0.1mm and 0.2mm

Stress level (MPa)	Scratching deepth	number	width(mm)	thick(mm)	Max load (kN)	Life(cycle)
52.5	0.1mm	2-12	20.02	9.47	9.953	3291
		4-107	19.85	9.33	9.723	7952
50	0.1mm	4-94	20.05	9.07	9.093	5064
		4-42	19.84	9.13	9.057	50000
	0.2mm	4-68	19.83	9.34	9.261	2442
		4-15	19.99	9.20	9.195	7701
		4-108	19.93	9.53	9.497	5326

[1] AVIC Shenyang Aircraft Design & Research Institute

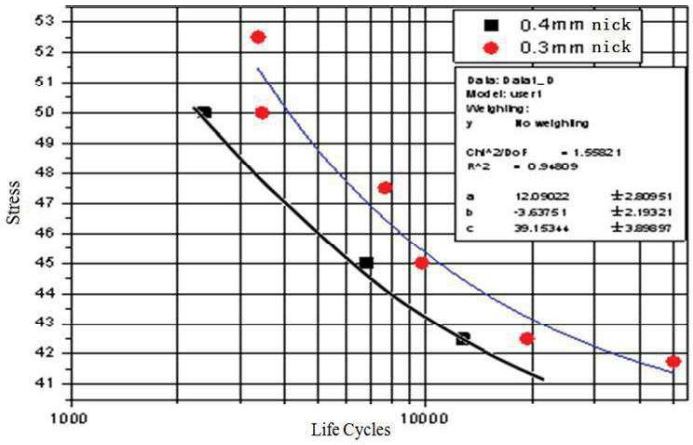

Figure 3. 24 S-N Curves for the Scratching Depths of 0.3mm and 0.4mm

Through the comparison of fatigue properties of the PMMA with the different scratching depths, the results of the experiment show that the scratching depth less than 0.2mm has no impact on the fatigue properties, but the scratching depth of 0.4mm will reduce the fatigue strength of the PMMA. And the impact of the scratching depth on fatigue life is obvious.

2) Stress spectrum confirmation

"PATRAN" was used to create a FEM for an airplane canopy (Figure 3. 25), and MPC was used to simulate the flexible attachment between the PMMA and frame. On this basis, by combining thermal stress and pressure stress, the effect on the canopy plexiglass was analyzed.

Figure 3. 25 FEM Model of The Airplane Canopy

3) Fatigue life analysis of the PMMA

After the colligating analysis to the experiment data, we can deduce the S-N curves of structures with different scratching damage forms. Then we will analyze the fatigue life of the PMMA using the way of Miner theory based on the S-N curves and stress spectrum.

Through the study and theory analysis, we validated the impact of scratching damage to fatigue life of the PMMA. Then we can provide the data reference and set up repair standards for the airplane canopy.

3.8 Research on Acoustic Fatigue Analysis Method for Typical Civil Aircraft Structure[1]

During the period of the aircraft's service life, acoustic fatigue damage may occur in some parts of civil aircraft due to the strong noise environment. Therefore, acoustic fatigue problem is one important term in civil aircraft airworthiness examination. In this paper, four kinds of engineering analysis method were employed in studying the acoustic response and fatigue characteristics of the typical commercial skin-stiffener aircraft structure. Then the predicted results (Figure 3. 26 and Figure 3. 27) from engineering methods for both skin and stringer were compared with the results calculated by finite

[1] COMAC Beijing Aeronautical Science & Technology Research Institute

element method (FEM). In regard to typical civil aircraft skin, the engineering results of root mean square (RMS) stress and acoustic fatigue life calculated using Nomograph method and AGARD method are in good agreement with the FEM prediction results. Whereas, the prediction results of DSR method and MBB method are not in good agreement with the FEM results. Also, the differences of sonic response stress among all the methods mentioned before are growing with the increase of the sound pressure level. However for the stringer, the predicted results of root mean square (RMS) stress and acoustic fatigue life by means of DSR method are very close to the FEM results, but the calculation results of Nomograph method and AGARD method are of great difference from the FEM results. It is concluded that different engineering analysis method is suitable for specific aircraft structure type. For a given structure, one method is only fit for estimating the acoustic fatigue life of a specific part of the structure.

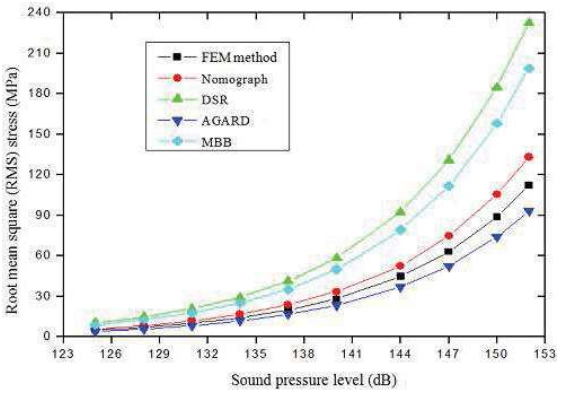

Figure 3. 26 Root Mean Square (RMS) Stress of Skin at Different Sound Pressure Level

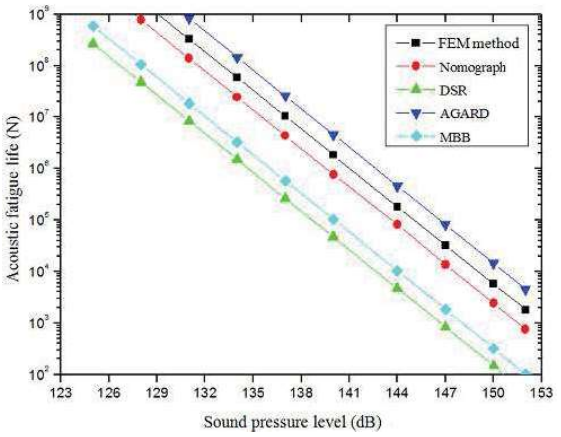

Figure 3. 27 Acoustic Fatigue Life of Skin at Different Sound Pressure Level

3.9 Failure Analysis and Test of the Composite Elevator Trailing Edge Structure[1]

Composite elevator is an important part of the aircraft structures. Safety performance of the aircraft has always been a concerned problem. The trailing edge of the composite elevator is subjected to the combination of the bending and shear load coming from the aerodynamic and inertia load, which may lead to much more complicated failure mode of the trailing edge.

The working performance and bearing capacity of the composite elevator are determined by the weakest part of the structure. Thus all the strength of the parts (such as the joint strength of the trailing edge, the local strength of the honeycomb sandwich structures, the buckling strength of the skin panel, etc.) are needed to be accurately evaluated and estimated. Because the joint of the trailing edge is under

[1] Shanghai Jiao Tong University

the out of plane load condition, the rivets of the joint have the tendency to be pulled out, which may cause the failure of the whole composite elevator. Many researchers have presented some important achievements about the pull out strength of the joints of composite structures by both numerical analysis and test validation.

Our experiment shows that the pull out strength is more critical than the in-plane strength for the joint connections of the composite structures, especially, when the thickness of the skin is very small. It seems that the critical load is very low if regarding the pull out strength as principle criterion. However, if the upper and lower skin could buckle before the load reached the pull out load of the rivet, the joint will be safe. And after unloading, the structure can recover to the original state. Actually, the loads will redistribute when the skin reaches the critical buckling load. The ribs will undertake most of the out of plane load which is undertaken by the skins before. This design concept is used in the fuselage panel which allows the skin being buckling even the load is very low.

The elevator is constructed with the aramid honeycomb sandwich being the upper and lower skin, and a set of ribs extending between the upper skin and lower skin. To avoid the joint disadvantages of sandwich structures, the honeycomb is vanish in the trailing edge area by tapering technology and the skins are turning to one laminate. See Figure 3. 28.

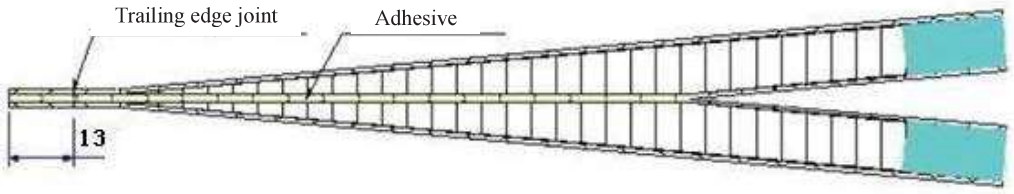

Figure 3. 28 Structure of Trailing Edge Joint of Composite Elevator

A pull-off strength experiment was conducted on six kinds of elevator trailing edge of honeycomb sandwich structure in different sizes. One kind is with one rivet and the other kinds are with two or three rivets, respectively. Considering different bending loads two different locations were chosen for the load points. The digital image technology was used to obtain the deformation of the trailing edge and a pair of load cells was used to get the load value of both sides. Figure 3. 29 gives the buckling and failure modes of the different types of specimens.

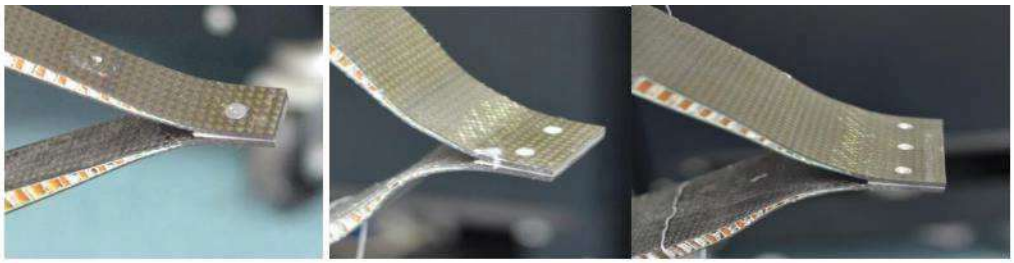

Figure 3. 29 Buckling and Failure Modes of Different Types of Specimens

Furthermore, a series of static strength tests was performed on the trailing edge of the composite elevator box. Figure 3. 30 illustrates the composite elevator box test of both pull out loading and bending loading.

(a) Pull-Out Loading (b) Bending Loading

Figure 3. 30 Test Installation of Composite Elevator Box

A three dimensional model, with progressive damage failure and the contact between the rivet and the composite laminate, was conducted. The failure load calculated by FEM agrees well with the experimental data which can provide reliable basis for design and retrofit for the structure strength of composite elevator structure. Figure 3. 31 illustrates the progressive failure mode of the joint hole of the trailing edge. Figure 3. 32 presents the stress distribution of the rivet-joint of the structure.

Figure 3. 31 Progressive Damage Process of Joint Hole

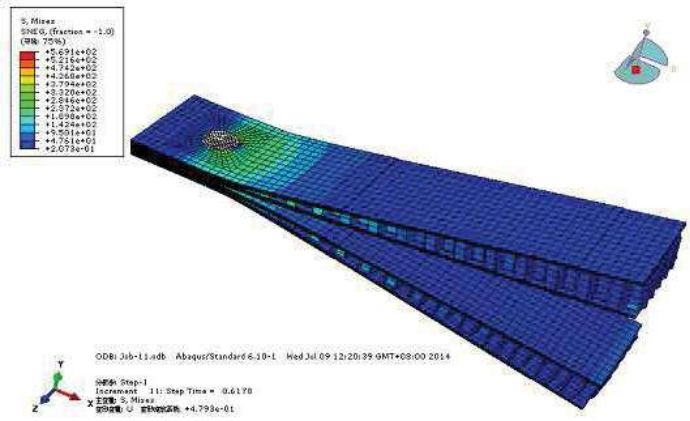

Figure 3. 32 Stress Distribution of Rivet-Joint Structure

Finite element simulation of the deformation conditions accords well with the experimental result. The result from analysis shows that bending failure of the upper and lower panel leads to the failure of the bearing capacity of the whole structure. It also tells that the rigidity of the upper and lower panel has a great influence on the load transmitting. The thickness of the composite plate of the upper and lower panel has a great impact on the stiffness. Flexible panel design can improve the efficiency of the structure because it can increase and redistribute the load path by allowing the skin to be buckling with the load. This conclusion can give a reference for optimization analysis of the sickness of upper and lower wall-board plate on the elevator box.

3.10 A Novel Composite-Metal Joint and Its Mechanical Performance and Fracture Behavior[1]

Introduction

The wide use of composite materials in aerospace increases the demand of more efficient and effective joining technologies between composites and metal [1]. Generally speaking, there are mainly three approaches to join the composite and metallic materials: mechanical fastening, adhesive bonding and a combination of both (Hybrid joint) [2]. Bolted joints are commonly used in primary loading structures since they are more reliable and robust, which can meet the damage tolerance design requirements of modern aircraft. However, the low stress relief ability of the composites and the high stress concentration around the fastener holes limit the joint efficiency. The fasteners also add weight to the joint. Comparing with bolted joints, adhesive bonding preserves the adherent's strength as far as possible and adds almost no additional weight to the structure. Furthermore, it can maintain smooth aerodynamic surfaces at the same time. But it is prone to crack at both ends of the joint in the presence of peel and out-of-plane shear stresses. The hybrid joint takes advantage of the both aforementioned methods, but also inherits the shortcomings of them. To overcome the shortcomings of the traditional joint approaches, a novel joint method, which can reinforce the joint in through-the-thickness direction has been developed and proposed in this study. The mechanical performance and fracture behavior of the joint also were investigated by both experimental and numerical methods.

Specimen Description

The geometric feature and dimensions of the single-lap composite-steel joints with twelve pins is shown in Figure 3. 33. The diameter of all the pins is 0.8 mm and their locations are also illustrated in Figure 3.28. The thickness of the steel plate is 3 mm. The CFRP plate is made of CYCOM carbon fiber/epoxy composite laminate, whose nominal cured ply thickness is 0.188 mm and stacking sequence is $[\pm 45/0/90]_{2s}$. The 0◦direction of the laminate is coincident with the length direction of the adherents and the thickness direction of the laminate is coincident with the thickness direction of the joint plates. The epoxy adhesive used to bond the two adherents together is Hysol EA9696 which is produced by Hexcel Company.

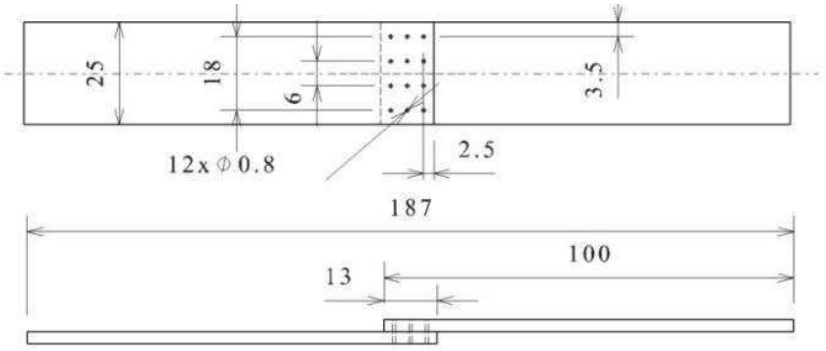

Figure 3. 33 Geometry and Dimensions of Single-Lap Joint (all dimensions in mm)

Test Setup

The specimens were tensioned by a MTS Landmark electron–hydraulic servo-controlled material testing machine (MTS-SANS 5305) in accordance with the American Society for Testing and Materials D5868[3]. Both the extensometer and digital image correlate (DIC) technology were used to measure the strain.

[1] Shanghai Jiao Tong University

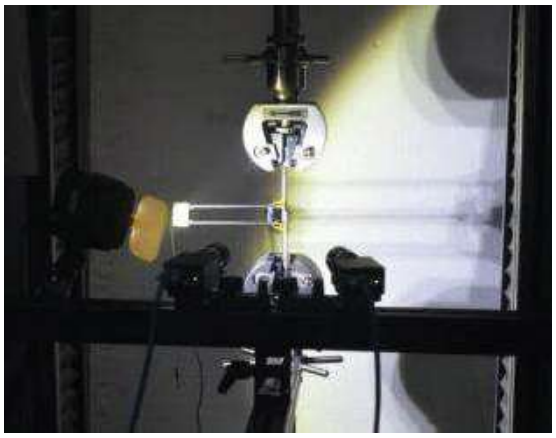

Figure 3. 34 Test Setup

Result analysis

The results of the specimens and the bonded specimens are described in Figure 3. 33 and the specimens with the similar features but without pins are illustrated in Figure 3. 34.

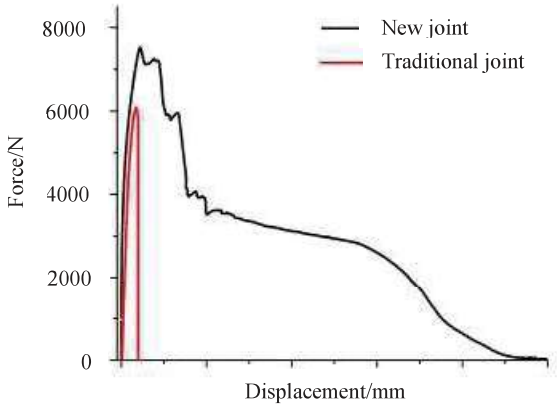

Figure 3. 35 Load-Displacement Test Results of The Dew Joint and Tranditional Bonded Joint

From the Figure 3. 35, it can be seen that the strength of the new joint is about 1.2 times of the traditional adhesive bonded joints'. The energy-absorption ability of the proposed joint is much higher than the traditional bonded joint.

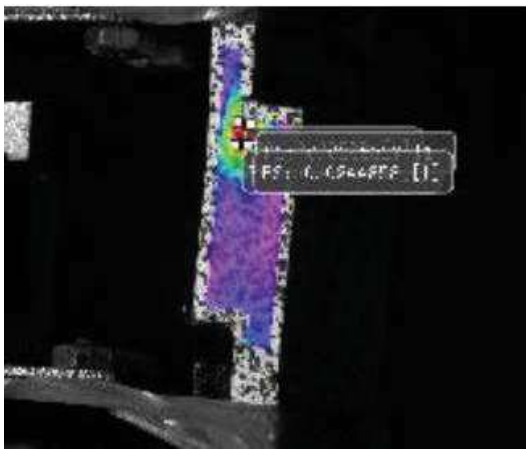

Figure 3. 36 DIC Result of Novel Joint at the Time of Crack Initiation

A nonlinear three-dimensional finite element model was constructed using the commercial finite element code, Abaqus/standard, which is shown in Figure 3. 37. The crack process of the joints was analyzed. The novel joint developed in this paper shows an advantage over bolted and bonded joints as the damage tolerance and durability performances are concerned.

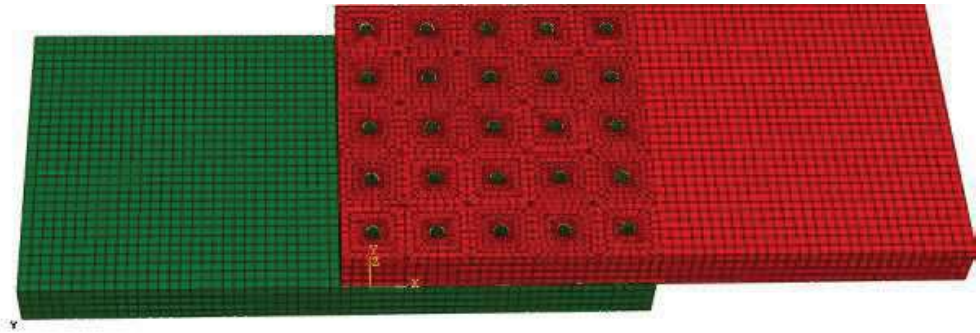

Figure 3. 37 The Finite Element Model of the Joint

Acknowledgements

The work was sponsored by Natural Science Foundation of Shanghai (14ZR1422500).

References:

[1] S. Stelzer, S. Ucsnik, G. Pinter. Fatigue behaviour of composite-composite joints reinforced with cold metal transfer welded pins. Int. J. Fatigue 2015; 81:37-47

[2] P.N. Parkes, R. Butler, J. Meyer, A. de Oliveira. Static strength of metal-composite joints with penetrative Reinforcement. Compos. Struct. 2014; 118:250-256

[3]ASTM International, ASTM D 5868. Standard Test Method for Lap Shear Adhesion for Fiber Reinforced Plastic (FRP) Bonding, West Conshohocken, 2014.

3.11 Reliability Life Evaluation Method of Roller Wheel Based on Contact stress[1]

Flap motion mechanism is an essential part for the high-lift system of aircraft. The safety of the motion mechanism directly affects the normal function of aircraft. Catastrophic accidents may happen if it is not designed and verified properly. As a main part of the motion mechanism, the dominant failure mode of the roller and sliding rail system is the abrasion. This will reduce the motion accuracy and structural strength, and may lead to the stagnation or even functionality failure of the motion mechanism. It is shown that plenty of accidents are due to the abrasion of the roller and sliding rail system. Therefore, in the present work, the flap roller and sliding rail system in civil aircraft was tested. Hereafter, contact stress was derived by Hertz theory, and then it was integrated into Archard cumulative damage models. Accordingly, a contact fatigue model was developed.

Furthermore, a statistical method was applied based on the contact fatigue model. A kind of reliability evaluation method of fatigue life was proposed and also verified by experiments. This research will give a theoretical support for the replacement and maintenance of complex kinematic machines.

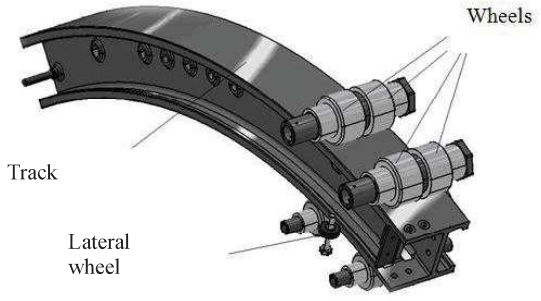

Figure 3. 38 Wheel and Track

[1] AVIC Aircraft Strength Research Institute

The research idea can be described as below:

Step 1: obtaining the contact stress and the contact face width based on Hertz theory;

Step 2: building the abrasion model according to Archard/ Miner theory;

Step 3: introducing probability theory and calculating the Roller wheel's reliability life by Monte Carlo method

Step 4: experimental verification.

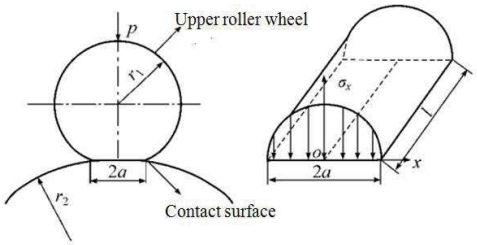

Figure 3. 39 Contact Model in Hertz Theory

3.12 The Reliable Life Evaluation of Aircraft Structure Details[1]

It's important to determine the reliable life of aircraft structure details on which the fatigue cracks are always initiated. However, there are a few of the same details, especially with fatigue cracks. In such a case, the life estimation method is studied based on the normal information diffusion estimation and the grey system theory by taking the randomicity of crack propagation into account.

Parameters Determination of Weibull Distribution

The principle of information diffusion can benefit the understanding of the population of the random variables, so the law as shown in formula (1) will improve the accuracy of cumulative failure distribution estimation in a few samples. Assuming that the detail life follows the three-parameter Weibull distribution, the simulation result in Figure 3. 40 shows that the results estimated by normal information diffusion estimation are pretty better than ones by mean rank formula. And then dealing the samples with gray system theory will determine the parameters of the distribution.

$$\widehat{F}(x) = \int_{-\infty}^{x} \frac{1}{\sqrt{2\pi}nh} \sum_{i=1}^{n} exp\left[-\frac{(x-x_i)^2}{2h^2}\right] \quad (3.12\text{-}1)$$

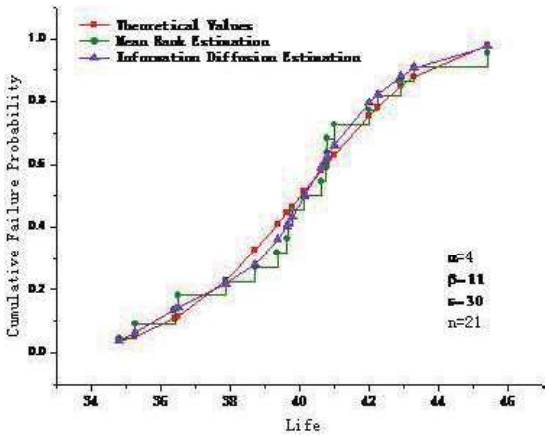

Figure 3. 40 Estimatied Results of Weibull Distribution by Different Means

[1] AVIC Aircraft Strength Research Institute

The Reliable Life Estimation Method of Details

The following crack growth model is used for estimating the life time.

$$a(t) = a(0)exp(Qt) \tag{3.12-2}$$

Where $a(0)$ is the equalent initial flaw size (EIFS) which is a random variable following the Weibull consistent distribution; Q is also a random variable following the logarithm normal distribution and a parameter which is a function of the loading spectra, structural and material properties, etc.. The two distributions can be determined by the fractographic data. Then the expression of reliable life can be obtained as follow:

$$\begin{aligned} R(t) &= 1 - \int_0^{\infty} F(t|Q=q)\cdot f_Q(q)dq \\ &= 1 - \frac{1}{\sqrt{2\pi}\sigma} < \int_0^{Q_c} \frac{1}{q} exp\left[-\frac{1}{2}\left(\frac{lnq-\mu}{\sigma}\right)^2\right] dq \\ &\quad - \int_{Q_c}^{\infty} \frac{1}{q} exp\left\{-\left[\frac{qt+ln(x_u/x_e)}{B}\right]^{\alpha} - \frac{1}{2}\left(\frac{lnq-\mu}{\sigma}\right)^2\right\} dq > \end{aligned} \tag{3.12-3}$$

Where Q_c is a parameter related to x_e and x_u , which are respectively the critical crack length and the upper bound of $EIFS$.

The estimation method developed above is applied to the aircraft structure with 13 damaged stringers in the center wing-box. Figure 3. 41 and Figure 3. 42 respectively show the crack and the fatigue fracture morphology of one damaged stringer. The estimation result is consistent with the experiment.

Figure 3. 41 Crack of Stringer

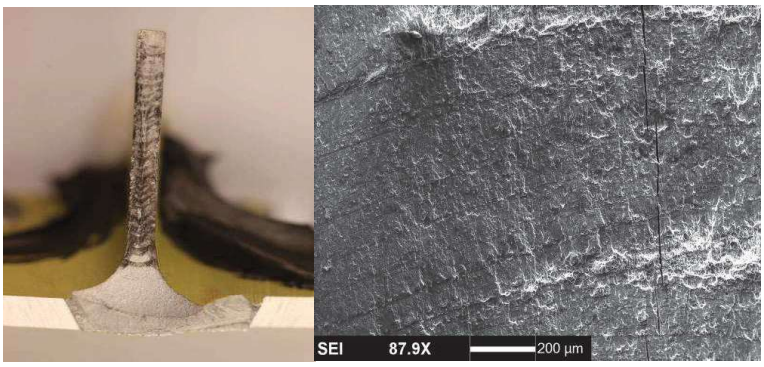

Figure 3. 42 Morphology of Fatigue Fracture

3.13 Risk Assessment of Multiple Site Damage (MSD) Fuselage Lap Splices[1]

Parts of the research results by Civil Aviation University of China on Widespread-Fatigue Damage (WFD) were introduced, which mainly concentrated in risk assessment of multiple-site damage in fuselage lap splices, including:

[1] Civil Aviation University of China

1. Based on the theory of statistics in fatigue and fracture mechanics as well as the existed experimental results, A quantitative analysis method on the occurrence probability of multiple site damage was developed. In different failure modes, the reliability model showed different failure probability characteristics, which proved that the accuracy of quantitative analysis method depended on the failure mode assumed.

2. Referring to the fuselage lap splices of Boeing 737, a simplified model was established by ANSYS. Applying the crack propagation modeling software FRANC3D, the stress intensity factors of crack tips in MSD were calculated. Through changing the initial crack condition, it calculated the stress intensity factor of three kinks of crack mode, which are included crack of hole edge, crack to crack and connecting crack. And the influence of three conditions on the stress intensity factor at the crack tip was analyzed.

3. Based on the combination method to calculate stress intensity factor on the crack tip, this article analyzed the probability of occurring WFD on collinear porous wall through combining the probability method of simulating crack initiation and deterministic method of crack propagation.

4. Based on the database of stress intensity factor, a calculation program of crack propagation was developed to simulate the crack propagation of MSD. The crack propagation life can be obtained under different initial crack condition.

5. Six test pieces of longitudinal lap splices were tested under fatigue loading. Experiment data involved the life of crack initiation, the length of initial crack, the position of crack initiation and the length of crack. The behavior of MSD crack propagation in testing process was analyzed. At last, the reliability of fatigue life based on the test data was achieved.

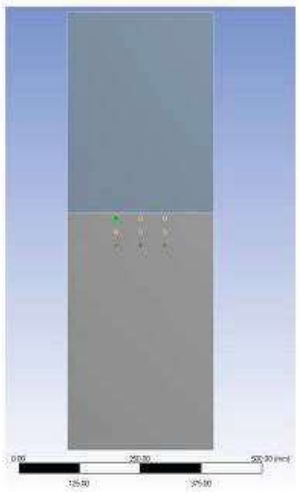

Figure 3. 43 Finite Element Model of Riveted Lap-Joints

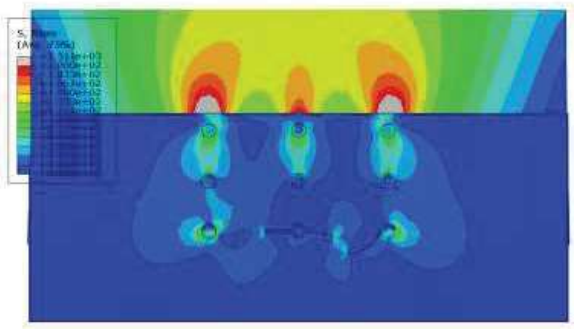

Figure 3. 44 Crack Propagation Result

Figure 3. 45 Multiple-Site Damage in Riveted Lap-Joints Experiment

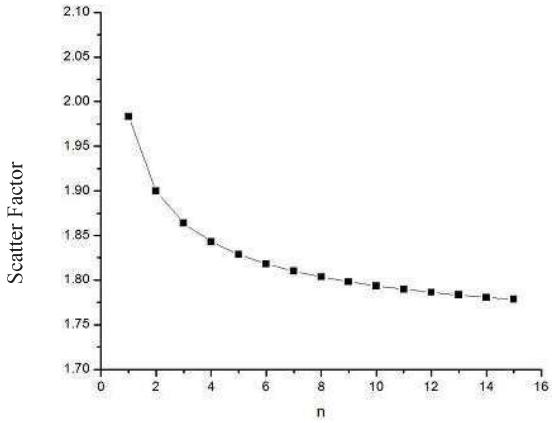

Figure 3. 46 Experimental Results Analyzed by Fatigue Life Scatter Factor Method

References:

[1] Cartwright D J, Rooke D P. Approximate stress intensity factors compounded from known solutions[J].Engineering Fracture Mechanics, 1974, 6(3): 563-571.
[2] M Liao, Y Bombardier, G Renaud, N Bellinger. Advanced damage tolerance and risk analysis methodologies and tools for aircraft structures containing multiple-site and multiple-element fatigue damages[J]. Proceedings of the Institution of Mechanical Engineering, Part G:Journal of Aerospace Engineering, 2001(29):1412-1423.
[3] Ripudaman Singh, Jai H.Park, Satya N. Atluri. Growth of Multiple Cracks and Their Link up In a Fuselage Lap Joint[J].AIAA JOURNAL, 1994, 32(11)：2260-2268.
[4] Lucas F.M. Silva, J.P.M. Goncalves, F.M.F. Oliveira, P.M.S.T. de Castro. Multiple-site damage in riveted lap-joints: experimental simulation and finite element prediction[J]. International Journal of Fatigue, 2000, 319-338.
[5] Mayville R A, Warren T J. A Laboratory study of fracture in presence of lap splice multiple site damage[J]. Atluri Sampath, Tong (Eds), Structural integrity of aging airplanes. Berlin Heidelberg: Stringer Verlag, 1991: 263~273.

3.14 Stress Intensity Factor Solutions to Edge Hole Cracks Emanating from Multiple Colinear Hole[1]

Introduction

Multiple site damage (MSD) has been a great threat to the aircraft safety. One of the most significant accident related to MSD is the fuselage failure of Aloha 737 on April, 1988[1-2]. To prevent such failures, procedures for maintaining the structural integrity of aging aircraft have been established [3]. However, on April 1, 2011, a 15 years old Boeing 737 of United States Southwest Airlines experienced a rapid depressurization in flight caused by MSD [4]. These accidents call for advanced methods for analyzing structures with MSD. An accurate, efficient and versatile method, the weight function method (WFM), was used and further developed by the present authors Xu and Wu[5-8] to obtain the stress intensity factors (SIF), crack opening displacements (COD) and residual strength of panels with multiple collinear cracks. In this paper, the weight function is used to study two typical crack configurations, periodic collinear edge hole cracks and arbitrary small cracks emanating from collinear holes. These two crack configurations are ideal representations of riveted hole cracks in the aircraft fuselage as shown in.

[1] Shanghai Jiao Tong University

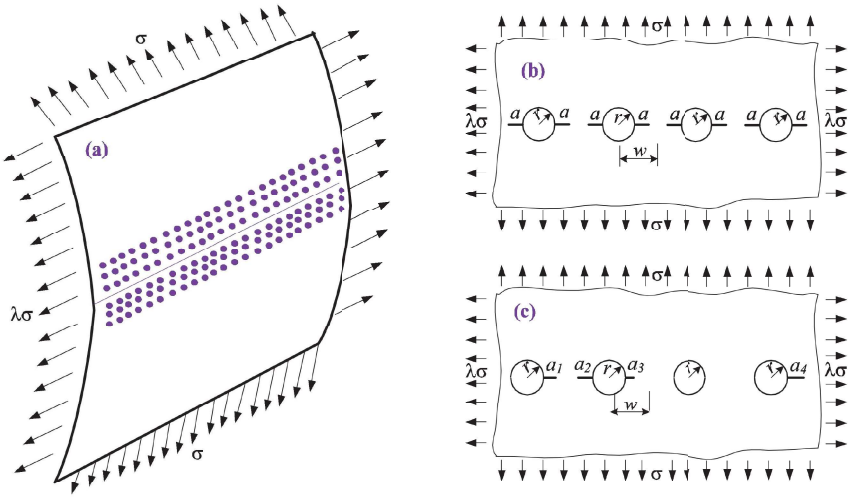

Figure 3. 47 Two ideal representations of edge hole cracks emanating from a fuselage, (a) a sketch of a fuselage skin under bi-axial tension; (b) periodic edge hole cracks in an infinite sheet subjected to bi-axial tension; and (c) arbitrary small cracks emanating from multiple collinear holes

Primary Results

The weight function method is firstly developed for periodic collinear cracks as shown in Figure 3. 47b. This crack configuration is one of the limiting case of the complex MSD configuration. Using the weight function method, Eq.(3.14-1), the stress intensity factor for various crack length a and $(a+r)/w$ are given in Figure 3. 48.

$$K = f\sigma\sqrt{\pi a} \tag{3.14-1a}$$

$$f = \int_0^a \frac{\sigma(x)}{\sigma} \cdot \frac{m(a, x, r/w, l/w)}{\sqrt{\pi a}} \cdot \mathrm{d}x \tag{3.14-1b}$$

where $m(a, x, r/w, l/w)$, $l=r+a$, is the weight function for the periodic edge hole cracks shown in Figure 3. 47b. To verify the present weight function method (WFM), the stress intensity factor obtained from finite element method (FEM) for Figure 3. 47b with $\lambda=0$ is also shown in Figure 3. 48, the maximum difference between these results are less than 2%. However, the present weight function is much more efficient than the finite element method for calculating the stress intensity factors for any length of crack. In addition, it is very efficient and accurate for crack opening displacement calculation.

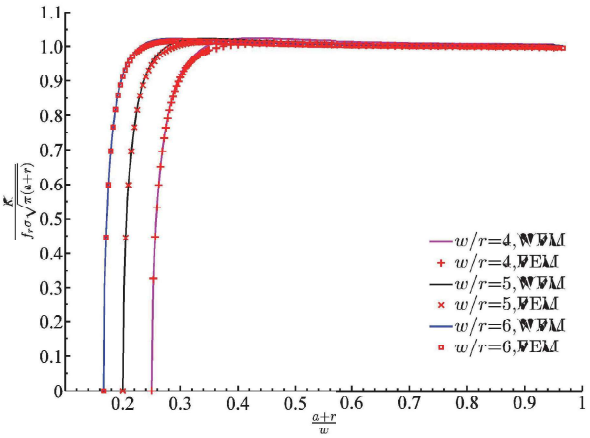

Figure 3. 48 Comparison Between the Normalized SIFs Obtained From FEM and WFM, Remote Uniform Tension in the y Direction

Conclusions

A novel weight function method is developed for edge cracks emanating from multiple collinear holes. It is accurate and efficient for the determination of stress intensity factor and crack opening displacement for cracks emanating from multiple collinear holes. The present weight function will enhance the capability of damage tolerance analysis of structure with MSD.

References:
[1] Swift, T. Damage tolerance capability. Int J Fatigue 1994; 16(1): 75–96.
[2] Schijve, J. Multiple site damage fatigue of riveted joints. Durability of metal aircraft structures, Proceedings of the international workshop on structural integrity of aging airplanes. Atlanta, G. A.,Stluri, S.N., Harris, C.E., Hoggard, A., Miller, N., Sampath, S.G. 1992.
[3] FAA. Aging Airplane Program: Widespread Fatigue Damage. Federal Register Rules and Regulations. 2010, 75(219): 69746-69789.
[4] NTSB Report AAB-13-02. www.ntsb.gov. National Transportation Safety Board.
[5] Wu, X.R., Xu, W.,2011. Strip yield cracks analysis for multiple site damage in infinite and finite panels – A weight function approach. Engng. Fract. Mech. 78(14), 2585-96.
[6] Xu, W., Wu, X.R., 2012. Weight functions and strip-yield model analysis for three collinear cracks. Engng. Fract. Mech. 85(1), 73-87.
[7] Xu, W., Wu, X.R., Wang, H.,2011. Weight functions and strip yield solution for two equal-length collinear cracks in an infinite sheet. Engng. Fract. Mech. 78(11), 2356-68.
[8] Xu,W., Wang, H., Wu,X.R, Zhang,X.J., Bai,G.J., Huang, X.L. A novel method for residual strength prediction for sheets with multiple site damage: Methodology and experimental validation. International Journal of Solids and Structures 2014; 51 (3), 551-565.

3.15 Interference Analysis of Multiple Cracks Propagation[1]

The engineering method and finite element analysis were adopted to analyze the interference of multiple cracks propagation. The plate specimen and stiffened plate specimen were designed, and the fatigue tests were completed under constant amplitude spectrum and random spectrum. For the Widespread-Fatigue Damage（WFD） problem of complex structure, the stress intensity factor was analyzed through embedded scripting in ABAQUS in view of extended finite element method (XFEM). Multiple cracks automatic propagation was implemented based on the crack growth rate and criteria for crack turning, which provides a research idea for WFD research. Figure 3. 49 and Figure 3. 50show some research in this field.

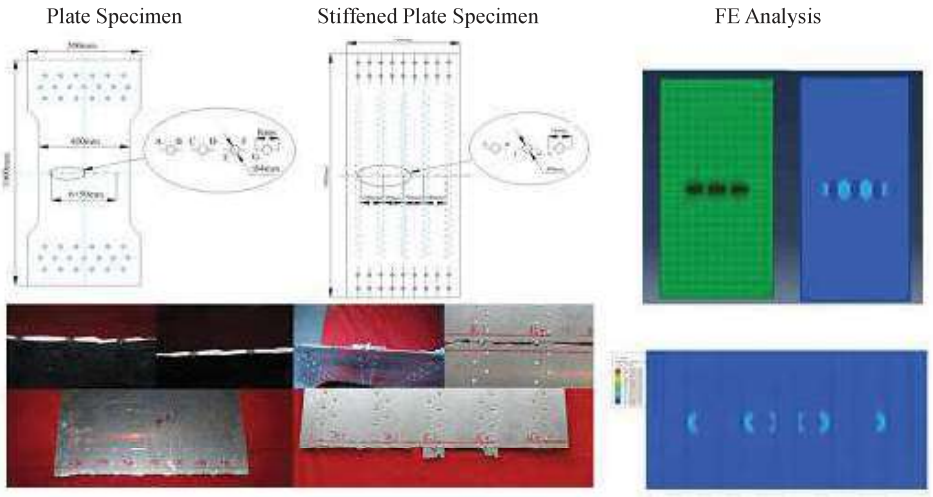

Figure 3. 49 Stiffened Plate Specimens and Results of Finite Element Analysis

[1] AVIC Aircraft Strength Research Institute

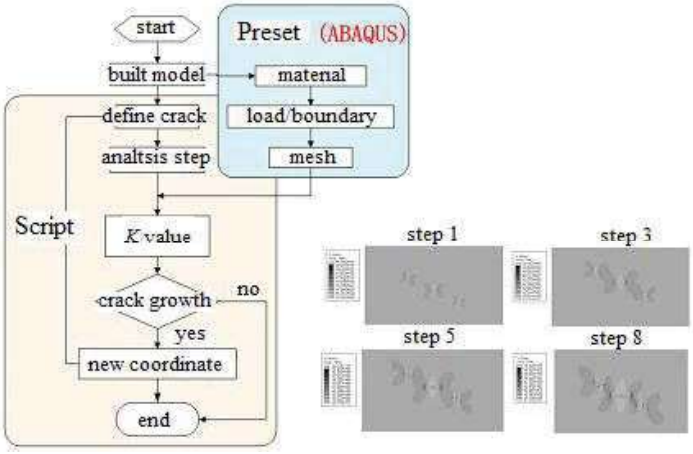

Figure 3. 50 Multiple Cracks Automatic Propagation Program and Results

3.16 Damage Analysis of Widespread Fatigue Damage（MSD）on Aircraft Critical structure[1]

Assumptions for MSD are described as following:

1 The fatigue life distribution follows two-parameter Weibull distribution, and the shape parameter is known.

2 If there are m cracks in sequence emerged in the structure containing N details, the distribution of crack is random. When the crack length is short, the load is not redistributed;

Based on MSD assumptions, the fatigue probability model of first crack initiation life on the structural with WFD was built up through the relationship between detail number and fatigue life, as shown in Eq.(3.16-1):

$$N_m = N_1 \cdot m^{1/b} \tag{3.16-1}$$

Where N_m—fatigue life of structure with m cracks

N_1—fatigue life of structure with single detail

b—shape parameter of two-parameter Weibull distribution

The proposed method can not only predict the first crack initiation life, but also analyze the multi-cracks lives in the multi-detailed structure. The first crack initiation life can be derived from the multi-cracks initiation lives. The feasibility of analytical method was verified by “build-block” design test, including the specimen with single/multiple hole and stiffened panel with a lap splice, as shown in Figure 3. 51-Figure 3. 53.

Full-scale testing results were analyzed in this research. Twelve cracks were discovered in the stringer R district of upper-panel in left and right central wing (26 similar-details), as shown in Figure 3. 54. Figure 3. 55 is distribution of principle stress in vector form.

The 95% reliability and 95% confidence of first crack initiation life was 7215 flights. The analytical life was 3166 flights by the proposed approach. Figure 3. 56 showed the comparisons of 12 cracks initiation lives between experiments and analysis. The blue curve was the experimental results; The green curve was that 2-12 cracks prediction lives derived from the first crack initiation life in the test; The other two curves are fully calculated by analytical methods: one is that 2-12 cracks initiation lives were calculated based on the first crack initiation life obtained by the method in Handbook; the other one was the results fully obtained by our proposed method. Some conclusions can be observed:

1) The life prediction of first crack initiation has a great influence on that of the subsequent

[1] AVIC Aircraft Strength Research Institute

cracks. The error estimation between test results and analytical results is approximately 50%, which can be acceptable considering the life dispersivity of tests.

2) Based on the multi-cracks life of test, the first crack initiation life can be derived, which have a better agreement with the test results compared with the other analytical methods.
3) The error estimation of multi-cracks life prediction by our proposed method (approximately 50%) came from that of the first crack life prediction.

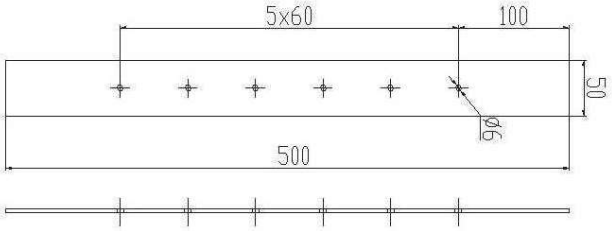

Figure 3. 51 6 Holes Specimen

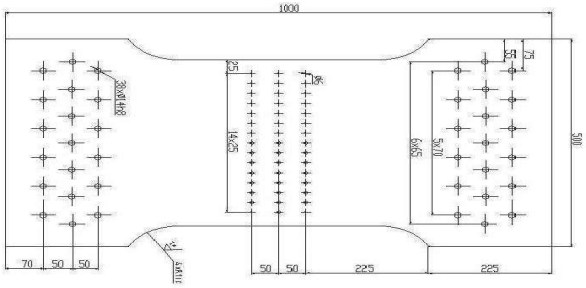

Figure 3. 52 45 Holes Specimen

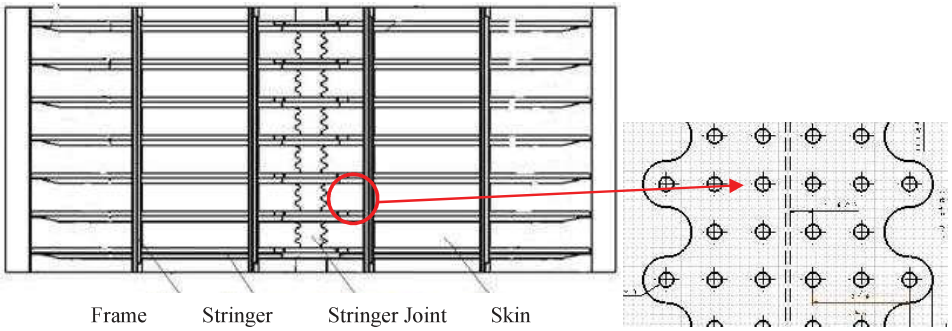

Figure 3. 53 Fuselage Panels Specimen

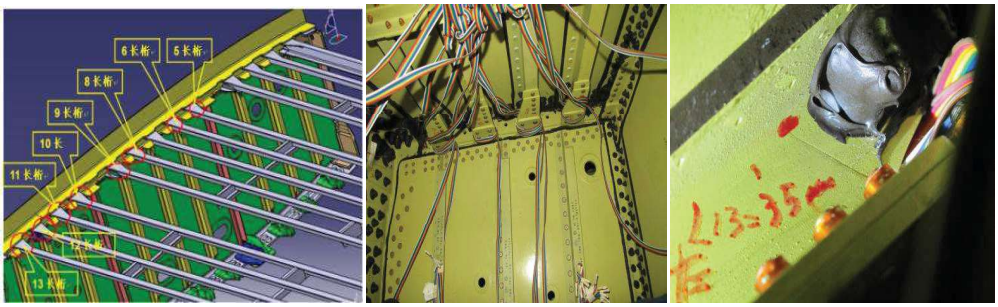

Figure 3. 54 Crack Locations of ARJ21-700 Full-scale Fatigue Test

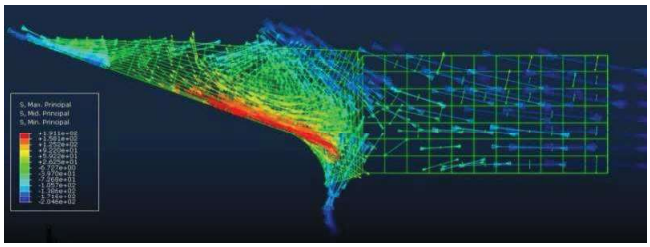

Figure 3. 55 Distribution of Principle Stress in R District

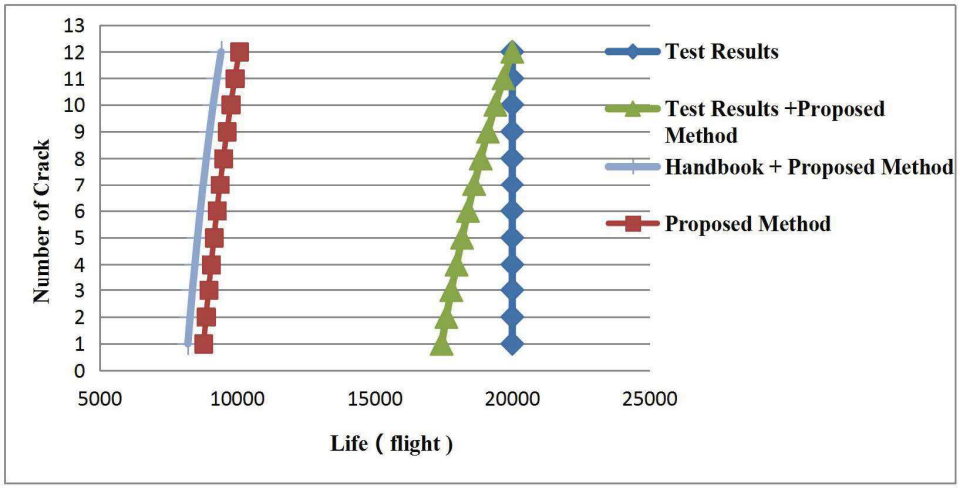

Figure 3. 56 Crack Numbers -Life Curve

3.17 Fatigue and Damage Tolerance Design and Evaluation Method for Civil Aircraft Structure Under Corrosive Environment[1]

Introduction

With the continuous development of aircraft structure life, especially in the aircraft in service, the corrosion problems are more and more serious. Fatigue and corrosion damage not only reduce the strength and stiffness of the aircraft structure, resulting in system and accessory function failure, affecting the service life and safety of the aircraft, but also greatly increase the costs of maintenance. Therefore, considering the environmental impact on service life caused by the airline, also known as the airworthiness of the security, concerns designer's attention.

Statement of Problem

Fatigue and damage tolerance assessment of civil aircraft structure needs to consider three forms of damage: fatigue damage, environmental damage and accidental damage. The inspection requirements are given by assessment. At present, the fatigue damage assessment of metal structures is based on fatigue and damage tolerance analysis and testing. The environment damage is checked and repaired through the development of corrosion protection and control program (CPCP). For accidental damage, the ground inspection is conducted after flight and the damage is repaired immediately after found. However, fatigue damage and environmental damage are usually coexistent, and in the absence of inspection and repair by CPCP. What effect will the corrosion have on fatigue damage? How much life time will be reduced? Many scholars and engineers have carried out research on this, considering the use of the impact of corrosion on the existing life after the reduction, and sometimes the reduction is very large. So light weight structure design is difficult to achieve, and also has a great gap with the reality of civil aircraft structure. After analysis and experimental research, this paper presents a complete set of fatigue and damage tolerance design and evaluation method of civil aircraft structure

[1] COMAC Shanghai Aircraft Design and Research Institute

under corrosion environment.

Research Ideas

In order to solve the problem of the interaction between environmental damage and fatigue damage, the structure characteristics of the damage tolerance are required for all the designed structure under the premise that the damage tolerance is the design standard of civil aircraft structure, such as slow crack propagation characteristics, structural accessibility, structural detectability, and structural maintainability. At the same time it needs to have a high durability, mainly in the high anti-fatigue properties, and corrosion resistance.

Therefore, starting from the structural design, the effective measures on material selection, structural layout, and part configuration options, details of connection, seal design, drainage design and surface protection system should be taken. The effect of protective system was studied on this basis. The influence of the protection system on the fatigue life of the structure before and after the failure was studied experimentally, and the effect of the crack propagation in the corrosion environment was studied. The following conclusions are drawn from the experimental study.

1) The corrosion environment has no effect on the fatigue life of the structure before the failure of the protection system, and the fatigue life of the structure was greatly affected by the corrosion environment after the failure of the protection system, which significantly reduced the service life.

2) The effect of corrosion on fatigue crack propagation is mainly concentrated at the crack tip area. Because of the formation of corrosive medium, the corrosive environment not only affects the micro-environment in the crack, but also affects the process of crack closure and the effective local stress intensity factor of the crack tip.

According to the experimental results, fatigue and damage tolerance design and evaluation of civil aircraft structure in the corrosive environment can take the following methods and steps.

1) Pay attention to anti-corrosion design, consider three aspects: material selection, protection system and structural detail design.

2) Develop the environmental spectrum, including ground-air-ground environmental spectrum and local environmental spectrum; determine the protection system that will not fail within the threshold period by test.

3) Conduct the materials and typical structural details fatigue and damage tolerance tests with considering of the corrosive environment, and obtain the analytical parameters.

4) Corrosion fatigue life is evaluated at the preliminary design stage in order to meet the design requirements.

5) Carry out the damage tolerance analysis of each PSE structure at the detailed design stage. Carry out the damage tolerance analysis and evaluation to determine the influence of corrosion in the determination of the repeat inspection interval.

6) Carry out the accelerated fatigue tests and crack propagation tests under corrosive environments on typical structural parts to provide parameters for analysis and evaluation and verify the key structural parts.

Assessment Method

In the case of the method described above, it's necessary to perform fatigue evaluation and damage tolerance evaluation in a corrosive environment.

1) Fatigue Assessment Method in Corrosive Environment

On the basis of general environmental fatigue analysis method, the influence coefficient M_D was introduced, and the fatigue resistance was reduced only after the protection system failed. In order to obtain M_D, it is necessary to decompose M into an influence coefficient M_{Dg} of ground stopping corrosion and an influence coefficient M_{Da} of airborne corrosion, which $M_D=M_{Dg}\times M_{Da}$. The effects of corrosion and corrosion fatigue on the structural life of the typical structural parts are studied by using the accelerated environmental spectrum. The curves of influence coefficient of ground parking corrosion and the air environment corrosion are obtained.

2) Damage Tolerance Assessment Method in Corrosive Environment

Based on the Paris formula of general environmental crack propagation, the correction experiment is carried out under the environmental conditions. Use the Paris formula:

$$\frac{\mathrm{da}}{dN} = C_{st}(\Delta K)^n \tag{3.17-1}$$

C_{st} is the crack growth characteristic constant in the corrosive environment, obtained through tests.

Method 1: For civil aircraft parts of the structure of the material, load and a variety of corrosive media, using the standard test parts for the crack propagation test, C_{st} is the crack propagation characteristic constant under the combined effect of various corrosive media and the corresponding stress spectrum in the selected material. In general, C_{st} is greater than C, indicating the acceleration of the environment on crack propagation. The specific conditions of the method for the various parts can only be determined by test.

Method 2: Make full use of the crack propagation test data of domestic aviation materials in various parts of the aircraft structure obtained by encountering a variety of typical environment. The crack propagation constant under environment conditions can be obtained directly by combinatorial method without the need of new tests.

$$\mathrm{C}_{st} = \sum_{i,j}\left[\left(m_{ei}m_R m_f\right)^{-n} w_{ji}\right]C \tag{3.17-2}$$

C_{st} is based on the Paris formula of the structural material obtained in the conventional crack propagation test. Eight typical experimental environment factors m_{ei} are used, and the load spectrum and frequency influence coefficients m_R and m_f are taken into account. Then the weight coefficient w_{ji} of corrosion environment is determined.

Conclusion

This design and analysis method can effectively quantify the interaction between environmental damage and fatigue damage of metal structures, give the fatigue and damage tolerance assessment results that meet the requirements of airworthiness, and can be used for civil aircraft model development.

3.18 Research on accelerated equivalent conversion theory of dissimilar metal structure on aircraft[1]

From designing to service process, corrosion problems of aircraft are throughout. Method of laboratory acceleration is the only way to protect and control corrosion, evaluate the changing rules with time of parking on the ground for corrosion damage of aircraft structure. It is viable to achieve the same effect of corrosion in a short time as parking on the ground for long time by establishing an accelerated corrosion spectrum and corrosion test. But during compiling accelerated environment spectrum at present, the equivalent relationship is based on a single metal, and the galvanic corrosion of different metals coupling on actual structure is ignored.

To get a result of accelerate corrosion test in laboratory closer to the one in real environments, 2A12-T4 aluminum alloy and TA15 titanium alloy are chosen as study subjects. Conversion coefficients of 2A12-T4 aluminum alloy coupled with TA15 titanium alloy in the NaCl solution of different concentration and the aqueous media as well as in the NaCl solution of different concentration and pH and the aqueous media are explored.

First of all, polarization curves of 2A12-T4 aluminum alloy and TA15 titanium alloy in NaCl solution of different concentration are measured by electrochemical tests (Shown in Figure 3. 57). Self-corrosion current density and self-corrosion potential are obtained (Shown in Figure 3. 58), and the changing rules of them in different solution are analyzed. It indicates that the self-corrosion current density increases first, and then decreases with concentration increasing, and the self-corrosion potential move to negative direction with the concentration increasing.

[1] Naval Aeronautical Engineering Institute

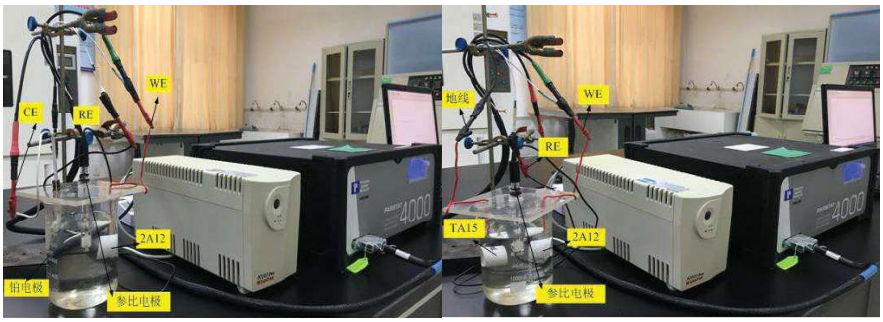

（a）Survey Sheet of Polarization Curve （b）Survey Sheet of Galvanic Current

Figure 3. 57 Survey Sheet of Electrochemical Test

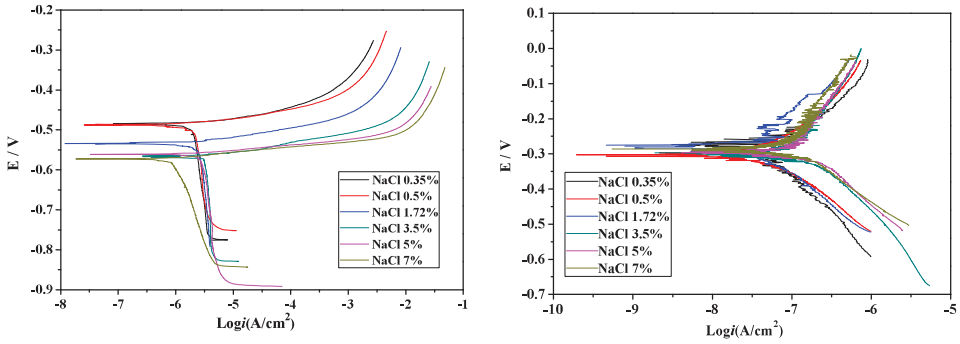

(a) Polarization Curves of Aluminium Alloy (b) Polarization Curves of Alloy

Figure 3. 58 Polarization Curves of Two Metals Alloy in NaCl Solution with Different Doncentrations

Then a galvanic corrosion simulation model (Figure 3. 59) is established by a multi-physics finite element software called Comsol.

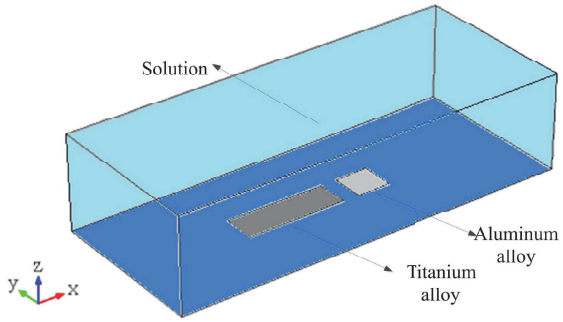

Figure 3. 59 Model of Galvanic Corrosion

Corresponding boundary conditions are input and simulation result of galvanic corrosion current is obtained in different conditions (Shown in Table 3. 5). Compared with galvanic corrosion current obtained by electrochemical test (Shown in Figure 3. 60), it was found that the simulation results of galvanic current coincide well with electrochemical test results (Figure 3. 61), and the simulation model can be used for simulating galvanic corrosion.

Table 3. 5 Current of Galvanic Corrosion with Cathode/Anticathode Area Ratio of 3:1 by Numerical Simulation

Solution Concentration	0.35%	0.50%	1.72%	3.50%	5%	7%
Galvanic Current(μA)	1.115	1.723	4.183	5.605	12.807	19.189

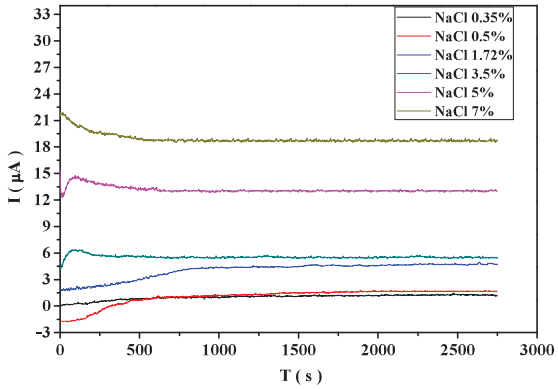

Figure 3. 60 Current of Galvanic Corrosion with Cathode/Anticathode Area Ratio of 3:1

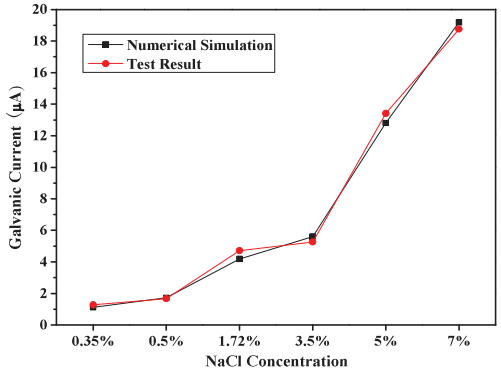

Figure 3. 61 Relationship of Galvanic Corrosion Current by Two Methods

Finally, on the basis of the simulation results, conversion coefficients of 2A12-T4 aluminum alloy coupled with TA15 titanium alloy in the NaCl solution of different concentration and the aqueous media are calculated through an equivalent conversion coefficient method (Shown in Figure 3. 62). The equivalent relationship is proved correct through test, which provides equivalent of accelerated environment spectrum for basis.

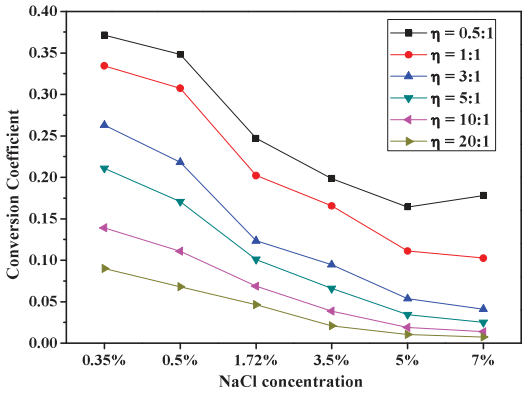

Figure 3. 62 Conversion Coefficient for Different Concentration NaCl Solution

3.19 An Optimal Multiple Linear Regression Model for Aircraft Structural Load Analysis[1]

[1] AVIC Chengdu Aircraft Design & Research Institute

Loading spectrum is essential for the aircraft structural durability/damage tolerance analysis, and the structural load analysis is a key technique of individual aircraft life monitoring and structural health management. How to accurately monitor in-service loading is important for the evaluation of aircraft life consumption and real time monitoring of structure health status. At present, this problem has not been well solved in engineering because load sensors are usually not available to be equipped on the aircrafts in service due to the restriction of weight, cost, reliability and maintenance. In this situation, in-service loading of aircraft structures can only be identified and analyzed based on on-board flight data. Flight parameters as original input, multiple linear regression is widely used, and construction of an optimal multiple linear regression model is necessary for the accuracy of in-service structural load monitoring at critical locations.

The optimal means that on the premises of regression equation's high goodness of fit, with independent variables as little as possible, each independent variable should have significant influence on the dependent variable, and meanwhile multi-collinearity between independent variables is quite weak. In the literature on aircraft structural load analysis and damage monitoring, how to synthetically build an optimal multiple linear regression load model has not been referred to. Based on multi-collinearity diagnosis, residual analysis and stepwise regression, this paper proposes an approach for synthetically building an optimal multiple linear regression load model. First of all, the multi-collinearity between independent variables should be diagnosed and attenuated; then, residual analysis is carried out to remove abnormal observations; finally, stepwise regression is used to find the best combination of independent variables.

This paper points out that traditional multi-collinearity diagnosis methods make little sense in practical application and puts forward two more feasible methods for reducing the multi-collinearity. The diagnosis method based on which the optimal regression equation is relatively better is finally chosen.

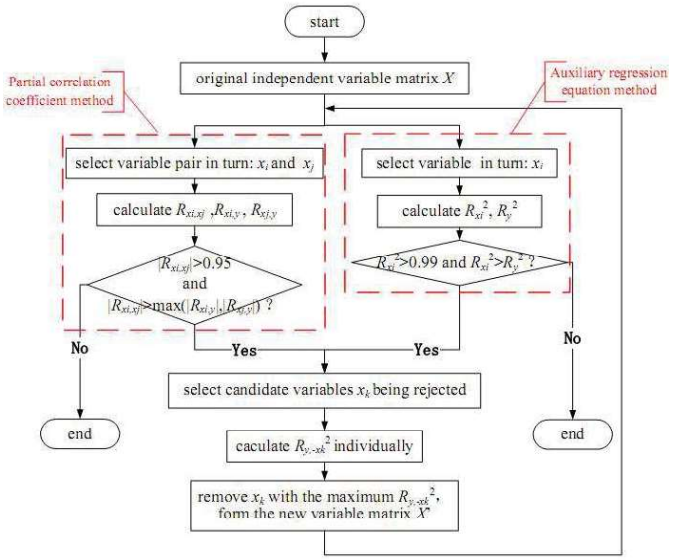

Figure 3. 63 Overall Flowchart of Multi-Collinearity Diagnosis

As a case study, load and stress samples of a critical wing attachment bulkhead location are used to illustrate the procedures of how to establish an optimal regression equation. It is proved that the approach can not only ensure the accuracy of aircraft structural load analysis, but also select the parameters of great statistical significance, which has significant engineering practical value and meaning.

First, in the multi-collinearity diagnosis based on partial correlation coefficient method, the term x1 is finally eliminated, the process listed in Table 3. 6.

Table 3. 6 Multi-collinearity Diagnosis Based on Partial Correlation Coefficient Method

NO.	Candidate Variable Pairs	$R_{x_i x_j}$	x_k	$R_{yx_k}{}^2$	Deleted Variable	Remaining Variables
1	x_1 and x_4	0.9623	x_1	0.9831	x_1	x_2~x_6
	x_3 and x_6	0.9507	x_3	0.9830		

Then, through the residual analysis with remaining variables in the model, two sample points should be deleted, of which the deviation is significant, obviously shown as Figure 3. 64 a). Afterwards, stepwise regression is conducted, the process listed in Table 3. 7. Through seven sequences, the final variable combination is x3, x4 and x6, which can be sorted by significance: x4>x3>x6. With adjusted determination coefficient =0.999423, the regression equation fits the observed values quite well, shown as Figure 3. 64 b).

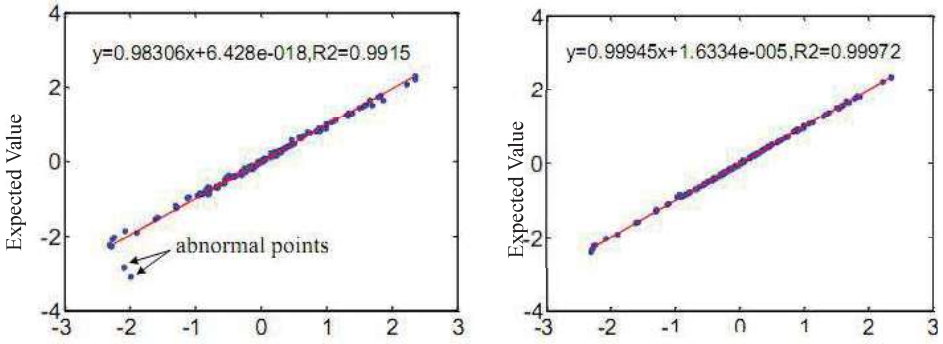

Figure 3. 64 Comparison between Observed Value and Expected Value.

Table 3. 7 The Process of Stepwise Regression

NO.	Terms in the Model					Removed Term	Remaining Terms					Term Being Moved in
	x_2	x_3	x_4	x_5	x_6	/	x_2	x_3	x_4	x_5	x_6	
1	×	×	×	×	×	/	8.12	49.16	155.33	7.53	55.28	x_4
2	×	×	155.33	×	×	/	-7.41	14.02	√	14.45	0.85*	x_5
3	×	×	207.52	14.45	×	/	-10.62	2.24	√	√	-8.76	x_2
4	-10.62	×	231.16	17.67	×	/	√	7.53	√	√	0.26*	x_3
5	-14.26	7.53	40.59	0.169*	×	x_5	/	/	/	/	/	/
6	-15.18	22.39	91.13	×	×	/	√	√	√	0.169	-8.45	x_6
7	1.38*	18.02	54.90	×	-8.45	x_2	/	/	/	/	/	/
8	×	34.76	92.43	×	-20.43	/	1.38	√	√	-0.64	√	End

×: the term is not currently in the model,

/: the process or calculation is not available in the current sequence,

√ : the term is currently in the model,

*: p-value of t statistic is greater than the entrance tolerance or the exit tolerance (both 0.05).

3.20 A Research on the Vertical Tail Buffet Fatigue Load Sequence Generation Technology[1]

[1] AVIC Chengdu Aircraft Design & Research Institute

The advanced aircraft has adopted V-shaped twin vertical tails aerodynamic configuration form for high maneuvering performance. However, in the high AOA flight conditions, the tail structures will be struck by the separation vortex from the aircraft forebody and resonate strongly. This phenomenon is called vertical tail buffet problem. This paper has taken the vertical tail structure buffet response power spectral density (PSD) from the flight test data as the research object, and adopted dynamic response and load recognition technologies to obtain the correspondence relations between acceleration response of the reference point and other buffet parameters. Meanwhile, the probability distribution model has been set up to forecast the acceleration peak responses of the reference point in every dominant mode in the buffet stochastic process. By a final comparison of two buffet response exceedance distributions, one from the fatigue load spectrum generation process, and the other from the flight and wind tunnel test results, the robustness and calculation accuracy of the vertical buffet fatigue sequence generation technology have been proved as a result. Therefore, the vertical buffet fatigue sequence generation technology established in this paper is suitable for the certain type of aircraft structure anti-buffet strength design and experimental verification.

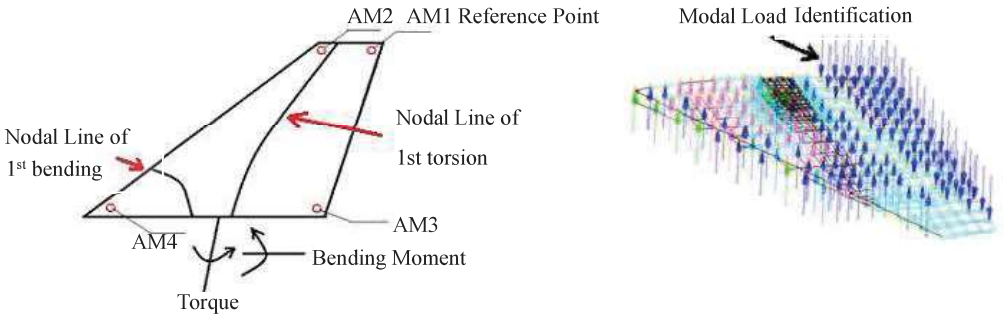

Figure 3. 65 Vertical Tail Mode Analysis and Dynamic Load Identification

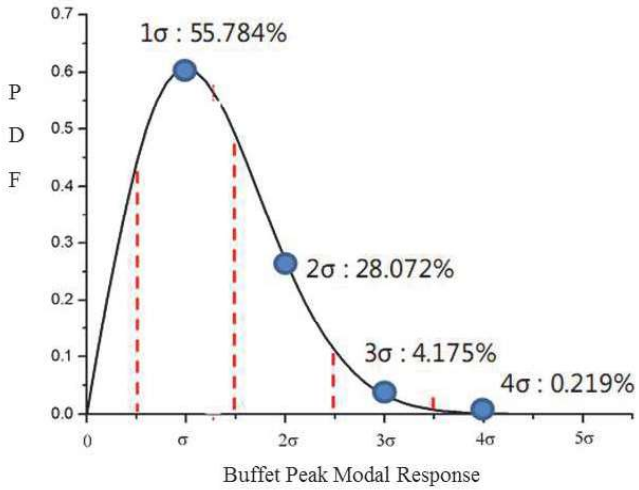

Figure 3. 66 the Rayleigh Distribution - the Model of PDF of the Buffet Peak Modal Response (PDF: Probability Density Function)

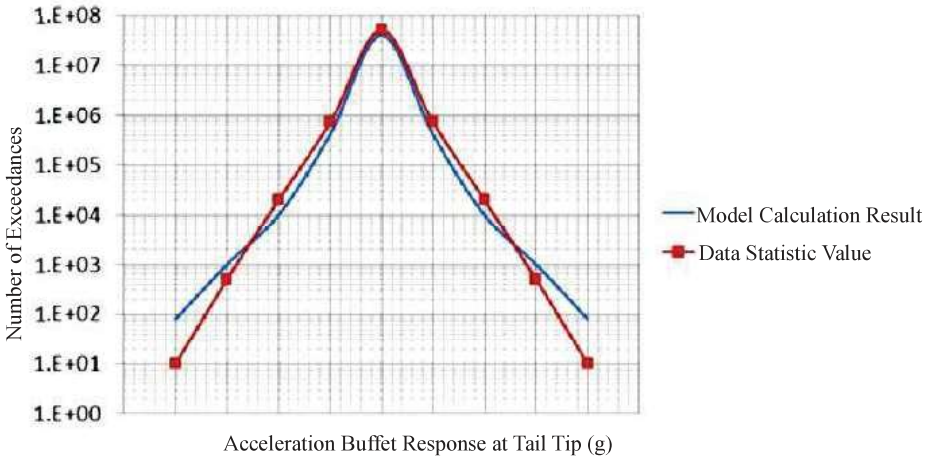

Figure 3. 67 Buffet Response (Acceleration at the Tail Tip Point) Exceedance Curve

4 Full-Scale Structure Fatigue Testing

4.1 Helicopter Corrosion Fatigue Research Status[1]

The Corrosion fatigue's influence on service life of structures has increasingly drawn scientists and engineers' attention of all countries with the exposure of severe problems caused by engineering structures of aircrafts and ships. Research work of corrosion fatigue started with foundational study during 1950s-1960s and turned to application study that has been more and more applied in aircraft design and other engineering structures.

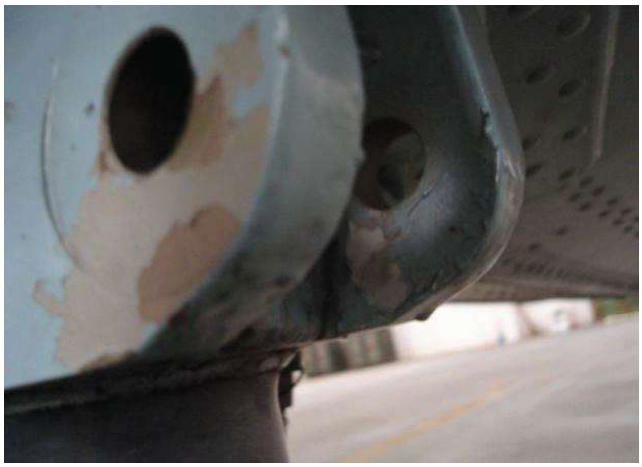

Figure 4. 1 Corrosion Situation Some Type of the Helicopter

Over 1970s, there have been released a lot of study results and papers on material's corrosion fatigue behavior and the influence of corrosion fatigue crack growth. U.S. Air Force conducted comprehensive investigations and evaluations on various types of aircrafts' damage type and frequency of occurrence. The conclusion shows that cracks and corrosion rank respectively the first and second as the uppermost damage types of all. Also, corrosion pits and dimples are the main causes of cracks. Lots of countries have devoted a large amount of manpower and material resources to control aircrafts' corrosion condition.

In China, plants, institutes and colleges related to aeronautics have made a lot of research work on fixed-wing planes like SH-5 and Q-6. Over 1990s, we have done a lot of work on a series of naval

[1] AVIC Helicopter Design & Research Institute

aircrafts' corrosion fatigue and achieved big progress especially on environmental spectrum, environmental test and equivalent relation. However, for the objects and features of our study work, many achievements are difficult to be applied directly to high cycle corrosion fatigue issues of helicopters' rotary parts.

In recent years, CHRDI carried out the 'Z8 corrosion fatigue research' project which focused on corrosion fatigue's influence on structures' service life and launched thorough research. The project adopted the latest fatigue test technology, corrosion preparation technique and corrosion level assessment technique based on digital image processing technology and successfully solved technical problems confronted in the research work.

The project conducted a series of research contents including Z8 environmental spectrum, equivalent relation of accelerated corrosion, coating protection system and engineering applicative corrosion level evaluation standard. Five typical metal materials' corrosion fatigue characteristics including LD2CS, LD10CS, LY12CZ, 15CrMnMoVA and 30CrMnSiA (failure mode without fretting) were tested. Corrosion fatigue experimental verification was accomplished including three kinds of full-scale structural components: main gear forward and backward brace rod and lateral booster pedestal. On this basis, we conducted research on environmental influence coefficient and corrosion fatigue life correction factor and set up a set of corrosion fatigue life evaluation and correction methods for helicopter structural components.

In the project we completed the corrosion and fatigue tests of a total of 2014 standard parts and 18 structural parts with 36 corrosion fatigue curves, made 244 measured load spectra and fulfilled the corrosion fatigue evaluation work of 19 parts which used to determine the lifetime for Z8 helicopter. The main research work is as follows:

1) Corrosion fatigue tests of 1080 test pieces of 5 different kinds of materials were accomplished. The test time was as long as 33192 hours with four fatigue machines working at the same time for more than a year, and 36 corrosion fatigue S-N curves were obtained;

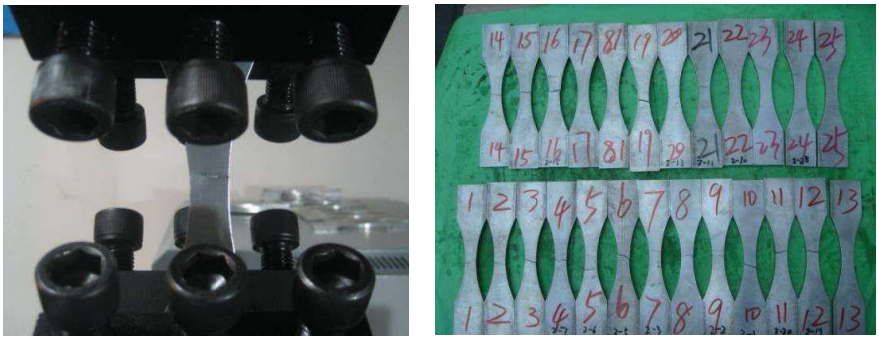

Figure 4. 2 Material Samples Test

2) Four-months' corrosion fatigue tests of 18 full-scale structural parts for MGB forward and backward rod, lateral booster pedestal were accomplished;

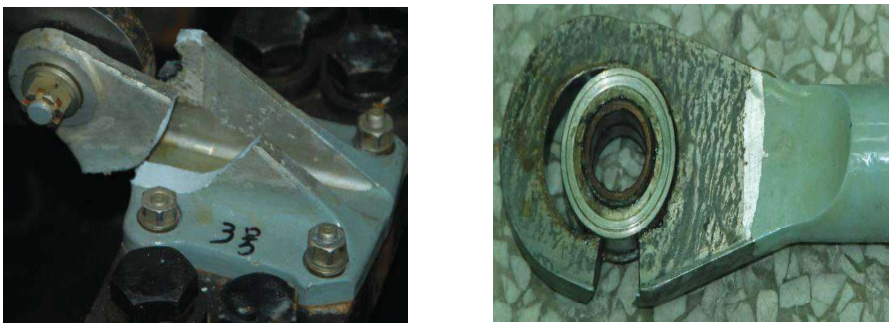

Figure 4. 3 Structure Corrosion Fatigue Test

3) 270 corrosion tests with 7 corrosion grades of aluminum alloy and alloy steel were accomplished and corrosion fatigue level evaluation standard for helicopter was made based on the corrosion

equivalent relationships obtained from the tests.

4) 396 accelerated corrosion tests with 7 corrosion grades of aluminum alloy and alloy steel were accomplished, which laid the foundation for preparation of accelerated corrosion test pieces and evaluation of corrosion fatigue level.

5) Environmental data of corrosion of Qingdao, Sanya and Ningbo were studied and Z8 helicopter's service environment spectrum was obtained.

6) 360 specimens with hygrothermal exposure test, ultraviolet irradiation test, low-temperature fatigue test and salt spray test of coating protection system were accomplished, which gave four corrosion calendar years limits of coating protection system for aluminum alloy and alloy steel.

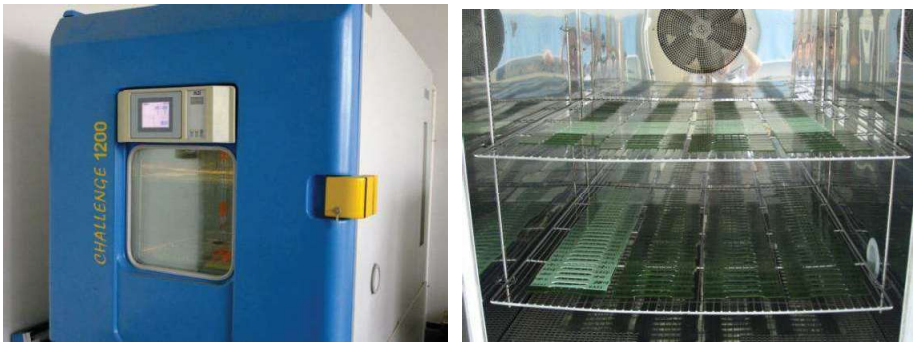

Figure 4. 4 Hygrothermal Exposure Test

Figure 4. 5 Ultraviolet Irradiation Test

Figure 4. 6 Salt Spray Test

7) Coordination and a detailed research of flight spectrum were carried out, and the corresponding detailed flight spectrum was presented. 130G measured load data were processed. 244 measured load spectra were made and thus revision of the original Z8 helicopter's load spectra was fulfilled.

8) How corrosion environment affects fatigue property was studied and the influence coefficient of

corrosion fatigue strength was got.

9) How calendar corrosion affects fatigue property was studied and the influence coefficient of calendar corrosion fatigue strength was got.

10) Restoration techniques of corrosion pits and its influence quantity on fatigue strength were studied, which provided technical support for the repair of corrosion parts and the decision of its service life.

11) High-cycle corrosion fatigue evaluation theory of helicopter was studied. Helicopter's evaluation systems of corrosion fatigue life and calendar life were established, based on which the corrosion fatigue life of 19 structural parts for Z8 helicopter was evaluated.

By fully absorbing advanced foreign technological tactics, the project achieved impressive results of revising the corrosion fatigue life's evaluation for Z8 helicopter after a lot of monographic studies. The project established revision technology of corrosion fatigue life evaluation for helicopter with international advanced level which was suitable for Chinese situation. It enabled our country's corrosion fatigue life evaluation of helicopter to reach the advanced international level successfully.

4.2 Damage Tolerance Test of Curved Panel with Longitudinal Crack Subjected to Pressurized Load[1]

In order to study the behavior of damage tolerance for fuselage curved panel, a test equipment was designed and manufactured according to the boundary requirements of internal pressure load. The test machine includes rigid steel frame, pressure-box, hydraulic cylinders and load plates as shown in Figure 4. 7. Pressure is applied to the concave side of the panel using an air supply source and a pneumatic control system. Some strain channels were used to monitor the fuselage skin and substructure elements.

Figure 4. 7 Pressure Test Machine

The fuselage panel tested in this study was representative of a narrow-body fuselage structure. The curved panel has a 1671-mm-radius, 2840-mm-length and 2054-mm-width with seven full length rod-stiffened stringers and five frames. The initial damage for panel consisted of a 25-mm-long longitudinal crack.

Damage tolerance experiment includes crack propagation test and residual strength test. The test was conducted in three phases with the loading conditions shown in Table 4. 1.

Table 4. 1 Test Phases and Applied Loads

Test phase	Purpose	Load Type	Pressure (MPa)
I	Strain-stress survey	Quasi-Static	0.055
II	Crack growth	Cyclic, R=0.1	0.055

[1] AVIC Aircraft Strength Research Institute

III	Residual strength	Quasi-Static	0.067

The quasi-static test results show that the test hoop stress is 4.6% lower than the theoretic hoop stress of thin-walled cylinder, and the test axial stress is 7.3% lower than theoretic axial stress. The results are reasonable since an actual airplane fuselage contains stiffening elements that carry load and generally reduce stress on the skin.

Figure 4. 8 shows the crack propagation path in left and right directions. It can be seen that the crack progress nearly along a straight line. Figure 4. 9 shows the experimental results of the crack growth in left and right directions. It can be seen that the left crack and the right one progresses at the same rate approximately. And they progress slowly significantly from 12.5 mm to 80 mm. However, the growth rate of the crack in both directions continuously increased after 80 mm. By the end of fatigue test, the crack propagation life was 131231 cycles.

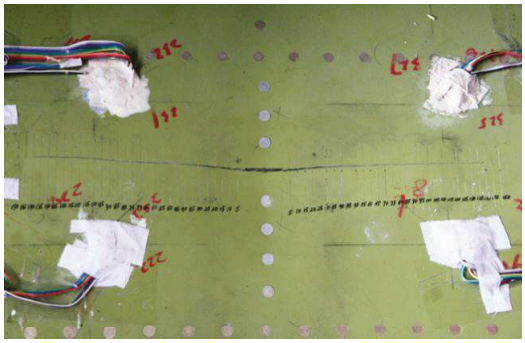

Figure 4. 8 Crack Propagation Path

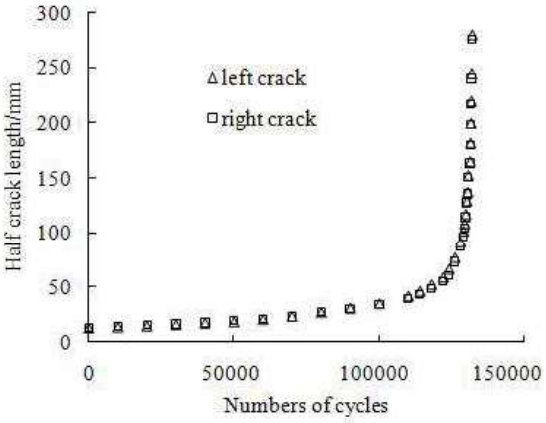

Figure 4. 9 Half Crack Length VS Number of Cycles

The residual strength test was carried out when the total crack was 556 mm after crack propagation test. A load was applied quasi-statically with a pressure increment of 0.002 MPa up to 0.066 MPa and an increment of 0.001 MPa afterwards. Further crack extension was observed at 0.068 MPa pressure. Catastrophic failure occurred at a pressure of 0.071 MPa. Figure 4. 10 shows the final state of damage after the residual strength test. The left crack tip abruptly extended through frame F2 and then stopped at frame F1 with a down turning. The right crack extended through frame F4 and then stopped at frame F5.

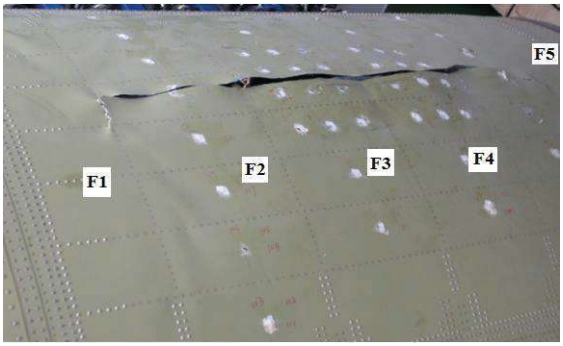

Figure 4. 10 Damage of the Residual Strength Test

4.3 The Automatically Variable Stroke Loading System of Aircraft Landing Gear Structure[1]

Recently, the common static test method of aircraft landing gear structure is to fix the landing gear as installed in an aircraft, and change its boundary form according to different operating conditions. And the loading spectrum in its fatigue test is always simplified to make the test easier to be operated and reduce the workloads between different operating conditions. The test results are not precise for the two traditional tests of landing gear structure.

This study presents a test equipment that can load the landing gear structure automatically and adjust its stroke. The equipment can be used to test all kinds of single pillar landing gears, and its test cycle will be shortened through avoiding manual intervention in the test. Moreover, the testing accuracy can be improved.

Equipment Design

The equipment is comprised of some main structures, such as framework, lifting platform and loading frame, and the other components like hydraulic loading device, rollers, screw, loading beam, electrical machine, and so on. The equipment is shown in Figure 4. 11.

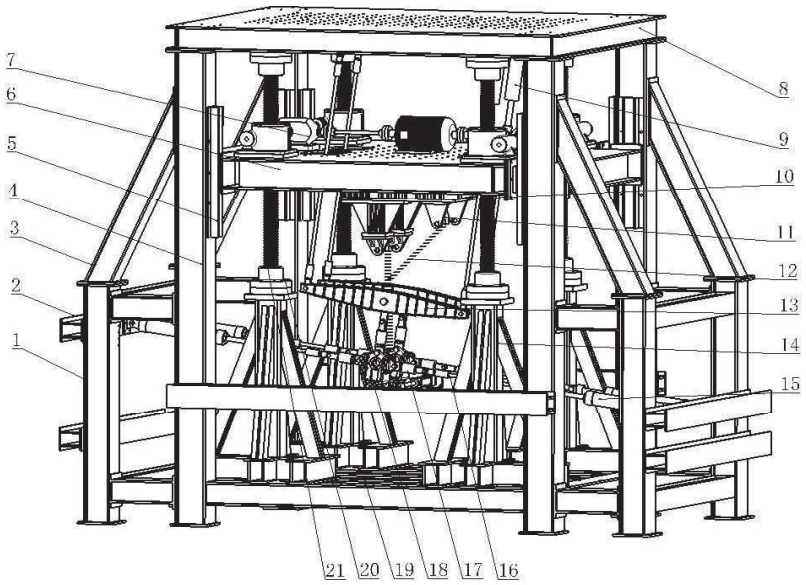

Figure 4. 11 Schematic of the Equipment

Operating Principle

[1] AVIC Aircraft Strength Research Institute

When using this equipment to operate static and fatigue test of landing gear structure, the structure is fixed the same as that in an aircraft. The axis of the landing gear is arranged perpendicular to the horizontal plane. When the loading condition of the landing gear changes, which means the travel changes, the lifting platform moves simultaneously in the opposite direction, and the position of the fake airplane wheel will keep still. Consequently, it can reduce the workloads when the operating condition changes during the whole test process.

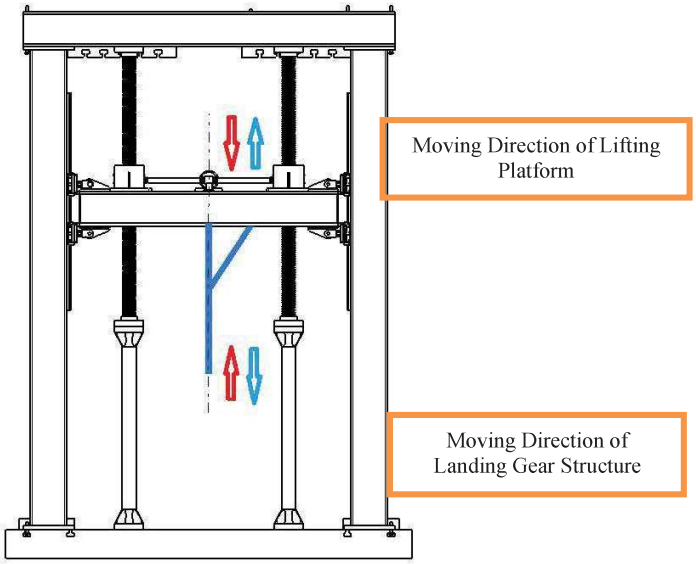

Figure 4. 12 Operating Principle of Keeping Loading Points Still

The installation state of landing gear structure and the operating principle of keeping the wheel still are shown in Figure 4. 12.

Function of the Equipment

This equipment can be used in the static and fatigue test of all kinds of single pillar landing gear structure, and the load can be operated automatically and precisely without manual interventions.

4.4 Configuration Selection Test of Nose Landing Gear and Ram Air Turbine (RAT) Compartment[1]

A configuration selection test of nose landing gear cabin and RAT cabin for commercial aircraft was conducted to assess the structures and to determine the design scheme of RAT cabin.

The test specimen is composed of nose structures and specimen bulkheads (as shown in Figure 4. 13). The nose structures consist of nose landing gear cabin, RAT cabin, floor beams, 8th to 21st frames and lower panels. Specimen bulkheads include forward bulkhead, aft bulkhead and upper bulkhead. The specimen is 3950mm in length, 3890mm in width and 1784mm in height.

[1] AVIC Aircraft Strength Research Institute

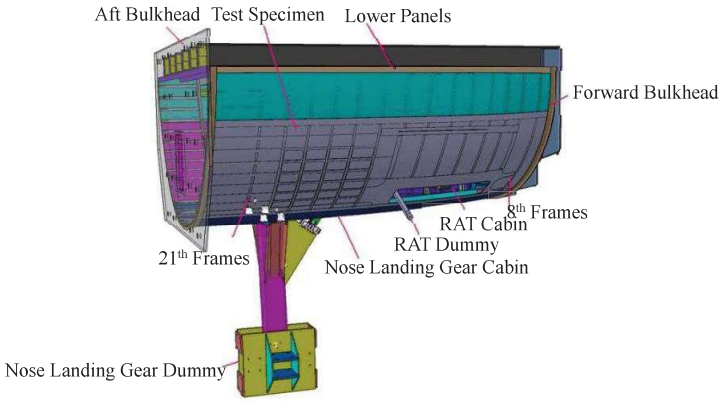

Figure 4. 13 Test Specimen and Dummies

Test loads included cabin pressure differential, RAT release load and nose landing gear load. Cabin pressure differentiation and nose landing gear load were applied separately. RAT release load was applied simultaneously with cabin pressure differential.

To simulate nose landing gear load, a dummy was designed to apply load on nose landing gear cabin. The nose landing gear load in course direction was applied by actuators in front of nose structures. Lateral load was applied by actuators on left side, while vertical load was applied by two levers from upside.

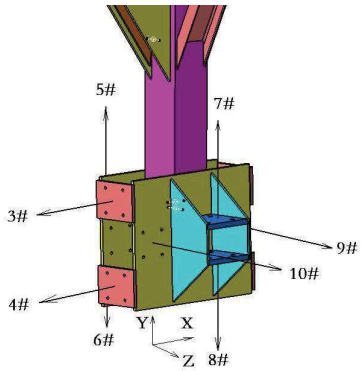

Figure 4. 14 Loading Schematic for Nose Landing Gear Loads

An RAT dummy was designed to apply RAT release loads. RAT load was applied by tightwire, as shown in Figure 4. 15. The actuator is fixed on loading track, and the load direction was changed by a wheel fixed on loading wall.

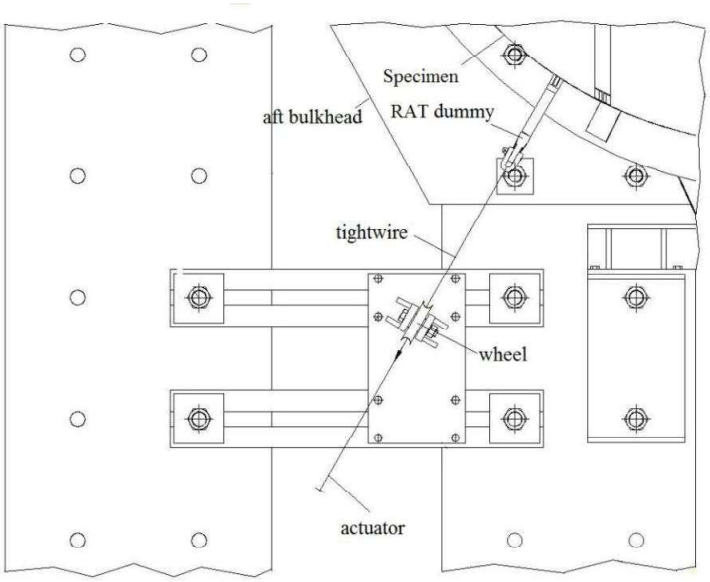

Figure 4. 15 Loading Schematic of RAT Release Load

Cabin pressure differential was applied by pneumatic facility. An air-water box is set up as a protective system. The locations of air inlet, pressure measurement hole and protective hole are shown in Figure 4. 16. The fastener holes on aft bulkhead were sealed by sealant, and the cutouts were sealed by armor plate and rubber plate. The sealing scheme is proven to be reliable.

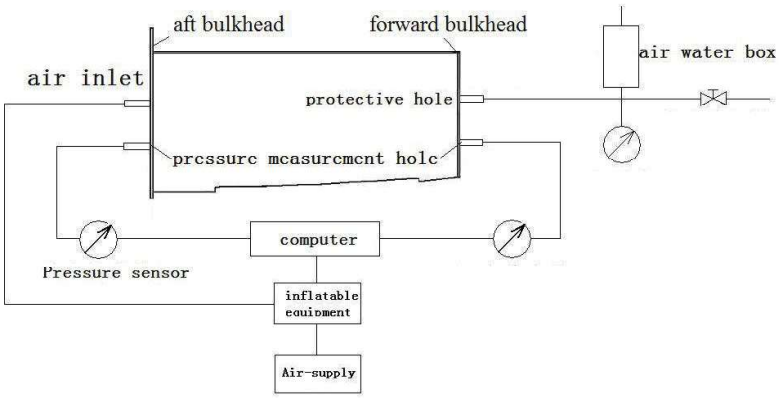

Figure 4. 16 Loading Schematic Diagram of Cabin Pressure Differential

The test setup is shown in Figure 4. 17.

Figure 4. 17 Test Setup

The test result demonstrated that the test specimen can withstand required loads. No visible permanent deformation was found after the test. When the reinforcement bars were removed, the strain did not show obvious change. Therefore, the reinforcement can be removed (Figure 4. 18).

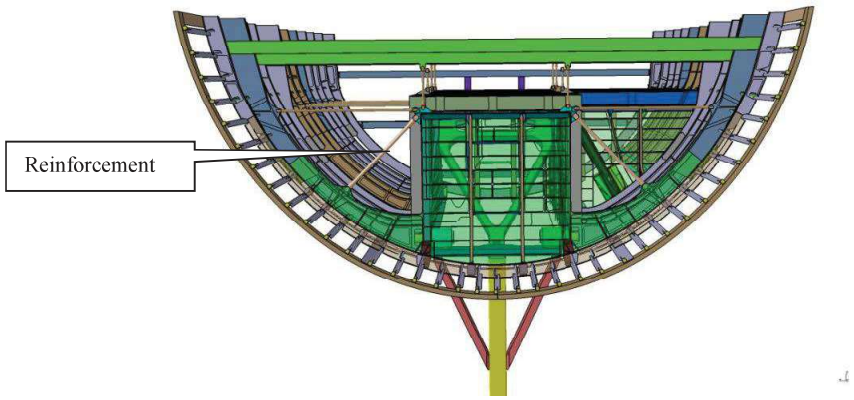

Figure 4. 18 Schematic of Reinforcement Location

4.5 The Fatigue Loading Method of Movable Flap on Track[1]

The experimental investigation on the flap motion mechanism is the main objective of this work. Aiming at this target, the present study has advanced a kind of loading methods for the verification of the movable wing mechanism. Test verification was conducted in order to validate the valuable loading method and to support other tests on large movable rudder.

As the motion track of flap mechanism is a half parabola shape, shown in Figure 9.13, it requires concomitant load in the process of movement. In practical engineering, it is difficult to simultaneously simulate the real flight loading process of flaps and its system. These problems are the same as the mutual influence between structure and mechanism. As a result, the current tests on the flap motion mechanism were developed with the wing surface fixed.

[1] AVIC Aircraft Strength Research Institute

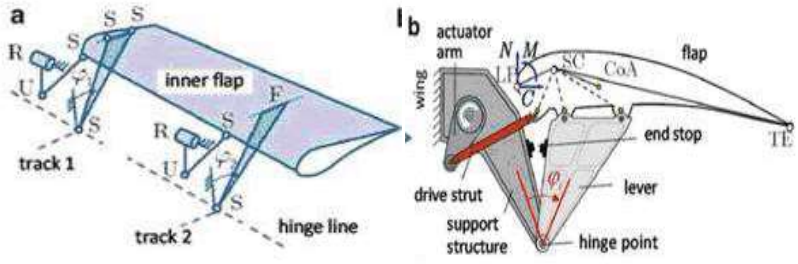

Figure 4. 19 Flap Motion Form

Firstly, in order to simulate the real boundary conditions of the wing structure and the real force transmission characteristics of reduction box section of the wing, this work advanced a boundary simulation method for the wing with adjustable bending and torsion deformation. The above method is based on the finite element simulation, given in Figure 4. 20. It can be used to solve the technical problem of boundary stiffness simulation during fatigue test. See Figure 4. 21.

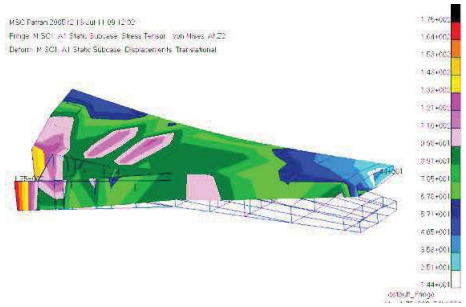

Figure 4. 20 The Finite Element Calculation Results

Figure 4. 21 The Flaps Test Stiffness on the Scene

The loading conditions in our test mainly simulate the changing process of aerodynamic load on the flap surface when aircraft is taking off and landing. The typical load spectrum is shown in Figure 4. 22.

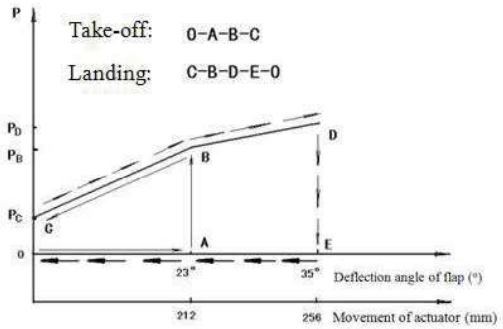

Figure 4. 22 Loading Diagram in the Flap Controlling Test

In order to ensure the authenticity of loading conditions for the movable wing surface, a kind of movable loading scheme was put forward to guarantee the magnitude and direction of load. The loading scheme in Figure 4. 23 was developed to ensure the accuracy of the wing surface load by adjusting the movement of the actuators through the force vector relation.

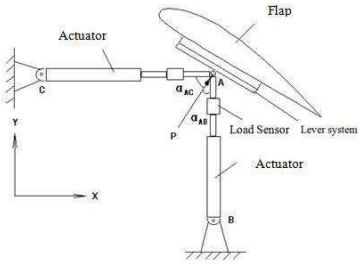

Figure 4. 23 Loading Schematic Diagram

The load points of lower surface of the wing were designed as the form of pulling and pressing pad. Two actuators are hinged on the mudsill, and they act on the pad glued on the wing surface. If the stress area is increased, the concentrated load of actuators will be redistributed averagely on the wing surface. This loading method can reduce the localized large stress distribution and avoid the failure of skin. Figure 4. 24 shows the test locality.

Figure 4. 24 Test Results

The main conclusions are given as below:

1) Using the developed loading scheme with hydraulic actuators, the test verification process is conducted successfully. Each actuator works very well, and there are no stagnancy, alarm and overload, which proves the feasibility of this method;

2) During the testing process, the measured load, strain and displacement of the wing surface show good repeatability. The loading precision is controlled less than 0.4% of the target load through a series of testing measurements.

3) The aerodynamic loads on the movable wing surface are able to be simulated by using several servo actuators based on the force vector relationship. The present work confirms that the current loading approach provides valuable reference for other tests on movable mechanism.

4.6 The Fatigue Testing Technique of Amphibious AG600[1]

Amphibious aircrafts have both the general aerodynamic characteristics of common aircraft and the hydrodynamic properties for taking off, landing and navigating on the water. At the same time, amphibians should have the ability to land on water repeatedly during the expected service life.

AG600 is a large amphibious aircraft developed in china. Except the conventional load, a water load

[1] AVIC Aircraft Strength Research Institute

brought from taking off and landing on water should be applied in its full scale test. It also needs to meet the new requirements of the new structure test.

Water Landing Loads Simulation Infliction Method

The water landing loads were processed by analyzing their four working conditions: the body step, the bow, the stern and the float approaching water. And different water-loading ways were studied, such as tension/compression pads, loading pads, vacuum acetabula, and ballonet. Figure 4. 25 is elements of vacuum acetabula inflicting load.

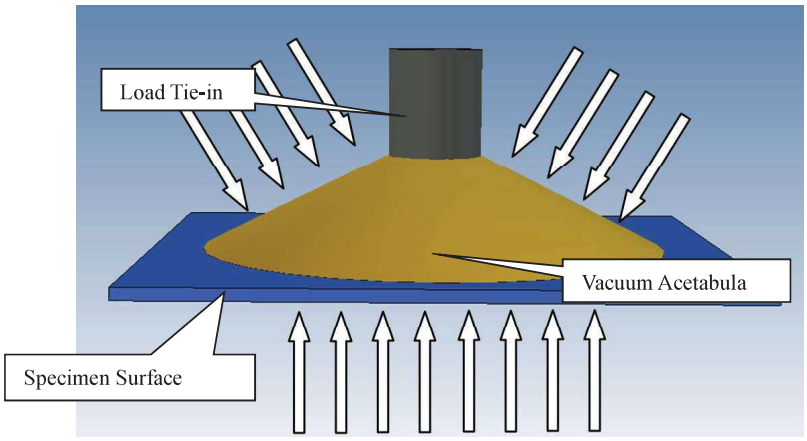

Figure 4. 25 Elements of Vacuum Acetabula Inflicting Load

The Method for Whole Airplane Suspended Support

The load space is reserved below the fuselage to inflict water landing load in the full size test by heaving the whole aircraft up. In this way, we can take full advantage of the nose and main landing gears with long strength and high stiffness, which can afford the steady and dependable restriction. So the statically determinate restriction is intercalated on the nose and main landing gears. It is used on sustain of non-testing state, and all testing state except the nose and main landing gear installation static test. Figure 4. 26 is the photo of full scale aircraft test.

Figure 4. 26 Full Scale Aircraft Test

Tracking Loading and Sustain Technique on Landing Gears in The Full Scale Aircraft Test

It is a “V” type at the bottom of the AG600 aircraft, and the main landing gear is a long hyperstatic structure. The tracking loading technique is used on landing gear during full scale aircraft test. The sustain installations on landing gear are shown in Figure 4. 27.

Figure 4. 27 Tracking Loading and Sustain Installation on Landing Gear

4.7 Static Strength Test of Main Landing Gear of AG600 Aircraft[1]

The test was designed to verify the structural strength of the main landing gear of AG600 aircraft and the accuracy of theoretical calculation model.

The landing gear struts is longer than others and produce greater deformation at the wheel center. The test needs to simulate the load applied and stiffness of aircraft structural correctly. In addition, it must guarantee the position of vertical loading point at the maximum load levels.

All the tests including actuating device testing, upper lock Position testing and ground load testing were conducted in a self-balance test frame.

Specimen

The specimen contains of mounting bracket, undercarriage supp, Lower lock, actuating device and emergency release device sketch , which are shown in Figure 4. 28.

Figure 4. 28 Specimen

Test Load

There are 3 test items: actuating device testing, upper lock position testing and ground load testing. Actuating device testing needs to apply pressure loading on the actuator of the actuating device. The loading apply position of upper lock position testing is on the axis of the upper lock. The loading apply position of ground load testing is in the center of the wheel axle and the touchdown point of wheel.

Test Fixture and Loading Scheme

The test fixture consists of component 1 to component 4 and other connection components. The specimen is supported by the joints on component 1.The test fixture is shown in Figure 4. 29.

[1] AVIC Aircraft Strength Research Institute

Figure 4. 29 Test Fixture

The actuating device testing contains of two installation attitude: folded up and full release (shown in Figure 4. 30).

Figure 4. 30 actuating device

The loading scheme of upper lock position testing is shown in Figure 4. 31.

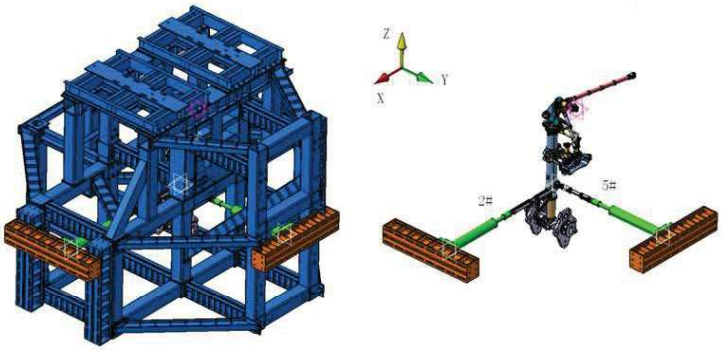

Figure 4. 31 Loading Scheme of Upper Lock Position Testing

The loading scheme of ground load testing is shown in Figure 4. 32. It has 8 loading points. The number of loading points is different in different conditions.

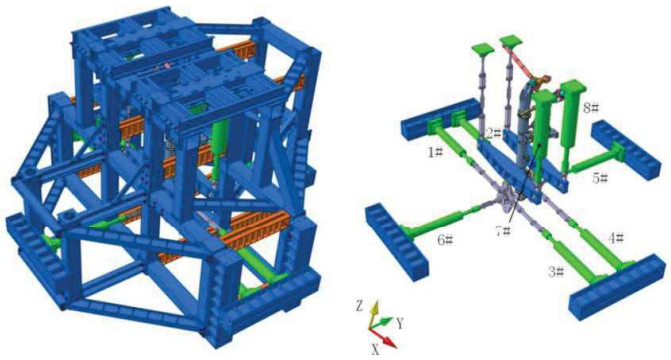

Figure 4. 32 Loading Scheme of Ground Load Testing

The long hole-solt design scheme is introduced to overcome the problem of position of vertical loading point in large deformation. The design scheme is shown in Figure 4. 33.

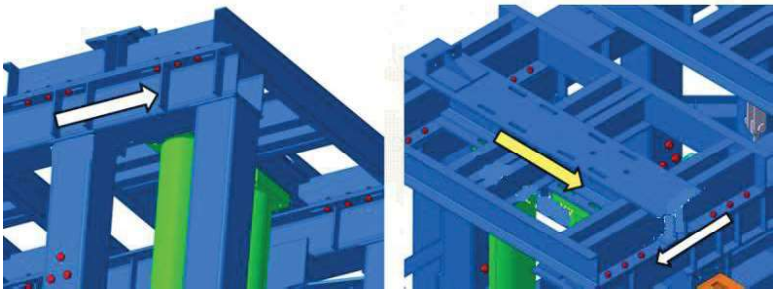

Figure 4. 33 Long-Slot Hole Design Scheme

4.8 Static and Fatigue Test Technique of Large-Scale Fuselage Panel Under Complex Loads[1]

Fuselage panel is an important structure form of aerotransport and its mechanic performance has a direct influence on the security and economy of aircraft. On the other hand, it's the foundation of structure configuration selection, structure design and modification. Considering the factors of cost and development cycle, it's common to optimize complicated and expensive fuselage structure into the form of large-scale fuselage panel in the research of configurations design.

1) Key Techniques

Several key techniques has been successfully solved in the static and fatigue test of large-scale fuselage panel under complex load, including boundary simulation of fuselage panel under complex loads, the imposed high-tonnage load, internal pressure sealing, interference separation between tensile (compress) and shear load. The developed device can apply single load and complex load. The more load cases it has, and the higher loads the device apply, the higher precision and the better complex load coordination we will obtain.

2) Technique Targets

The targets of the developed device, load cases and test panel sizes are respectively described inTable 4. 2, in Table 4. 3 and Figure 4. 34.

[1] AVIC Aircraft Strength Research Institute

Table 4. 2 Load Targets

Load Types	Load Targets
Internal pressure	0.15MPa
Tension	4000kN
Compression	4000kN
Torque load	3000kN•m

Table 4. 3 Load Cases

Case Categories	Load Cases	Case Categories	Load Cases	Case Categories	Load cases
4 Cases of Single load	Internal pressure	5 Cases of two combined loads	Internal pressure + Tension	2 Cases of Three Combined Loads	Internal Pressure + Tension+ Shear
	Tension		Internal pressure + Compression		Internal Pressure + Compression+Shear
	Compression		Internal pressure + Shear		
	Shear		Tension + Shear		
			Compression + Shear		

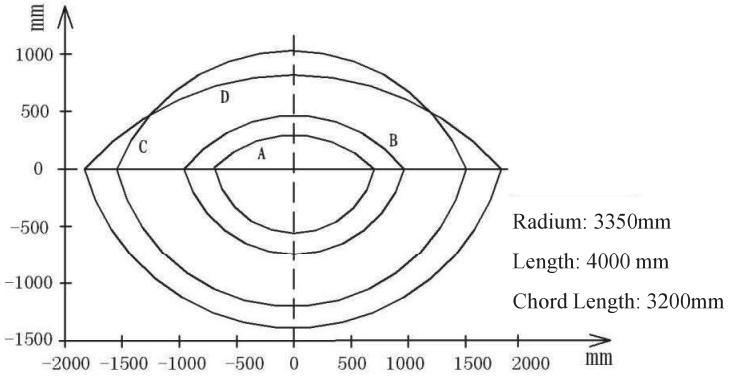

A: Regional Jet B: Single-Aisle Aircraft C: Wide Body D: Jumbo

Figure 4. 34 Test Panels Sizes

3) Boundary Simulation

Figure 4. 35 shows the boundary simulation of the large-scale fuselage panel under complex load. D-type jig is selected to simulate the boundary condition of the fuselage. The fuselage panel is connected with the D-type jig to form a ring structure, and the airtight plate is installed on its both ends to simulate the end effect of the fuselage panel.

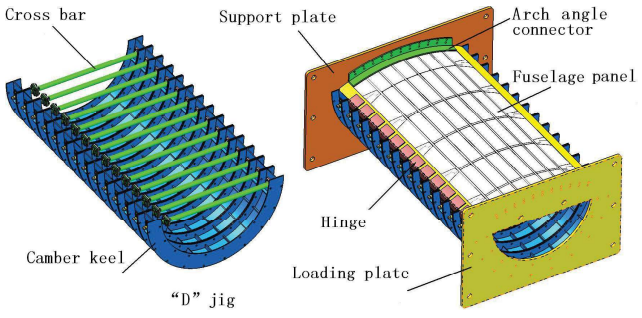

Figure 4. 35 Boundary Simulation

4) Test Device

The results of this research on the static/fatigue test technique of the large-scale fuselage panel under complex loads have been applied to the structural selection and test verification of the commercial aircraft fuselage panel. Figure 4. 36 shows the static/fatigue test device of the large-scale fuselage panel under complex loads.

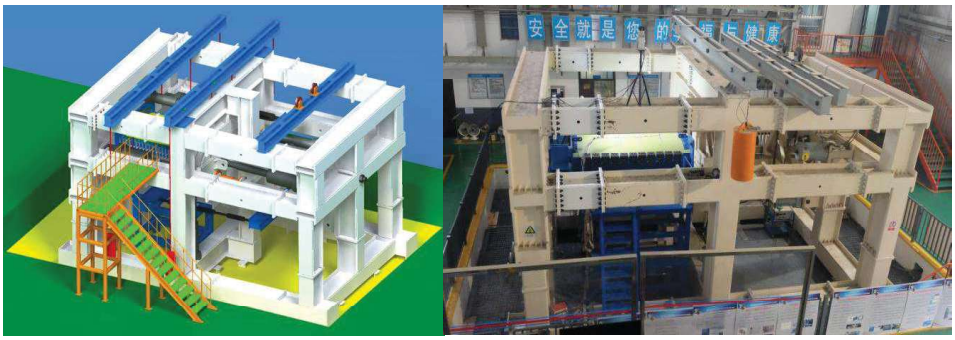

Figure 4. 36 Static/Fatigue Test Device of the Large-Scale Fuselage Panel Under Complex Loads

5 Structure Health Monitoring

5.1 The study of Load-Measuring Technology Using Smart Bolt in the Field of Structure Health Monitoring[1]

Smart bolt inside which sensor or memorizer /microprocessor chips are buried has the integration characteristic of structure and function. It usually has two aspects of functions: one is the ability of sentience temperature, load, pressure and other kinds of environment factors which is called the function of sensor applied in the field of measuring or Structural Prognostic and Health Management (SPHM), the other is the ability of data storage and status identification which is called the function of data label applied in the field of production assembly and operation maintenance.

AVIC—SADRI has developed a kind of smart senor-bolt with the function of load measuring which can be used to measure tensor load and shear load (Figure 5. 1). This kind of bolt has been applied in the study of the load distribution of typical multi-pin connecting structures, and got satisfied results with the load-measure precision of 2% and high sense for assembling clearance, preload and other influencing factors of bolt-loads distribution. At present a kind of aircraft bolt SPHM system are developed based on this kind of smart bolt.

a) Smart Bolt b) Tensile Test c) Simple Shear Test d) Double Shear Test

[1] AVIC Shenyang Aircraft Design & Research Institute

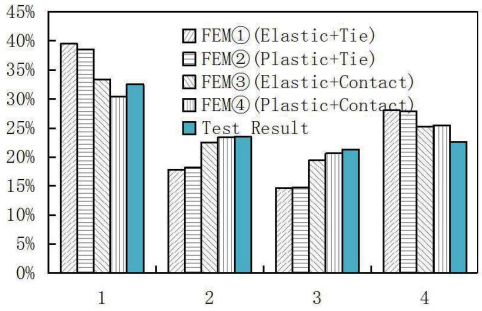

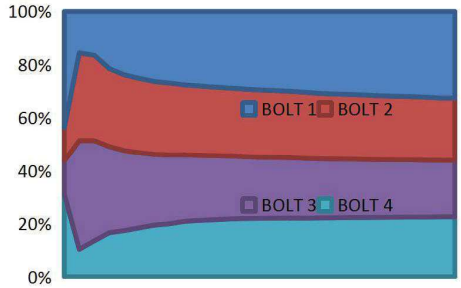

e) Comparison Between Experiment and Calculation f) Variation of Bolt Load Distribution Ratio

Figure 5. 1 Smart Bolt and Its Load Test Effect

Reference:
[1] http://digi.163.com/08/1208/09/4SKNK88M00162IEM.html.
[2] http://auto.takungpao.com/news/q/2014/0115/2180625.html.
[3] Wang Jianzhi, Qiu Tao. An Overview of Smart-bolt Technique [C]// Proceedings of the 2015 [4] Aeronautics Measurement & Control Technology Conference. Beijing: CSAA, 2015: 535-538. (in Chinese)
[4] Wang Jianzhi, Qiu Tao, Wu Defeng, He Gang. An Method of Detection Bolt Load: China. ZL2011104187 80.8 [P]. 2011-12-15. (in Chinese)

5.2 Application of Intellective Coating Monitoring Technique in Engineering[1]

Intellective coating sensor was successfully applied in fatigue crack monitoring on fatigue life prediction and extension of airframe structures.

Intellective coating monitoring technology is a rising technique on Structure Health Monitoring and Detection. Intellective Coating Monitoring Technology (ICMT) can achieve the functions of detecting, addressing and auto-warning of micro-crack in airframe structure. It can make the early-crack, which appears on critical elements, to be easily detected, make the health condition of airframe structure to be monitored all the time, and form a reliable support for flight safety, economical service and in-time maintenance.

Intellective Coating Monitoring System (ICMS) mainly consists of three sub-systems: sensor sub-system, information acquisition and data smart-management sub-system, structure crack/damage on-time identification sub-system.

Sensor sub-system is formed by three layers: driving layer, sensing layer and protecting layer. Driving layer and sensing layer are the key layers of smart coating.

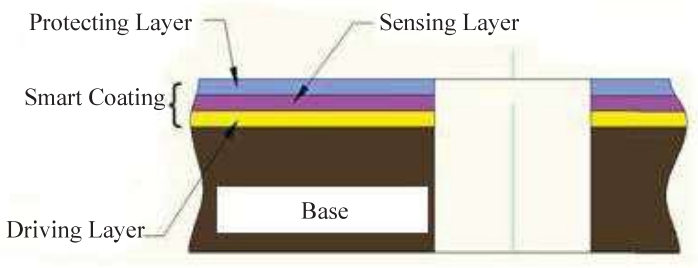

Figure 5. 2 Smart Coating Sensor Layer-Up

Information acquisition and data smart-management sub-system is mainly used to fulfill the basic function requirements of dealing with data of sensor net and information management, such as information separation, signal filtration, signal amplification, A/D transformation (information management), sampling control, signal pre-processing (abnormal value treatment and calibration).These information is the base to identify and monitor severity of structure crack and damage.

[1] AVIC Shenyang Aircraft Design & Research Institute

The main function of structure crack/damage on-time identification sub-system is to analysis the treated information by applying crack/damage calibration method and technology, then verify the situation(location, damage severity, damage type) of structure crack/damage by comprehensive analysis with structure characteristics.

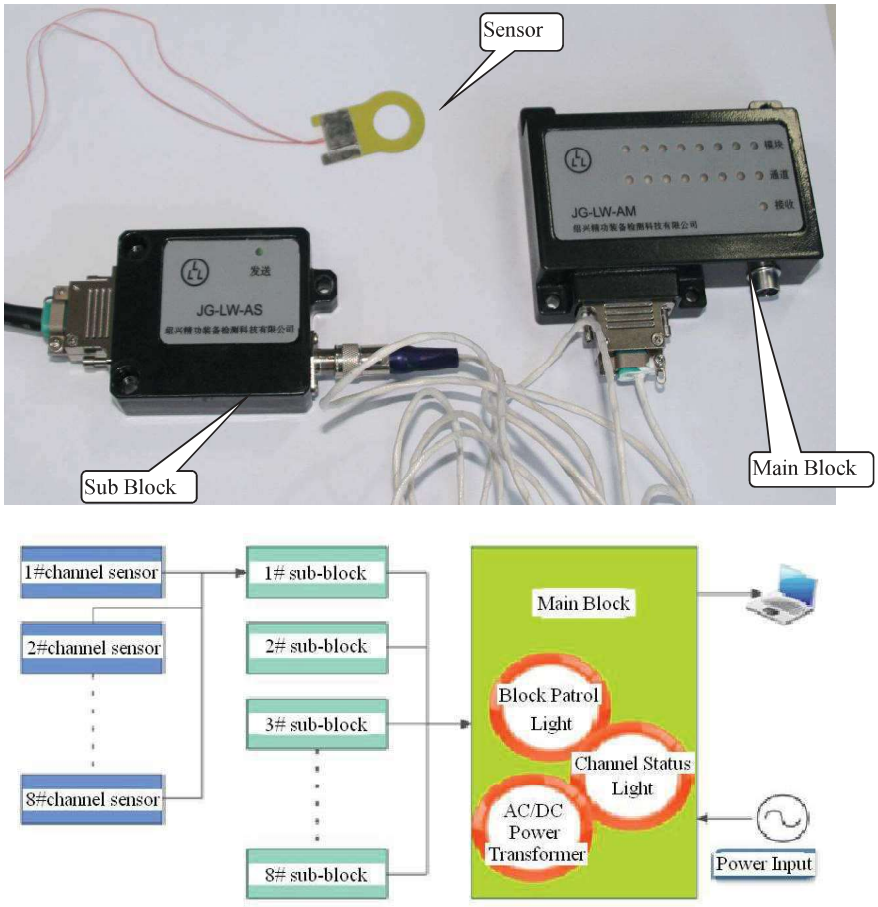

Figure 5. 3 ICMS Construction Map

Figure 5. 4 shows smart coating monitor technology engineering application in aircraft full-scale fatigue test.

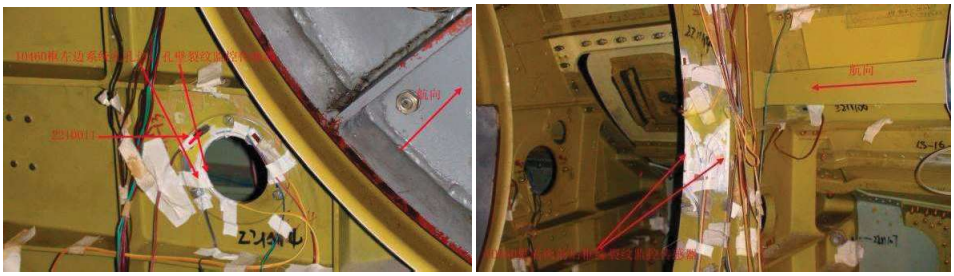

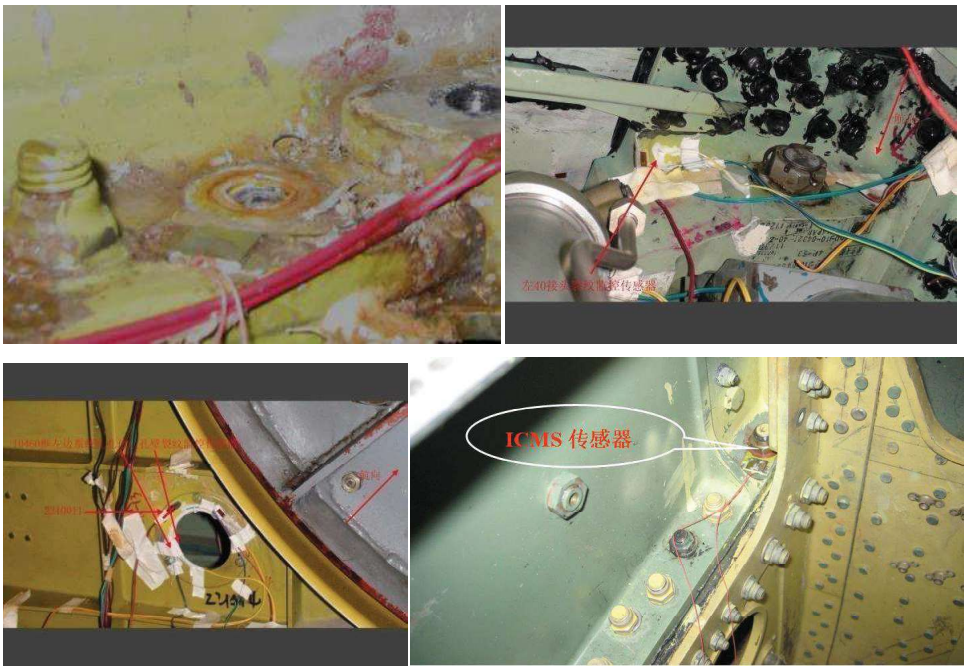

Figure 5. 4 ICMS Engineering Application in Full-Scale Fatigue Test of Aircraft

ICMS exhibits excellent performance in full-scale fatigue test of aircraft. It shows nice and stable working status in the activity of monitoring the critical structure elements all the time and sending real-time feedback. Its application in the test indicates that ICMS can satisfy the requirements of full-scale fatigue test for structure crack/damage monitoring; it is timely and efficient, and it can inform the operator in time with warning light and sound alarm. ICMS provides trustable data support for decision-making in fatigue test.

5.3 Aircraft Structural Load identification Technology with High Accuracy in SPHM System[1]

Structural Prognostic and Health Management (SPHM) of aircraft plays an important role in fatigue life monitoring and self-maintenance system, which is used to guarantee safety of structures, explore the potential service life, and enhance the capability of combating. An important work of SPHM is to obtain the load time histories of fatigue critical structures, so as to evaluate fatigue damage and predict remaining life of in-service aircraft. Traditionally, theoretical models based on wind tunnel test and CFD analysis were used for loading calculation in the stage of preliminary design, and in-flight load measurement programs were conducted to obtain in-service loading based on strain gage data. These traditional methods have some limitations and defects, that is, analytical model cannot be constantly updated to improve the accuracy between the analytical load and actual load. Depending on additional strain gages and/or other sensors may reduce structural maintenance and reliability.

In the past decade, the Artificial of Neural Network (ANN) has been widely used for load identification of helicopters and aircrafts, and lots of researches have been conducted to verify its efficiency and accuracy in contrast to traditional methods. Due to its ability to learn from legacy experience and identify underlying information from noisy data with high accuracy and reliability, ANN has the potential to play a leading role in SPHM system.

Reliability of SPHM requires a high precision of structural load identification. Since there is an approximately exponential relationship between fatigue life and load level, a 5% error of load may cause almost 20% errors in life or damage, and 90% reliability of life requires at least 97.5% reliability of load. In the literature, the application of ANN techniques can control the error below 5%~15%,

[1] AVIC Chengdu Aircraft Design & Research Institute

which is obviously not sufficient for the high reliability of life. Because outputs of ANN model are highly dependent on inputs (test data), three steps should be done to improve the accuracy as follows, after analysing the characteristics of flight parameters.

Step1: Maneuver Identification. This step eliminates all periods of inactive data in level flight and clusters the flight data in each identified maneuver for building ANN model individually.

Step2: Inputs Optimization. Based on maneuver type and load type, a preliminary group of relevant flight parameters are selected, and then through correlation analysis and stepwise regression, the optimal inputs for ANN model are determined.

Step3: Peak/valley Bias. A sample bias method is proposed to increase the occurrence probability of data near peak/valley points, so as to reduce the size of inputs and enhance the accuracy of outputs at peak/valley points.

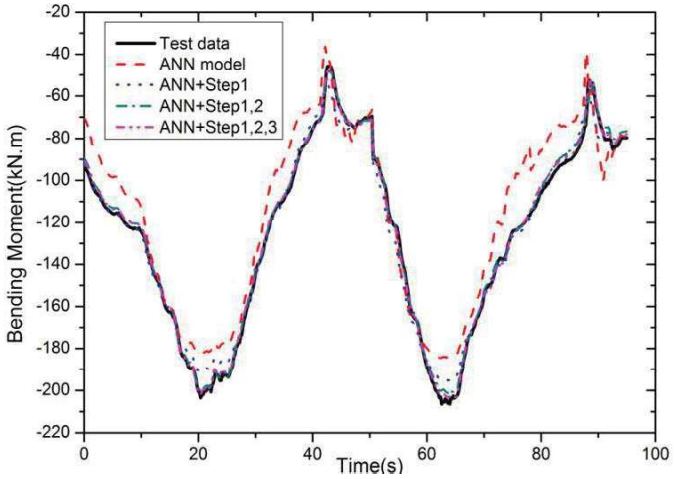

Figure 5. 5 Comparison of the ANN Results Using Different Methods

Figure 5. 5 shows the results obtained from the ANN model using the approach proposed in this paper. As indicated, all of the steps can enhance the accuracy of ANN model, and the final error is below 3%.

Conclusions: ANN model combined with maneuver identification, inputs optimization and peak/valley bias technology, are proposed in this paper, which can significantly improve the accuracy of aircraft structural load identification than simple ANN model.

References:

[1] Wang Yongjun，Dong Jiang，Liu Xiaodong，Zhang Lixin. Identification and standardization of maneuvers based upon operational flight data[J]. Chinese Journal of aeronautics, 2015,28(1):133-140.

[2] Steve Reed, Brian McCoubrey, Andy Mountfort. Introduction to Service of an Artificial Neural Network Based Fatigue Monitoring System[C]. 25th ICAF Symposium, 2009,1093-1119.

5.4 Bayesian Approach Based Probability Fatigue Life Prediction Method Under Random Load Spectrum[1]

A framework applying the Bayesian approach to the aircraft Structural Prognostic and Health Management (SPHM) system is constructed in this paper. A Bayesian approach based probability life prediction method under random load spectrum is presented using an improved Markov Chain Monte Carlo (MCMC) method.

The aim of the study is to improve the accuracy of damage prognostic and Remain Useful Life (RUL) prediction, so as to determine maintenance and inspections intervals reasonable and ensure safety and reliability of aircraft structures. In SPHM system, RUL of structures can be well prognosticated while the monitoring data is available and precision is improved with the increase of monitoring data. However, uncertainty always exists in the RUL prediction due to uncertainty in the crack growth model,

[1] AVIC Chengdu Aircraft Design & Research Institute

material and geometric properties, initial crack size, measured crack size. Thus, an important consideration in SHM-based prognosis is therefore to accurately predict RUL in the presence of uncertainty.

To address this issue, various methods to address uncertainty in fatigue have been proposed using Bayesian approach. However, almost all these papers focus on explore methods for damage or RUL prediction under constant loading. These methods may not suitable for random load spectrum, since it is more difficult sampling from posterior distribution of parameters using standard Markov Chain Monte Carlo (MCMC) simulation than constant loading case. But, few attempts have been made to address RUL prediction under random load spectrum using Bayesian approach. Therefore, a different method to establish posterior distribution of parameters in damage model is applied in random load spectrum case in this paper.

First, Parameters C and n in Walker's model are assumed as uncertain variables which are independent to each other, and parameters M1 and M2 are assumed as constant variables. Mean values of these four parameters are fitted using experimental crack growth data under constant loading. Prior distributions of C and n are assumed as uniform distributions which mean values equal to the fitted mean values of C and n.

Then, experimental crack growth data under random loading spectrum is combined with Bayes' theory to establish posterior distributions of C and n.

Finally, an improved MCMC method is proposed to solve the problem of extract samples from posterior distributions of parameters for random loading spectrum case. The main idea is embed a cycle-by-cycle crack growth prediction process in standard Metropolis-Hasting method (one of the MCMC methods).

Above methods presented in this paper are preliminarily identified using the test data of 7050-T7651 aluminum alloy plate with a center-through crack under random load spectrum. Figure 5. 6 demonstrates that posterior distributions of C and n move and change with the increase of available data and have a trend to keep in a specific location if more data is available. This means that uncertainties in the prior distribution are reduced using Bayesian approach.

It is found that the crack growth curves predicted using mean values of posterior distributions of C and n show gradual convergence to experimental crack growth curves and high accordance with experimental crack growth curves after several Bayesian updates. See Figure 5. 7. The results also show that probability distribution of fatigue life predicted using this method is reliable and credible. See Figure 5. 8. When 10 crack size data are available, mean value of predicted RUL(116 576 cycles) only 5.3% smaller than real RUL(123 100 cycles) in the test. Therefore, the probability distribution of RUL predicted based on methods presented in the paper is reliable and credible.

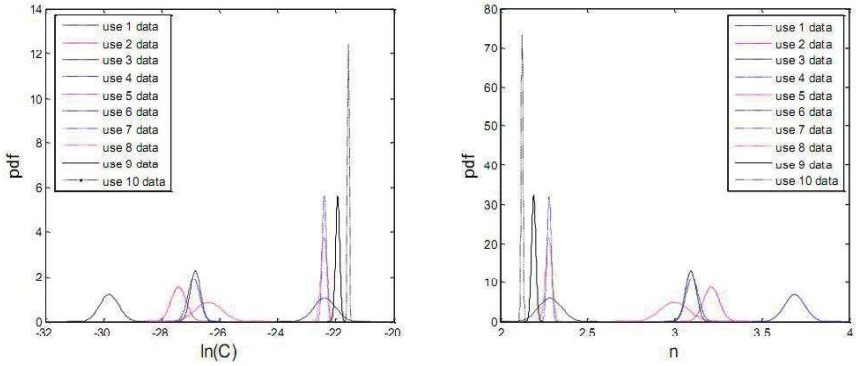

Figure 5. 6 Posterior Distributions of C and n When Different Number of Crack Size Data is Available

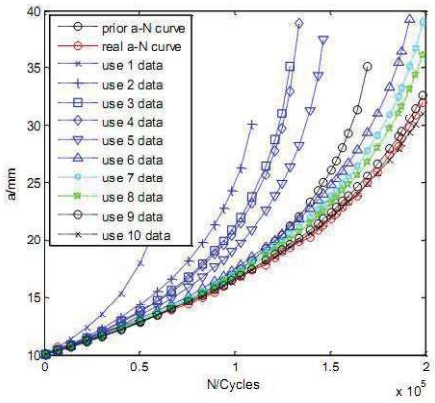

Figure 5. 7 Average a-N Curves Predicted using different Number of Data.

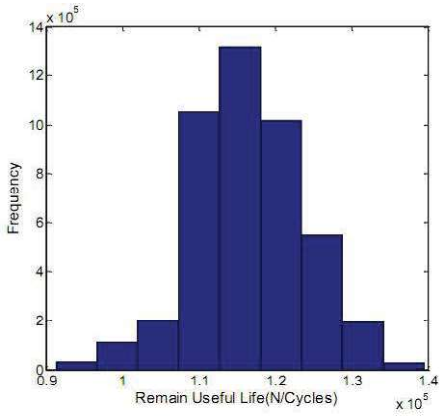

Figure 5. 8 RUL Predicted Using 10 Crack Size Data

Reference:
[1] Douc R, Maire F, Olsson J. On The Use of Markov Chain Monte Carlo Methods for The Sampling of Mixtrue Models:A Statistical Perspective [J]. Statistics and Computing. 2015,25(1):95–110.
[2] MOHANTY S. Bayesian Statistic Based Multivariate Gaussian Process Approach for Offline/Online Fatigue Crack Growth Prediction [J]. Experimental Mechanics, 2011, 51(6):833-843.
[3] KARANDIKAR J M, KIM N H, SCHMITZ T L. Prediction of Remaining Useful Life for Fatigue-Damaged Structures Using Bayesian Inference，Engineering Fracture Mechanics[J]. Engineering Fracture Mechanics, 2012,96(2):588-605.
[4] AN D. Options for Prognostics Methods: A review of data-driven and physics-based prognostics[C]// AIAA/asme/asce/ahs/asc Structures, Structural Dynamics, and Materials Conference. 2013:1-19.

6 Maintenance and Repair

6.1 Analysis of Repairing Methods for Fastening Hole with Manufacturing Error[1]

With scientific and economic development, higher requirements for the aircraft service life are proposed. The realization of aircraft's long life and high reliability mainly depend on the durability design of structure details and the control of the initial fatigue quality of aeronautic structure details during manufacturing. For connection structure, the quality of fastening hole is a crucially influential factor to structure life. Based on the current situation of domestic aviation industry, studying the fatigue life of the structure through selecting the typical fastener hole manufacturing error in connection structure, confirming structure with errors and fatigue life of changes of connection structure after being repaired in a certain way and qualifying the changes of detail fatigue rating (DFR) are significant researches for improving structure fatigue strength and providing theoretical basis for structure repair.

In actual producing and processing, designers usually handle problems such as fastening hole manufacturing error on the basis of experience and simple calculation without systematically theoretical or experimentally researches. Therefore, the repairing method adopted normally lacks theoretical support and does not have specific judgments about life changes of structure after repair, which leads to increase of check and maintenance cost in later period and greatly potential safety hazard for plane's flight safety.

Aiming at typical connection structure with manufacturing error, this thesis conducts an intensive research on typical aircraft structure fatigue analysis and life prediction by means of combing theory and experiment. After statistics, screening and study, research part and typical error types are identified as bolt holes errors on central wing and outer panel jointing area and small edge problems on the edge strip of front spar of central wing. This paper simplifies structure of the two parts and analyzes the fatigue life as well as detail fatigue rating by applying structure durability analysis theory. Through experimental verification, this paper studies the changes of fatigue life and detail fatigue rating between structure with manufacturing errors and the original structure. Through theoretical and experimental analysis, The validity of repair methods was proved for the fastening holes error in the current aviation industry and theoretical and experiment data were used for supporting repairing methods.

[1] AVIC Aircraft Strength Research Institute

Samples Designing

The sample of central wing and outer panel structure simplified is shown in Figure 6. 1. Type original, without errors, is designed as comprising sample. The manufacture error is designed in the middle fastening hole of the structure and this is type I sample. When the manufacture error is designed in the fifth fastening hole from left in Figure 6. 1 named type Ⅱ.

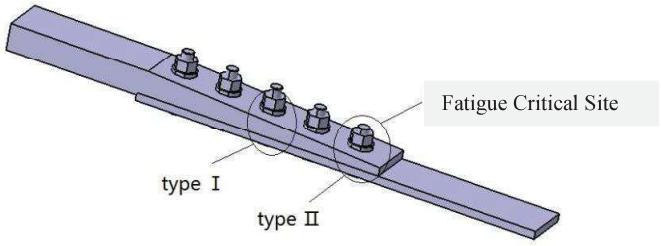

Figure 6. 1 Sample of Central-Outer Wing Panel Structure

The most common manufacturing error in the structure of front spar of central wing is small edge problems on the edge strip during manufacture. The original test sample is designed as Figure 6. 2. The error often happened in the fastening hole on the edge and is circled in Figure 6. 2. The repairing method is digging the edge and strengthening it in the area. To test the effect of the repairing method, other two types of sample were designed and are shown in Figure 6. 2 and Figure 6. 3.

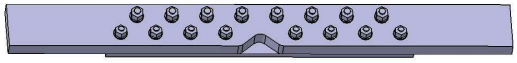

Figure 6. 2 Test Sample without Reinforcement

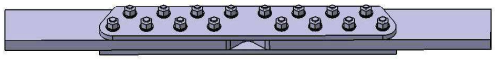

Figure 6. 3 Reinforced Test Sample

Test Facility

The test was completed on the INSTRON1332（10T）machine. The test samples were fixed and tested as the following Figure 6. 4.

Figure 6. 4 Fixed Method and Test Facility

Test Results and Analysis

Repair effect of central wing and outer panel structure is shown in Table 6. 1.

Table 6. 1 Repair Effect of Central-Outer Panel Structure

sample types	N95/95 compared with original structure	DFR compared with original structure
Original structure	1	1
Error type Ⅰ	86.9%	96.5%
Error type Ⅱ	40.3%	70%

Repair effect of front spar of central wing structure is shown in Table 6. 2.

Table 6. 2 Repair Effect of Front Spar of Central wing structure

sample types	N95/95 compared with original structure	DFR compared with original structure
Original structure	65024	1
Error type Ⅰ	16626	25.6%
Error type Ⅱ	53230	81.9%

Conclusion

The test of bolt holes errors on central wing and outer panel jointing area sample shows that the fatigue life and DFR (detail fatigue rating) decreased 30% and the repair effect obviously is not good. The test of front spar of central wing structure presents that it is necessary to repair the structure with errors in this area. The fatigue performance of reinforced structure basically reaches the same level as in original structure. The results of this test show that the repairing method is acceptable.

6.2 Research on Maintenance and Life Assessment of Typical Panel Structure[1]

Typical panel structure is an important structure of aircraft, which contains a large number of fastening holes, and the fatigue crack is the main form of damage. According to the fatigue structural damage, the cracks of different lengths were repaired by the traditional stop hole and advanced friction stir welding. Based on the combination of engineering calculation and experimental verification, the static and fatigue damage tolerance performance is evaluated.

Typical Panel Damage Structure

Panel structure widely exists in the aircraft structure. Following the simplified principle of the main contradiction, ignoring the influence of ribs and geometry, the fatigue test piece as shown in Figure 6. 5 was finally designed. The center of rectangular plate is 3mm diameter circular hole, the hole edge cutting half crack length of pre-fatigue crack is 2.5mm,the length L is 400mm,the width W is 100mm,the thickness t is 3.2mm.

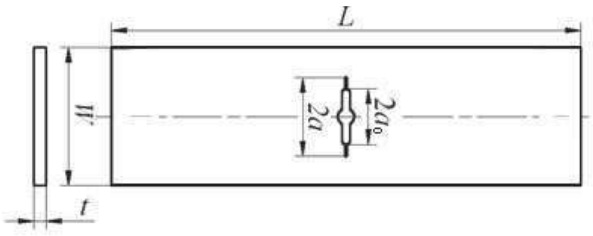

Figure 6. 5 Shapes and Size of Test Pieces

Maintenance Plan

Stop hole repair is the size of the circular holes drilled at the fatigue crack tip for eliminating the crack tip plastic zone and preventing the crack continue to expand. Friction stir welding repair uses the heat which created by the friction of high speed stirring head and wall to make the material flow, the crack is eliminated by the flow. The maintenance test is shown in Figure 6. 6.

[1] AVIC Aircraft Strength Research Institute

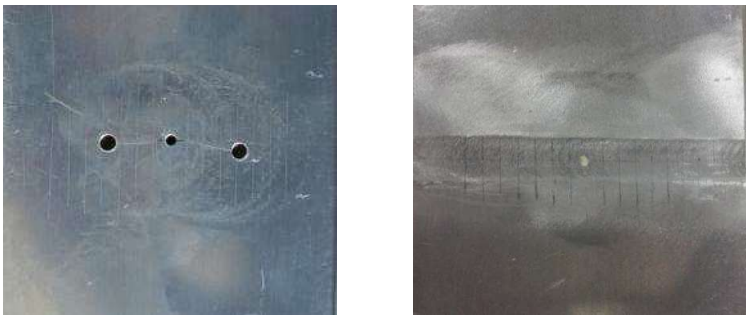

Figure 6. 6 Maintenance Test

Mechanical Property Evaluation

The content of static evaluation includes no repair, stop hole repair and FSW repair. The test results as shown in Figure 6. 7. The basic static tensile curve of FSW almost overlaps with the base material. The evaluation of the tensile strength of FSW is up to 89.4% of base material.

The material does not change between the stop hole repair and the base material. Considering the plate width, crack size and crack length, bearing capacity and other factors, static performance design of stop hole maintenance is drawn as Figure 6. 8.

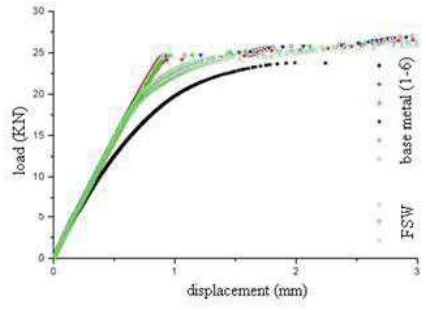

Figure 6. 7 Static Performance Comparison

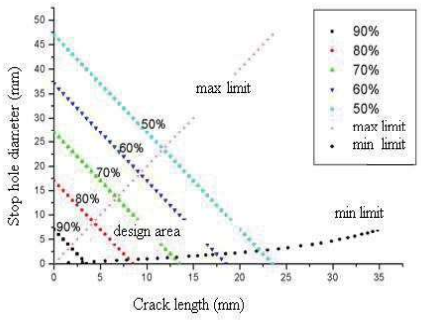

Figure 6. 8 Static Performance Design of Structure with Stop Hole repair

Comparing the stop-crack hole repair with FSW repair, the static performance of stop hole depends on the bearing capacity and crack length, and FSW is not depending on the crack length, showing its stability maintenance effect.

The main evaluation of crack propagation performance is curve of propagation life to crack growth rate. Based on the analysis method of crack growth rate test, the crack growth rate curves under different survival rates are presented.

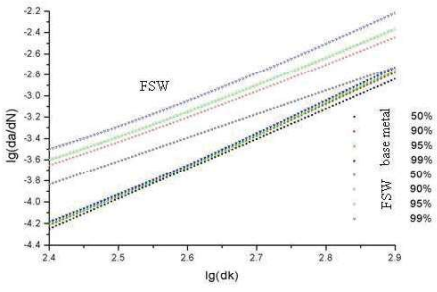

Figure 6. 9 Comparison of Crack Growth Rate

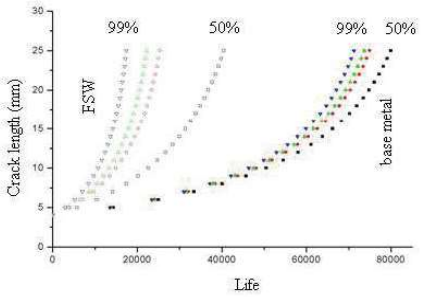

Figure 6. 10 Comparison of Crack Growth Life

It is showed that FSW crack growth rate is higher than stop hole repair in Figure 6. 9. The higher

survival rate causes higher crack growth. Figure 6. 10 shows the life of same delta crack which begins from 4mm to 25mm. The life of FSW repair is shorter than stop hole repair. It can also be concluded that FSW is more conservative than stop hole repair.

Conclusion & Prospect

Considering the static and crack growth properties, the FSW repair shows the superiority than stop hole repair. If this new technology was used in maintenance in future, the miniaturization, welding equipment engineering and standardization should be paid attention, and the welding parameters optimization of geometry and materials in various aircrafts.